Right ventricular diastolic dysfunction in pulmonary arterial hypertension

Rain, S.

2015

document version
Publisher's PDF, also known as Version of record

Right ventricular diastolic dysfunction in pulmonary arterial hypertension

Silvia Rain

Financial support for printing this thesis was kindly provided by the Vrije Universiteit

The work presented in this thesis was performed at the departments of Pulmonology and Physiology, Institute for Cardiovascular Research of the VU Medical Center, Amsterdam, The Netherlands.

Cover design Silvia Rai &, Sebas Apeldoorn
Print Offpage, Amsterdam www.offpage.nl
ISBN ----------

VRIJE UNIVERSITEIT

Right ventricular diastolic dysfunction in pulmonary arterial hypertension

ACADEMISCH PROEFSCHRIFT

ter verkrijging van de graad Doctor aan
de Vrije Universiteit Amsterdam,
op gezag van de rector magnificus
prof.dr. F.A. van der Duyn Schouten,
in het openbaar te verdedigen
ten overstaan van de promotiecommissie
van de Faculteit der Geneeskunde
op maandag 14 september 2015 om 11.45 uur
in de aula van de universiteit,
De Boelelaan 1105

door

Silvia Rain

geboren te Ploiesti, Roemenië

promotoren:	prof.dr. A. Vonk Noordegraaf
	prof.dr. J. van der Velden
copromotor:	dr. F.S. de Man

Content

Chapter 1

Introduction and thesis outline

Definition of pulmonary arterial hypertension

Pulmonary arterial hypertension (PAH) is defined by a mean pulmonary arterial pressure of more than 25mmHg and a pulmonary wedge pressure lower than 15mmHg.[1,2] The estimated prevalence is of 15-50 cases per million, with substantially higher prevalence in risk groups (HIV 0.5%, systemic sclerosis 7-12%). Although primary a lung disease, the progression and survival in PAH is related to the incapacity of the right ventricle to adapt to the increased afterload.[3-10]

Table 1 – Clinical classification Pulmonary Hypertension

Group 1	Pulmonary arterial hypertension(PAH) Idiopathic / Familial (iPAH) Toxin- and drug-induced Connective tissue disease (PAH-CTD) Congenital heart defects (PAH-CHD) Other causes (HIV, Sickle Cell Disease)
Group 2	Pulmonary hypertension due to left heart failure (PH-LHF)
Group 3	Pulmonary hypertension due to lung disease (PH-Lung)
Group 4	Chronic thromboembolic pulmonary hypertension (CTEPH)
Group 5	Other multifactorial causes of pulmonary hypertension

Right ventricular diastolic dysfunction – From bed to bench side

Right ventricular (RV) remodeling in response to the increased afterload is considered to follow a two-step sequence. In an initial stage, the hypertrophic response is prominent and helps the thin-walled RV to cope with the increase in pulmonary pressure. However, in most patients this step is rapidly followed by extensive RV dilation and progression to irreversible (end-stage) heart failure.[11,12] At this end-stage systolic function is clearly compromised (as shown by a low RV stroke volume and ejection fraction) and patients present with signs and symptoms of heart failure: minimal exercise capacity (shown in 6-minutes-walk-test), sensation of dyspnea and peripheral edema.[13] Whether RV diastolic function is also compromised in patient with PAH and further contributes to disease worsening is not known. Therefore the aim of this thesis is to characterize RV diastolic function in PAH.[14,15]

Part 1 – Basic science perspective

Load-independent RV diastolic function determination

Determining RV diastolic function is challenging in PAH since non-invasive ultrasound parameters (E/A, E/E, tau) commonly used to determine left ventricular diastolic function are less applicable on the right heart due to their load-dependency. A prospective study on PAH showed that RV echocardiography is only in 50% of the cases accurate in determining the hemodynamic estimates of the right ventricle.[16,17] Furthermore, echocardiography could not differentiate between early versus late diastolic abnormalities, which makes this non-invasive technique less valuable to diagnose RV diastolic function.[18]

Right atrial pressure (RAP), a clinical parameter used in common clinical practice to characterize RV diastolic function, is only an indirect marker of diastolic dysfunction and does not fully reflect intrinsic RV diastolic function.[19-2021] Since tricuspid regurgitation is common in PAH (>80% patients with a pulmonary artery systolic pressure >35mmHg) and leads to an abnormally high RAP due to atrial volume-overload and flow underestimation, determining RAP may not truly reflect RV diastolic dysfunction.[22]

Figure 1 – RV systolic and diastolic function assessed by pressure-volume analysis

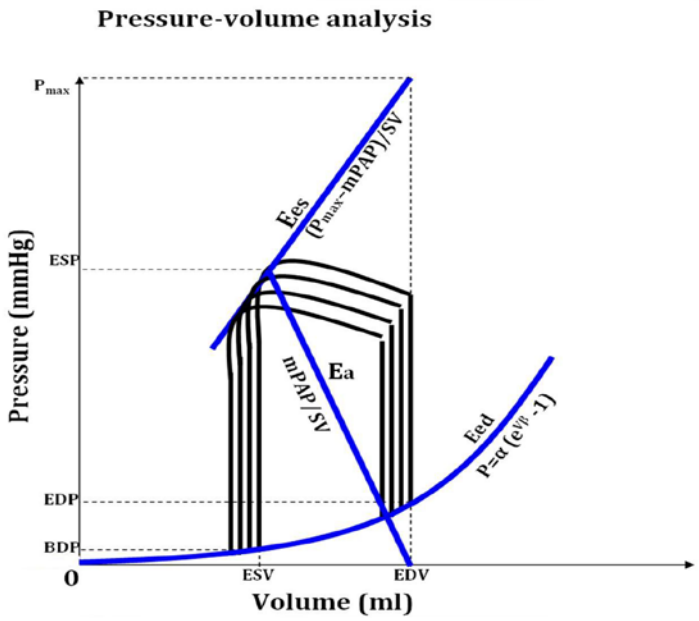

Pmax: maximal isovolumic pressure; EDP: end-diastolic pressure; BDP: minimal diastolic pressure; ESV: end-systolic volume; SV: stroke volume; EDP: end-diastolic volume; Ees: systolic elastance; Ea: arterial elastance; Eed: end-diastolic elastance.

Intrinsic RV diastolic function can be measured invasively in animal models by load-independent methods which compute end diastolic elastance (Eed) from pressure-volume analysis. (Fig. 1)[23,24] To determine Eed one needs to perform preload reducing maneuvers, such as vena cava occlusion. During this procedure the preload to the right ventricle is progressively decreased, leading to a gradual lowering in RV filling pressures and a leftward-downward displacement of the pressure-volume loops. Eed is then calculated by fitting an exponential line through the end-diastolic pressure-volume points, where the exponential factor $\boldsymbol{\beta}$ ($P=\alpha\ (e^{V\beta}-1)$) reflects the diastolic stiffness of the ventricle. This method is feasible in animal studies. However in PAH patients it carries risks related to the pre-existing poor cardiac function and the preload reduction intervention therefore cannot be used safely. In ***Chapter 2*** we aimed to develop a new method to determine RV diastolic function which is suitable for common clinical practice by circumventing the preload reduction maneuvers and has the advantage of reflecting the intrinsic muscle properties on the right ventricle.[14-2526]

Figure 2 – Impaired cardiomyocyte function

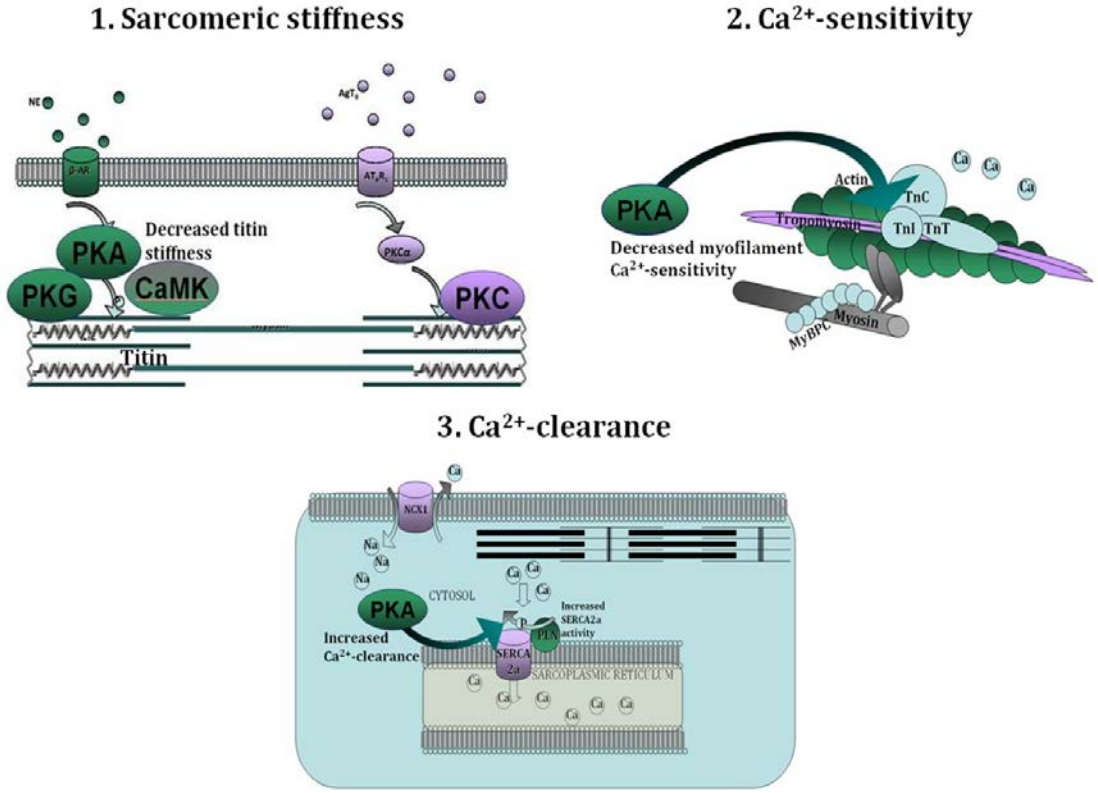

PKA: protein kinase A; PKC: protein kinase C; CaMK: Ca^{2+}-calmodulin dependent kinase; NE: norepinephrine; AgT_{II}: angiotensin II; β-AR: beta adrenergic receptor; $AT_{II}R_1$: angiotensin II receptor type 1; Ca: calcium; Na: sodium; TnI/C/T: troponin I/C/T; MyBPC: myosin binding protein C; NCX1: sodium-calcium exchanger; $SERCA_{2a}$: sarcoplasmic reticulum Ca^{2+}-ATPase; PLN: phospholamban.

Cellular mechanisms contributing diastolic dysfunction

Heart failure with preserved ejection (HFPEF) fraction is the hallmark disease of left ventricular diastolic dysfunction.[27] Several cellular morphological and functional mechanisms were shown to be implicated in HFPEF.[27] First, a prominent increase in cardiac muscle cell size was observed in samples from HFPEF patients. Furthermore, ventricular hypertrophy was associated with altered cardiomyocyte relaxation properties. Cardiomyocyte dysfunction (Figure 2) was related to increased stiffness of the contractile apparatus, higher residual diastolic actin-myosin cross-linking, altered myofilament Ca^{2+}-sensitivity and decreased diastolic Ca^{2+}-clearance.[28-34][35]

1) Cardiomyocyte stiffness

Titin was previously shown to be the major contributor to left ventricular cardiomyocyte stiffness. This giant sarcomeric protein anchors at the z-disk level and acts as a molecular spring, determining the sarcomeric elasticity upon stretch.[36] Titin stiffness is modulated by a fast acting mechanism involving the phosphorylation of specific titin domains and a relatively slow acting mechanism where one of the two titin isoforms is preferentially expressed.[37] Phosphorylation of titin N2B domain by

specific kinases (PKA/PKG/$CaMK_{II}\delta$) induces a decrease in sarcomeric stiffness, while PEVK domain phosphorylation (PKC) increases its stiffness.[38-3940]

2) Myofilament Ca^{2+}-sensitivity
An increase in myofilament Ca^{2+}-sensitivity can also contribute to cardiomyocyte diastolic impairment by enhancing residual actin-myosin interactions at low [Ca^{2+}] concentration (as found during the diastolic phase). Previous studies in samples from patients with end-stage left heart failure show that decreased protein kinase A (PKA) phosphorylation of sarcomeric proteins troponin I (TnI) and myosin binding protein C (MyBPC) have a net effect of increasing myofilament Ca^{2+}-sensitivity, which may underlie diastolic function.[41]

3) Impaired diastolic Ca^{2+}-clearance
Similar mechanisms of increased residual actin-myosin interactions involve alterations in the diastolic [Ca^{2+}] concentration during diastole by insufficient Ca^{2+}-reuptake into the sarcoplasmic reticulum (SR). An abnormally high diastolic [Ca^{2+}] may impair the capacity of the cardiomyocyte to fully relax. Several important ATPase pumps, Ca^{2+}-channels and regulatory proteins are implicated in the diastolic Ca^{2+}-clearance. Most of the cytoplasmatic Ca^{2+} is removed at the end of systole by the sarcoplasmatic reticulum calcium ATPase 2a (SERCA2a), which uses ATP breakdown to pump back Ca^{2+} into the sarcoplasmic reticulum. SERCA2a function is dependent on the inhibitory effect of phospholamban (PLN) which blocks SERCA2a activity if not phosphorylated. Therefore, a decrease in SERCA2a expression and activity or increased PLN inhibition via insufficient PLN phosphorylation or increased PLN expression can lead to an abnormally high diastolic Ca^{2+}-concentration in the cytoplasm and prolonged sarcomeric contraction in the diastolic phase.[42] Furthermore, the Na^{+}/Ca^{2+}-exchanger (NCX) is responsible for extruding Ca^{2+} from the cardiomyocyte into the extracellular space in exchange for Na^{+}. Altered NCX function can have the same diastolic consequences as abnormal SERCA2a-PLN function, with the distinction that an increase in NCX function can lead to excessive Ca^{2+} loss in the extracellular space and the inability of the cell to use this Ca^{2+} during sarcomeric contraction.[43,44]

The cellular changes mentioned above were observed in left ventricular failure. However, these mechanisms could be chamber specific and they can not be extrapolated to the right ventricle due to important differences in disease etiologies and ventricle-specific embryology, morphology and hemodynamics. Therefore in ***Chapter 2 and 3*** we aimed to determine whether the diastolic properties of the RV cardiomyocytes are impaired in PAH and which molecular mechanisms are responsible for these changes.

Neurohormonal activation in PAH
As the cardiac output progressively decreases with worsening of cardiac function, specific neurohormonal activation, such as the sympathetic nervous system and the renin-angiotensin-aldosterone system (RAAS), ensure that the perfusion of vital organs is maintained and the cardiac output is restored by enhanced contractility, heart rate and volume expansion.[45,46] By an increase in preload the heart can respond with an elevation in end–diastolic volume, which via the Frank-Starling mechanism results in a

rise in stroke volume.
However, long-standing neurohormonal activation and high circulating catecolamines or angiotensin II/aldosterone hormones are accompanied by negative disease outcome.[47] Catecolamines are initially able to enhance contractility and increased heart rate, but at the same time induce myocardial ischemia, promote apoptotic cardiomyocyte death or induce the expression of maladaptive fetal isoforms of proteins involved in contraction.[48,49]
In the attempt to counteract the negative effects of neurohormonal activation, cardiomyocytes are believed to downregulate the density of hormone membrane receptors and thus block further pro-apoptotic intracellular pathways. Studies from Bristow et al. showed that the density of the β1-adrenergic receptor-1 (β1-AR) is not only down-regulated in left heart failure, but also in the right ventricle of PAH patients. The consequences of this downregulation have never been studied, though they may be linked to an abnormal diastolic function of RV cardiomyocytes. A decrease in β1-AR signaling could be coupled to insufficient adenylate cyclase/ protein kinase A (PKA)-mediated phosphorylation of important proteins involved in proper relaxation of RV cardiomyocytes.[50,51]
In left heart failure PKA was shown to phosphorylate titin and reduce sarcomeric stiffness, phosphorylate troponin I and decrease myofilament Ca^{2+}-sensitivity and phosphorylate PLN and enhance SERCA2a diastolic Ca^{2+}-reuptake function. Downregulated β1-AR may contribute to RV diastolic dysfunction in PAH via these mechanisms. Of note, Bristow et al also showed that β2-AR is up-regulated in PAH. Therefore, the net effect on the adrenergic system – PKA-mediated protein phosphorylation status – was investigated in cardiac samples of PAH patients in ***Chapter 3.***

RV diastolic dysfunction and fibrosis

The neurohormonal systems are also implicated in the regulation of fibrosis, which together with cardiomyocyte-related relaxation impairments determine overall ventricular diastolic dysfunction. The amount of myocardial fibrosis is modulated by RAAS by a series of pathways which regulate collagen synthesis, preferential collagen isoform expression, degradation and cross-linking. In a previous study by de Man et al. increased levels of renin, angiotensin (Ang) I, and AngII were associated with PAH progression.[52] The exacerbated RAAS signaling could be responsible for the increase in myocardial fibrosis. Increased levels of AngII further can activate TGF-β in the ventricular fibroblasts with a net effect of increasing collagen fiber secretion, decreasing matrix-metalloproteinases (MMPs) and increasing tissue inhibitors of metalloproteinases (TIMPS) and ultimately enhancing myocardial collagen production and deposition. Aldosterone signaling was also shown to be responsible for increasing myocardial fibrosis via the activation of mitogen-activated protein kinases (MAPKs), including extracellular signal-regulated kinases (ERK1/2) with increased mRNA levels of collagen types I, III, and IV.
If both cellular and extracellular components show diastolic alterations, it is important to determine their relative contribution to stiffness in order to understand which component deserves priority in PAH treatment. Furthermore, since the pathways implicated in cardiomyocyte stiffness and fibrosis are distinct, they require targeted treatment tailored to the specific mechanistic impairment (pathomechanism).

Therefore, in ***Chapter 4*** we aimed to determine the relevance of RV fibrosis in relation with cardiomyocyte stiffness and reveal the most important molecular mechanisms implicated in these changes.

Part 2 – Clinical perspective

Clinical relevance of RV diastolic dysfunction

The presence of diastolic dysfunction could be related or contribute to disease severity in PAH-induced RV disease. Therefore in ***Chapter 2*** we investigated whether functional markers of disease severity (mean right atrial pressure, stroke volume, NT-proBNP levels and 6-Minute-Walk-Distance) are correlated with RV diastolic function.

Diastolic dysfunction could contribute to the worsening of the disease or could merely represent an epiphenomenon in disease progression. It is believed that the diastolic function is the first to be impaired in the course of the disease and at the expense of compensating systolic function. Therefore, diastolic dysfunction may contribute to the transition of the right ventricle from a compensated stage to heart failure, as the initial compensatory mechanisms become insufficient to maintain systolic function.[53] It remains unclear whether RV diastolic impairment is present at an early disease stage and whether it is associated with clinical progression of the disease. Since the RV is hypertrophied in an early disease stage, this could initially lead to an increase in RV diastolic stiffness. However, end-stage PAH is characterized by extensive dilation and a further increase in diastolic stiffness may be related to intrinsic cardiomyocyte diastolic stiffening. Therefore in ***Chapter 6 and 7*** we investigated whether diastolic stiffness is associated with clinical progression and disease survival. IPAH patients at baseline (treatment-naive) and after a variable period of treatment were studied and the role of diastolic function was assessed in relation with disease worsening. We further investigated whether diastolic stiffness was associated with survival in iPAH patients. For that we studied treatment-naive patients and determined whether a better survival was associated with maintaining a better diastolic function or lower diastolic stiffness at clinical presentation.

REFERENCES

1. Humbert M *et al.* Pulmonary arterial hypertension in France: results from a national registry. *Am. J. Respir. Crit. Care Med.* 2006; 173, 1023–1030.
2. Hurdman J *et al.* ASPIRE registry: Assessing the Spectrum of Pulmonary hypertension Identified at a Referral centre. *Eur. Respir. J.* 2012; 39, 945–955.
3. Galiè N *et al.* Guidelines for the diagnosis and treatment of pulmonary hypertension: the Task Force for the Diagnosis and Treatment of Pulmonary Hypertension of the European Society of Cardiology (ESC) and the European Respiratory Society (ERS), endorsed by the International Society of Heart and Lung Transplantation (ISHLT). *Eur. Heart J.* 2009; 30, 2493–2537.
4. Van de Veerdonk MC *et al.* Progressive right ventricular dysfunction in patients with pulmonary arterial hypertension responding to therapy. *J. Am. Coll. Cardiol.* 2011; 58, 2511–2519.
5. Humbert M *et al.* Survival in patients with idiopathic, familial, and anorexigen-associated pulmonary arterial hypertension in the modern management era. *Circulation* 2010; 122, 156–163.
6. Haddad F *et al.* Right Ventricular Function in Cardiovascular Disease, Part II Pathophysiology, Clinical Importance, and Management of Right Ventricular Failure. *Circulation.* 2008; 117, 1717–1731.
7. D'Alonzo GE *et al.* Survival in patients with primary pulmonary hypertension. Results from a national prospective registry. *Ann. Intern. Med.* 1991; 115, 343–349.
8. Voelkel NF *et al.* Pathobiology of pulmonary arterial hypertension and right ventricular failure. *Eur. Respir. J.* 2012; 40, 1555–1565.
9. Vonk Noordegraaf A *et al.* The role of the right ventricle in pulmonary arterial hypertension. *Eur. Respir. Rev. Off. J. Eur. Respir. Soc.* 2011; 20, 243–253.
10. Bogaard HJ *et al.* The right ventricle under pressure: cellular and molecular mechanisms of right-heart failure in pulmonary hypertension. *Chest* 2009; 135, 794–804.
11. Hagger D *et al.* Ventricular mass index correlates with pulmonary artery pressure and predicts survival in suspected systemic sclerosis-associated pulmonary arterial hypertension. *Rheumatol. Oxf. Engl.* 2009; 48, 1137–1142.
12. Van Wolferen SA *et al.* Prognostic value of right ventricular mass, volume, and function in idiopathic pulmonary arterial hypertension. *Eur. Heart J.* 28, 1250–1257 (2007).
13. De Man FS *et al.* Effects of exercise training in patients with idiopathic pulmonary arterial hypertension. *Eur. Respir. J.* 2009; 34, 669–675.
14. Rain S *et al.* Right Ventricular Diastolic Impairment in Patients with Pulmonary Arterial Hypertension. *Circulation.* 2013; 128:2016-25.
15. Gan TJ *et al.* Right ventricular diastolic dysfunction and the acute effects of sildenafil in pulmonary hypertension patients. *Chest.* 2007; 132, 11–17.
16. Fisher MR *et al.* Accuracy of Doppler echocardiography in the hemodynamic assessment of pulmonary hypertension. *Am. J. Respir. Crit. Care Med.* 2009; 179, 615–621.
17. Constantinescu T *et al.* New Echocardiographic Tehniques in Pulmonary Arterial Hypertension vs. Right Heart Catheterization - A Pilot Study. *Mædica.* 2013; 8, 116–123.
18. Okumura K *et al.* Right ventricular diastolic performance in children with pulmonary arterial hypertension associated with congenital heart disease: correlation of echocardiographic parameters with invasive reference standards by high-fidelity micromanometer catheter. *Circ. Cardiovasc. Imaging.* 2014; 7, 491–501.
19. Pasipoularides A *et al.* Evaluation of right and left ventricular diastolic filling. *J Cardiovasc. Transl. Res.* 2013; 6, 623–639.
20. Cortina C *et al.* Noninvasive assessment of the right ventricular filling pressure gradient. *Circulation.* 2007; 116, 1015–1023.
21. Huez S *et al.* Tissue Doppler imaging evaluation of cardiac adaptation to severe pulmonary hypertension. *Am. J. Cardiol.* 2007; 100, 1473–1478.
22. Arcasoy SM *et al.* Echocardiographic assessment of pulmonary hypertension in patients with advanced lung disease. *Am. J. Respir. Crit. Care Med.* 2003; 167, 735–740.
23. De Man FS *et al.* Bisoprolol delays progression towards right heart failure in experimental pulmonary hypertension. *Circ. Heart Fail.* 2012; 5, 97–105.
24. Hessel MHM *et al.* Characterization of right ventricular function after monocrotaline-induced pulmonary hypertension in the intact rat. *Am. J. Physiol. Heart Circ. Physiol.* 2006; 291, H2424–2430.
25. Klotz S *et al.* A computational method of prediction of the end-diastolic pressure-volume relationship by single beat. *Nat. Protoc.* 2007; 2, 2152–2158.

26. Brimioulle S *et al.* Single-beat estimation of right ventricular end-systolic pressure-volume relationship. *Am. J. Physiol. Heart Circ. Physiol.* 2003; 284, H1625–1630.
27. Paulus WJ *et al.* How to diagnose diastolic heart failure: a consensus statement on the diagnosis of heart failure with normal left ventricular ejection fraction by the Heart Failure and Echocardiography Associations of the European Society of Cardiology. *Eur. Heart J.* 2007; 28, 2539–2550.
28. Chung CS *et al.* Contribution of titin and extracellular matrix to passive pressure and measurement of sarcomere length in the mouse left ventricle. *J. Mol. Cell. Cardiol.* 2011; 50, 731–739.
29. Granzier HL *et al.* Passive tension in cardiac muscle: contribution of collagen, titin, microtubules, and intermediate filaments. *Biophys. J.* 1995; 68, 1027–1044.
30. LeWinter MM *et al.* Cardiac titin: a multifunctional giant. *Circulation.* 2010; 121, 2137–2145.
31. Kooij V *et al.* Effect of troponin I Ser23/24 phosphorylation on Ca2+-sensitivity in human myocardium depends on the phosphorylation background. *J. Mol. Cell. Cardiol.* 2010; 48, 954–963.
32. Wijnker PJM *et al.* Protein phosphatase 2A affects myofilament contractility in non-failing but not in failing human myocardium. *J. Muscle Res. Cell Motil.* 2011; 32, 221–233.
33. Bers DM Cardiac excitation-contraction coupling. *Nature.* 2002; 415, 198–205.
34. Benoist D *et al.* Cardiac arrhythmia mechanisms in rats with heart failure induced by pulmonary hypertension. *Am. J. Physiol. Heart Circ. Physiol.* 2012; 302, H2381–2395.
35. Sande JB *et al.* Reduced level of serine(16) phosphorylated phospholamban in the failing rat myocardium: a major contributor to reduced SERCA2 activity. *Cardiovasc. Res.* 2002; 53, 382–391.
36. Fukuda N *et al.* Physiological functions of the giant elastic protein titin in mammalian striated muscle. *J. Physiol. Sci. JPS.* 2008; 58, 151–159.
37. Linke WA Sense and stretchability: the role of titin and titin-associated proteins in myocardial stress-sensing and mechanical dysfunction. *Cardiovasc. Res.* 2008; 77, 637–648.
38. Hidalgo CG *et al.* PKC phosphorylation of titin's PEVK element: a novel and conserved pathway for modulating myocardial stiffness. *Circ. Res.* 2009; 105, 631–638.
39. Hidalgo CG *et al.* The multifunctional Ca(2+)/calmodulin-dependent protein kinase II delta (CaMKIIδ) phosphorylates cardiac titin's spring elements. *J. Mol. Cell. Cardiol.* 2013; 54, 90–97.
40. Hudson B *et al.* Hyperphosphorylation of mouse cardiac titin contributes to transverse aortic constriction-induced diastolic dysfunction. *Circ. Res.* 2011; 109, 858–866.
41. Van der Velden J *et al.* Effect of protein kinase A on calcium sensitivity of force and its sarcomere length dependence in human cardiomyocytes. *Cardiovasc. Res.* 2000; 46, 487–495.
42. Muller A *et al.* Modulation of SERCA2 expression by thyroid hormone and norepinephrine in cardiocytes: role of contractility. *Am. J. Physiol.* 1997; 272, H1876–1885.
43. Quaile MP *et al.* Reduced sarcoplasmic reticulum Ca(2+) load mediates impaired contractile reserve in right ventricular pressure overload. *J. Mol. Cell. Cardiol.* 2007; 43, 552–563.
44. Wang Z *et al.* A. Na+-Ca2+ exchanger remodeling in pressure overload cardiac hypertrophy. *J. Biol. Chem.* 2001; 276, 17706–17711.
45. Lymperopoulos A *et al.* Adrenergic Nervous System in Heart Failure Pathophysiology and Therapy. *Circ. Res.* 2013; 113, 739–753.
46. Francis GS *et al.* The neurohumoral axis in congestive heart failure. *Ann. Intern. Med.* 1984; 101, 370–377.
47. Florea VG *et al.* The autonomic nervous system and heart failure. *Circ. Res.* 2014; 114, 1815–1826.
48. Iwai-Kanai E *et al.* Intracellular signaling pathways for norepinephrine- and endothelin-1-mediated regulation of myocardial cell apoptosis. *Mol. Cell. Biochem.* 2004; 259, 163–168.
49. Al Darazi F *et al.* Small dedifferentiated cardiomyocytes bordering on microdomains of fibrosis: evidence for reverse remodeling with assisted recovery. *J. Cardiovasc. Pharmacol.* 2014; 64:237-46.
50. Bristow MR *et al.* Beta 1- and beta 2-adrenergic-receptor subpopulations in nonfailing and failing human ventricular myocardium: coupling of both receptor subtypes to muscle contraction and selective beta 1-receptor down-regulation in heart failure. *Circ. Res.* 1986; 59, 297–309.
51. Rain S *et al.* Protein changes contributing to right ventricular cardiomyocyte diastolic dysfunction in pulmonary arterial hypertension. *J. Am. Heart Assoc.* 2014; 3, e000716.
52. De Man FS *et al.* Dysregulated renin-angiotensin-aldosterone system contributes to pulmonary arterial hypertension. *Am. J. Respir. Crit. Care Med.* 2012; 186, 780–789.
53. Rain S *et al.* Pressure-overload-induced right heart failure. *Pflüg. Arch. Eur. J. Physiol.* 2014; 466, 1055–1063.

Chapter 2

Right ventricular diastolic impairment in patients with pulmonary arterial hypertension

Rain S, Handoko ML, Trip P, Gan CT, Westerhof N, Stienen GJ, Paulus WJ, Ottenheijm CA, Marcus JT, Dorfmüller P, Guignabert C, Humbert M, Macdonald P, Dos Remedios C, Postmus PE, Saripalli C, Hidalgo CG, Granzier HL, Vonk-Noordegraaf A, van der Velden J, de Man FS.

Circulation. 2013
doi: **10.1161/CIRCULATIONAHA.113.001873**

ABSTRACT

Background – The role of right ventricular (RV) diastolic stiffness in pulmonary arterial hypertension (PAH) is not well-established. Therefore, we investigated the presence and possible underlying mechanisms of RV diastolic stiffness in PAH-patients.

Methods and Results – Single-beat RV pressure-volume analyses were performed in 21 PAH-patients and 7 controls to study RV diastolic stiffness. Data presented as mean ± SEM. RV diastolic stiffness (β) was significantly increased in PAH-patients (PAH: 0.050±0.005 vs. control: 0.029±0.003; $p<0.05$) and closely associated to disease severity. Subsequently, we searched for possible underlying mechanisms, using RV tissue of PAH-patients undergoing heart-lung transplantation and non-failing donors. Histological analyses revealed increased cardiomyocyte cross-sectional areas (PAH: 453±31 vs. control: 218±21 μm^2; $p<0.001$), indicating RV hypertrophy. In addition, the amount of RV fibrosis was enhanced in PAH tissue (PAH: 9.6±0.7 vs. control: 7.2±0.6%; $p<0.01$). To investigate the contribution of stiffening of the sarcomere (the contractile apparatus of RV cardiomyocytes) to RV diastolic stiffness, we isolated and membrane-permeabilized single RV cardiomyocytes. Passive tension at different sarcomere lengths was significantly higher in PAH compared to controls (+200%; $p_{interaction}<0.001$), indicating stiffening of RV sarcomeres. An important regulator of sarcomeric stiffening is the sarcomeric protein titin. Therefore, we investigated titin isoform composition and phosphorylation. No alterations were observed in titin isoform composition (N2BA/N2B ratio PAH: 0.78±0.07 vs. control 0.91±0.08), but titin phosphorylation in RV-tissue of PAH-patients was significantly reduced (PAH: 0.16±0.01 vs. control 0.20±0.01 a.u.; $p<0.05$).

Conclusions – RV diastolic stiffness is significantly increased in PAH-patients, with important contributions from increased collagen and intrinsic stiffening of the RV cardiomyocyte sarcomeres.

INTRODUCTION

Idiopathic pulmonary arterial hypertension (PAH) is a rare but fatal disease with a survival rate of 58% in 3 years.[1] Present therapy is unable to normalize pulmonary arterial pressures and PAH-patients ultimately develop right heart failure.[2] Previous studies have demonstrated that PAH-patients have reduced systolic function as measured by RV ejection fraction. However, the knowledge on the role of RV diastolic stiffness in PAH is limited. Measuring RV diastolic stiffness has been hindered until now, because non-invasive techniques (echocardiography, magnetic resonance imaging) provide only information on relaxation velocities and not on diastolic stiffness per se.[3] In addition, these measures are highly sensitive to the confounding effects of increased pre- and afterload, and are therefore not reliable in the setting of PAH.[4] On the other hand, the gold standard of measuring load-independent diastolic stiffness by pressure-volume (PV) analysis is not without risk in PAH-patients, since it requires temporal preload reduction.[3] In left heart failure this was circumvented by the development of single-beat analyses of diastolic PV relationship.[5,6] However, it is unclear whether this analysis could also be used for the right ventricle in PAH. There are several possible contributing factors explaining RV diastolic stiffness in PAH. Hypertrophy and fibrosis are known to increase ventricular stiffness.[7] But RV diastolic stiffness could also be caused by changes in the contractile apparatus of RV cardiomyocytes: the sarcomeres. Sarcomeric stiffness is tightly regulated by the giant sarcomeric protein titin.[8] Titin consists of two isoforms: the stiff N2B isoform and the compliant N2BA isoform. Besides changes in isoform composition, titin compliance is regulated by phosphorylation. Whether these factors are altered in human PAH pathophysiology is unknown. Therefore, the aim of this study is to determine the presence of RV diastolic stiffness in PAH-patients and explore the contribution of collagen formation, sarcomeric stiffening and post- translational modifications of titin in RV tissue of PAH-patients.

METHODS

Part 1 – Experimental PAH Model – Single-beat method development

The experimental support for the single-beat method was performed in a rat model of PAH. All animal experiments were approved by the Institutional Animal Care and Use Committee of the VU University Amsterdam, The Netherlands. The study was performed in 15 Male Wistar rats. Pulmonary Arterial Hypertension (PAH) was induced by a single dose monocrotaline (60mg/Kg) subcutaneously injected (n= 9). Rats used as controls received a saline injection (n=6). The study was ended 31 days after monocrotaline or saline injection or after development of manifest right heart failure.[9]

Echocardiography Transthoracic Doppler Ultrasound (ProSound SSD-4000 system equipped with 13MHz linear transducer (UST-5542), Aloka, Tokyo, Japan) was performed in all spontaneously breathing rats under general anesthesia at the end of the study (isoflurane 2.0% in 1:1 02/air mix, Pharmachemie, Haarlem, The Netherlands). Right ventricular function was measured by the following parameters: Doppler derived stroke volume, cardiac output and tricuspid annular plane systolic

excursion (TAPSE). Right ventricular morphology was described by the following parameters: RV end diastolic diameter and RV wall thickness.[10]

Invasive RV pressure-volume analysis

After transthoracic echocardiography, cardiac function was assessed invasively by performing right heart catheterization with dual pressure – volume catheters. Rats underwent general anesthesia by Isoflurane inhalation (induction: 4.0% in 1:1 O2/iar mix; maintenance: 2.0% in 1:1 O2/air mix), were intubated (16G Teflon tube) and mechanically ventilated with a frequency of 75/min, at a pressure of 9/0 cmH20 and 1:1 inspiratory/expiratory ratio (Micro-Ventilator, UNO, Zevenaar, The Netherlands). During the procedure body temperature was maintained at normal values by placing the rats on warming pads. The thorax was then open and the inferior vena cava was encircled by performing a lose ligature around its trunk. The apex of the heart was then pierced with a needle (23G), a cotton swap was used to stop the hemorrhage and the combined pressure-volume catheter (SPR-869, Millar Instruments, Houston, TX) was inserted into the right ventricle.[11]

Figure 1 – Vena Cava Occlusion

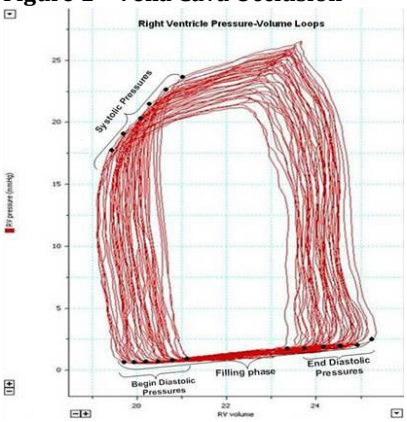

During VCO the preload to the RV is gradually reduced, which results in a decrease in systolic and diastolic pressures and a shift of the pressure-volume loops downwards and leftwards.

Pressure-volume loops were recorded at rest and after preload reduction secondary to vena cava gradual occlusion (VCO). Analysis was made off line using custom-made algorithms (programmed in MATLAB 2007b, The MathWorks, Natick MA) (Fig. 1).
Doppler ultrasound derived stroke volume was used to convert catheter volume units in milliliters. One catheterization unit was calculated to its corresponding volume (ml) by dividing the ultrasound obtained stroke volume (ml) by the catheterization stroke volume (units). Catheterization stroke volume was previously obtained from subtracting the end systolic volume (units) from the end diastolic volume (units). Due to procedure limitations to record absolute RV volumes (End Systolic Volume and End Diastolic Volume) but only RV changes, all end diastolic volumes were normalized at 1.5ml and end systolic volumes were calculated by subtracting the stroke volume (ml) from the reference point (1.5ml).

To quantify RV diastolic stiffness, multiple pressure-volume loops were recorded with a dual pressure-volume catheter placed in the right ventricle, both at steady state and during vena cava occlusion. The diastolic pressure-volume relation was then constructed using an exponential fit: ***Equation 1: $P=\alpha (e^{V\beta}-1)$*** through the decreasing pressure-volume points (after vena cava occlusion) and the diastolic stiffness factor $\beta_{multiple}$ was calculated.

The same equation was used to calculate RV diastolic stiffness β_{single} from a single beat pressure-volume loop (recorded before vena cava occlusion was started, at steady-state). For this exponential fit only 3 points were used:
1) $0_{pressure}$,0_{volume} point
2) begin diastolic point
3) end diastolic point

The classical pressure-volume relation implies the construction of an exponential pressure-volume curve through decreasing pressure-volume points (Fig. 2). Furthermore, the pressure-volume relation is considered to intersect the volume axes at pressure=0mmHg and a certain intercept volume (V_d). To calculate β_{single}, V_d was set to 0. However physiologically inaccurate, we considered the 0pressure-0volume point as a good substitute for the intercept since:
1. 0_{volume} is always lower or equal to V_d.
2. prolonging the diastolic exponential pressure-volume curve to volumes lower than the Vd (undetermined value) does not modify the exponential term β (further used to quantify RV diastolic stiffness).

Figure 2 – Multiple loops method and single beat method

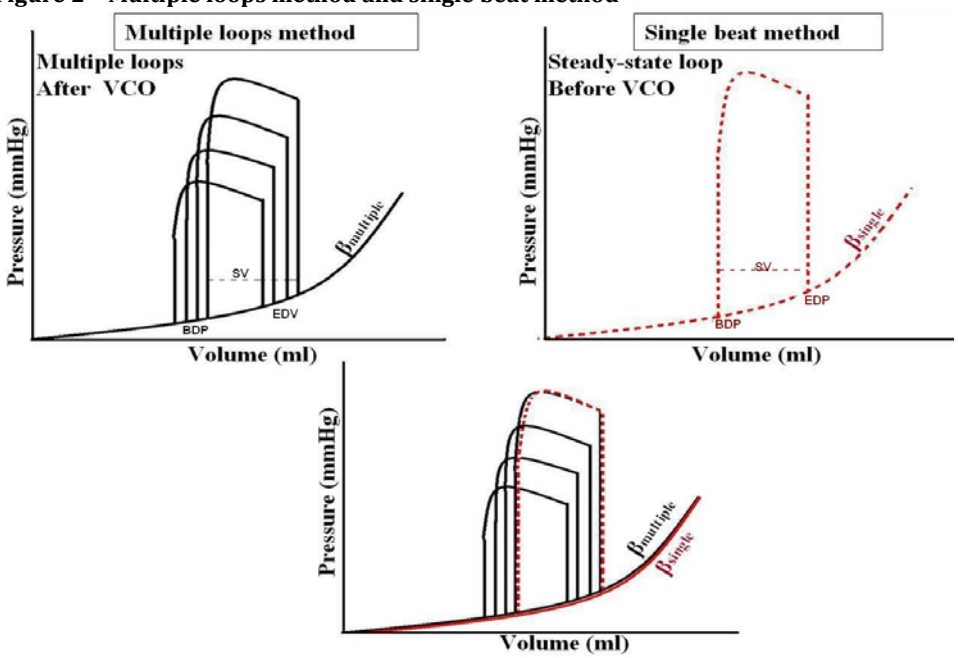

Begin and end diastolic pressures were recorded from RV catheterization, while stroke volume was derived from Doppler ultrasound.

Part 2 – Patient study

Assessment of RV diastolic stiffness

Hemodynamic data was obtained from digitally stored routine clinical measurements. Patients eligible for this study were referred to the VU University Medical Center for evaluation of pulmonary hypertension between September 2001 and November 2011 (Table 1). Standard clinical care included right heart catheterization (balloon-tipped flow-direct 7F Swan-Ganz catheter - 131HF7, Baxter Healthcare Corporation, Irvine, CA) and cardiac MRI (1.5-T whole-body system, Siemens Sonata, Siemens Medical Solutions, Erlangen, Germany). During right heart catheterization, radial or femoral blood samples were collected and standard laboratory tests including N-terminal pro-brain natriuretic peptide level (NT-proBNP) were performed.[12] New York Heart Association (NYHA) class and six-minute-walk-distance (6MWD) were registered during the same clinical evaluation. All patients were evaluated in stable hemodynamic condition, lying supinely and breathing at normal frequencies.[2] Patients were selected based on the following criteria: good-quality recordings of right heart catheterization pressure curves with cardiac MRI performed within the same hospital admission and under the same hemodynamic condition (n=28). PAH was diagnosed according to the PAH diagnostic guidelines (n=21).[13] Controls were selected from referred patients suspected with PAH but in whom the condition was ruled out after recording normal pulmonary pressures during right heart catheterization (n=7).

Right heart catheterization

The following invasive variables were recorded: right atrial pressure (RAP), RV pressure, mean pulmonary artery pressure (mPAP) and pulmonary capillary wedge pressure (PCWP). Cardiac output (CO) was determined by Fick method and pulmonary vascular resistance (PVR) was calculated using PVR=(mPAP-PCWP)/CO.[14] Diastolic filling pressures were measured at minimum pressure point (recorded after tricuspid valve opening) and noted as begin-diastolic pressure (BDP). End diastolic pressure (EDP) was recorded at maximal diastolic filling pressure point before the onset of isovolumic contraction (Fig. 3).

Cardiac MRI

RV volumes were calculated using Mass software (MEDIS, Medical Imaging Systems, Leiden, the Netherlands) from multiple short axial-slice MRI analysis.[2] ESV were considered to correspond to BDP and is further referred as BDV, while EDV corresponded to EDP (Fig. 3). Stroke volume was calculated from MRI-derived pulmonary artery flow and used to accurately determine RV BDV. RV volumetric filling curves were obtained from the stack of short-axis cine images for the quantification of RV early (E) and atrium (A) induced peak filling rate (E/A ratio) as previously described.[14]

Table 1 – Demographic characteristics

RV sample	Diagnosis	NYHA class	Gender	Age
1	Idiopathic PAH	IV	Female	38
2	Idiopathic PAH	IV	Female	44
3	Idiopathic PAH	IV	Female	51
4	PAH-Eisenmenger	IV	Female	46
5	PAH-Eisenmenger	IV	Female	14
6	PAH-Eisenmenger	IV	Female	20
7	PAH-Eisenmenger	IV	Female	31
8	PAH-Eisenmenger	IV	Female	21
9	PAH-Eisenmenger	IV	Male	46
10	PAH-Eisenmenger	IV	Female	50
11	PAH-Eisenmenger	IV	Female	41
12	Donor		Female	41
13	Donor		Female	23
14	Donor		Female	19
15	Donor		Female	53
16	Donor		Male	65
17	Donor		Female	49
18	Donor		Male	45
19	Donor		Female	38
20	Donor		Male	37

Single-beat pressure-volume analysis

PV relations were constructed by fitting a non linear exponential curve through the diastolic PV points using the following formula: $P=\alpha\ (e^{V\beta}-1)$[5,6] where α: curve-fitting constant; β: diastolic stiffness constant. The slope of the curve was characterized by the exponential term β and the curve constant α, which were further used to quantify RV diastolic stiffness. The first two points used to construct the PV relation were the BDP-BDV point and the EDP-EDV point. The third PV point used to construct the diastolic PV relation was set at $0_{pressure}$,0_{volume}, since prolonging the PV curves to volumes lower than the intercept volume does not modify the exponential term β and the curve constant α (Fig. 4). Due to large variation in EDV in control patients compared to PAH-patients, the EDV was normalized to the maximal EDV recorded among the patients. Consecutively, the BDV was calculated by subtracting the corresponding stroke volume from the normalized EDV. To avoid measurement errors due to the positioning of the RV catheter, BDP was normalized at 1mmHg, while the EDP was calculated with the following formula: $EDP_{normalized}=1+(EDP_{initial}-BDP_{initial})$

Figure 3 – Single-beat diastolic pressure-volume analysis

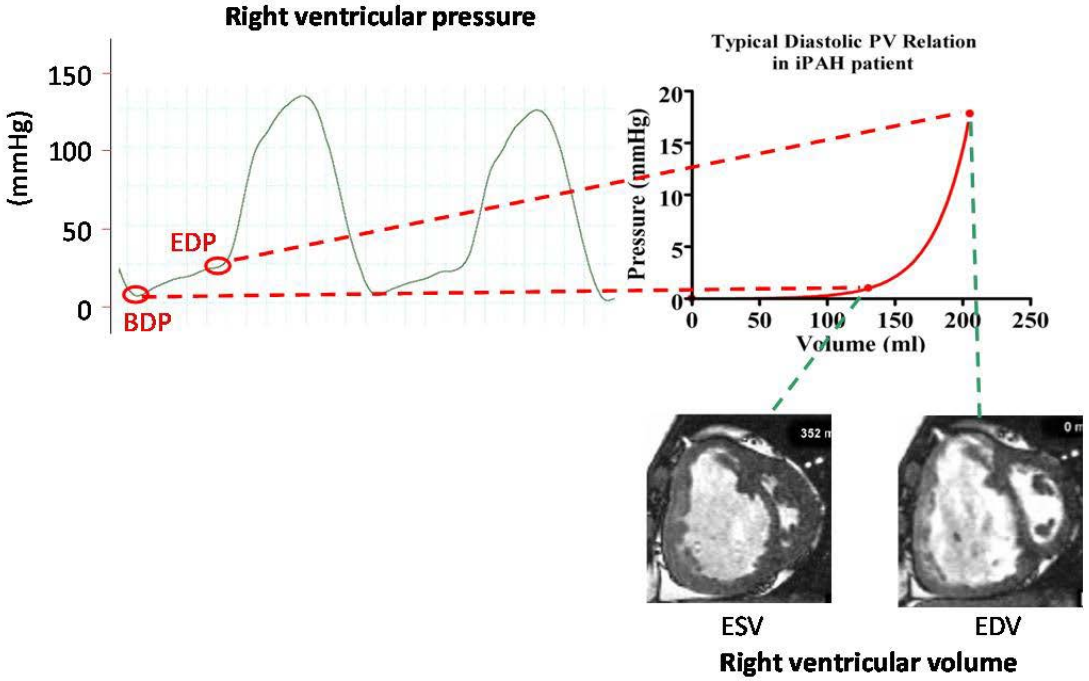

End diastolic pressures (EDP) and begin diastolic pressures (BDP) were determined from right heart catheterization, while end diastolic volume (EDV) and end systolic volume (ESV) were determined from right heart MRI.

To account for covariance in α and β, derived α and β of each individual subject were used to calculate the V at a common P of 20mmHg (V_{20ml}).[15] Experimental support for the use of single-beat instead of multiple-beat RV diastolic PV relation was obtained in rats with PAH-induced right heart failure undergoing right heart catheterization with a conductance catheter and echocardiography.

Assessment of RV end-systolic elastance

The slope of the end-systolic pressure volume relation (end-systolic elastance, Ees) was calculated as previously described: $\boldsymbol{Ees=(P_{iso}-mPAP)/SV}$ [16]

The isovolumic pressure (P_{iso}) was obtained by fitting an inverted cosine wave over the RV pressure curve using the isovolumic contraction period (from end-diastole to the point of maximal rate of pressure rise (dP/dt_{max}) and the isovolumic relaxation period (from minimal dP/dt to start diastole) by a semi-automatic Matlab R2008a program (The MathWorks, Natick, MA).[17]

RV histological analyses

Explanted RV tissue samples were collected from PAH-patients undergoing heart/lung transplantation (n=10). Control RV tissue was obtained from non-failing donors (n=9). Written informed consent was obtained and the study protocol was approved by the local ethics committees. All samples were immediately frozen and stored in liquid nitrogen. The degree of RV hypertrophy was analyzed on 5µm-thick tissue sections

stained with antibodies against the extracellular protein Laminin (1:200; L9393, Sigma-Aldrich). Minimally 40 cells per sample were used in order to calculate cross-sectional area. Cardiomyocytes with non-transversal cross-sections were not included in the analysis.[9,10,18,19] RV fibrosis was determined on 5µm-thick tissue sections stained with Picrosirius red and analyzed under double-polarized light.[9,10] Images were collected by the use of a Leica DMRB microscope (Wetzlar, Germany), a Sony XC-77CE camera (Towada, Japan) and a LG-3 frame grabber (Scion, Frederick MD). For each PAH and control sample, a minimum of 10 pictures obtained from different areas was analyzed. ImageJ for Windows 1.42 software (National Institutes of Health, Bethesda MD) was used for image analysis, taking the pixel to-aspect ratio into account. Collagen content was quantified as area percentage of the recorded images under a microscopy magnification of 20X.

RV cardiomyocyte force measurements

Tissue pieces were defrosted in relaxing solution and single cardiac cells were isolated mechanically as described before (7 control and 7 PAH samples).[20] A minimum of 3 cells per sample were measured and the average total, active and passive tension were calculated. Cardiomyocytes were incubated for 5 minutes in relaxing solution containing 1% Triton X- 100 to premeabilize membranes.[21] To remove Triton, the cardiomyocyte solution was washed six times with relaxing solution, after which a single cell was attached with silicone adhesive between a force transducer and a piezoelectric motor. Force measurements were performed at 1.8 and 2.2 µm sarcomere length in activating solutions with maximal and submaximal calcium concentrations ranging from 1 to 30 µmol/L. After maximal force development in activating solutions, the cell was shortened to 70% of its original length in order to determine total force development (F_{total}). A similar shortening was performed in the relaxing solution to record passive tension ($F_{passive}$). Active force (F_{active}) was calculated by subtracting $F_{passive}$ from F_{total}. Force values at submaximal [Ca^{2+}] were normalized to the maximal force value obtained at 30µmol/L [Ca^{2+}] to determine Ca^{2+}-sensitivity of the myofilaments expressed as EC_{50}, i.e. the [Ca^{2+}] at which 50% of maximal force was obtained. Steady-state $F_{passive}$ measurements were performed at increasing sarcomere lengths (1.8 – 2.6µm).

To determine tension, we corrected for differences in RV cross-sectional area between control and PAH. Individual force values were normalized for the cardiomyocyte width and depth recorded at 2.2µm sarcomere length. Contribution of actomyosin interaction to passive tension was determined by incubating skinned cardiomyocytes with actomyosin inhibitor 2,3-butanedione-monoxime (BDM; 25mM) at 15°C, for 10 minutes.[22] After 10 minutes active tension was measured in maximal activation solution to determine the efficiency of the compound. Subsequently, passive tension was recorded at increasing sarcomere lengths (1.8 – 2.4µm) and compared to passive tension recorded before BDM incubation.

Titin isoform composition and phosphorylation

Frozen RV tissue samples were weighed and pulverized in liquid nitrogen using a mortar and pestle. Tissue powder was solubilized in 8M urea buffer with DTT and 50% glycerol solution with protease inhibitors (4X Leupeptin, E-64 and PMSF). Equal dilutions were calculated based on Myosin Heavy Chain (MHC) content; protein

homogenate samples were loaded on custom-made 1% agarose gels. Solubilized human soleus muscle was used as reference. Gels were washed overnight in presoak solution, stained with Coomassie Blue and destained. Protein composition was determined using 1D-Scan software program. Titin N2B, N2BA, degradation products and MHC were quantified and Titin N2B/N2BA ratio was determined.
To quantify titin phosphorylation, gels were stained for 2 hours with ProQ diamond (Molecular Probes). Thereafter, the gels were washed and subsequently stained with SYPRO Ruby (Molecular Probes).[23]

Statistical analyses
Statistical analyses were performed using Prism 5 for Windows (GraphPad Software Inc, San Diego, CA). Normal distribution was tested and logarithm transformation was performed if necessary. P-values lower than 0.05 were considered significant. Changes in patient characteristics and diastolic stiffness were tested for significance with unpaired student t-tests or non-parametric Mann-WithneyU test (RAP, NT-proBNP). The relation between diastolic stiffness and several variables for disease severity (SV, 6MWD, RAP and NT-proBNP levels) was tested with Pearson's correlation. To adjust for possible confounding by body surface area, age, treatment duration and pulmonary vascular resistance, multivariable regression analyses was performed. Histological data were analyzed using multilevel analysis to correct for non-independence of successive measurements per patient (MLwiN 2.02.03, Center for Multilevel Modeling, Bristol, UK).[24] Changes in cardiomyocyte maximal tension, Ca^{2+}-sensitivity and passive stiffness were tested for significance by repeated measures ANOVA followed by Bonferroni post-hoc test.

RESULTS

Part 1 – Experimental PAH Model - Single-beat method development

RV Diastolic stiffness obtained with the classical method using multiple pressure-volume loops ($\beta_{multiple}$) was compared to diastolic stiffness obtained from a single beat steady-state loop (β_{single}) (Fig. 5 A,B).[25,26] Since no significant difference was found between the methods (Fig. 5 C), we further used the single beat approach for the clinical setting, where vena cava occlusion and multiple pressure-volume loops recording are contraindicated.

Figure 4 – Diastolic exponential fitting through the $O_{pressure}$-0_{volume} point

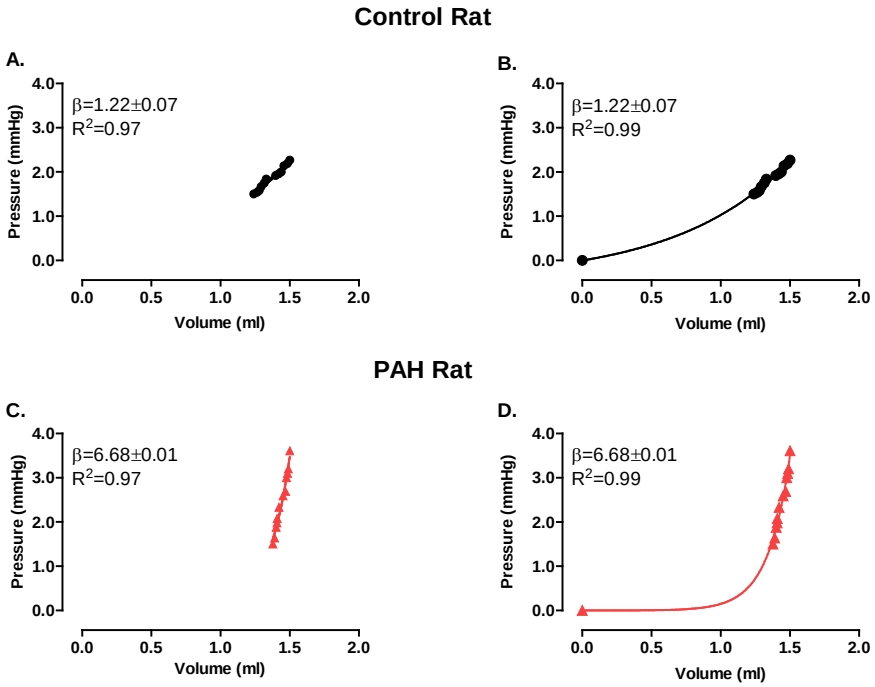

A&C. Diastolic stiffness β is obtained by fitting an exponential curve through multiple decreasing pressure-volume points. B&D. Diastolic stiffness β is obtained by fitting an exponential curve through multiple pressure-volume points and the pressure=0mmHg and volume=0ml point.

Figure 5 – Single beat vs multiple beat method correlation

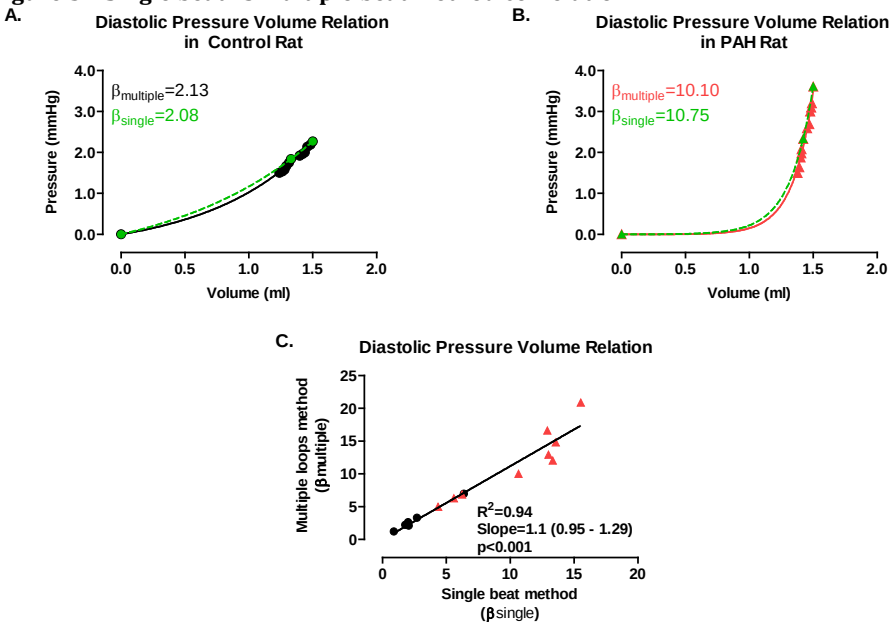

A&B. Example of control and PAH diastolic pressure-volume relations C. Method correlation between diastolic stiffness $\beta_{multiple}$ and β_{single} in control rats and PAH rats.

Part 2 – Patient study

Table 2 – Patient characteristics

	PAH (n=21)	Controls (n=7)	p-value
Age (years)	45 ± 12	54 ± 13	0.13
Gender (F/M)	20/1	7/0	1.00
BMI (kg/m^2)	24.6 ± 3.4	24.8 ± 5.3	0.90
NYHA (II/III/IV)	17/3/1		
6MWD (meters)	480 ± 96	480 ± 100	0.99
mPAP (mmHg)	47 ± 11	16 ± 4	<0.001
CO (L/min)	5.6 ± 1.2	6.3 ± 1.3	0.19
PVR (dynes.s/cm^5)	628 ± 249	117 ± 89	<0.001
RVEF (%)	36 ± 4	57 ± 5	<0.01
PCWP (mmHg)	8 ± 3	7 ± 3	0.83
RAP (mmHg)	7 ± 6	3 ± 2	<0.05
HR (beats/min)	86 ± 15	71 ± 7	<0.05
NT-proBNP (pg/L)	1603 ± 2332	125 ± 155	<0.05
Years on treatment	4.2 ± 2.7		
Monotherapy	5/21		
Multiple drug therapy	16/21		
Treatment strategies			
Sildenafil	16/21		
Bosentan	14/21		
Epoprostenol	5/21		
Terguride	3/21		
Treprostenil	4/21		
Sitaxentan	1/21		

Data presented as mean ± SD. PAH: pulmonary arterial hypertension. BMI: body mass index. NYHA: New York Heart Association. 6MWD: six-minute-walk-distance. mPAP: mean pulmonary arterial pressure; CO: cardiac output; PVR: pulmonary vascular resistance; RVEF: right ventricular ejection fraction; PCWP: pulmonary capillary wedge pressure; RAP: right atrial pressure; HR: heart rate; NT-proBNP; N-terminal pro-hormone brain natriuretic peptide.

Assessment of RV diastolic stiffness RV diastolic stiffness was calculated in PAH-patients (n=21) and controls (n=7). The clinical characteristics of the patients enrolled in this part of the study are described in Table 2.
PAH-patients were in majority women (20 of 21) with an average age of 45 years. Control patients matched in terms of age, sex and body mass index.

Compared to controls, PAH patients had significantly increased mPAP and PVR and normal PCWP. RAP and NT-proBNP levels were significantly higher in PAH-patients compared to controls. Furthermore, RV ejection fraction was lower in PAH-patients, as well as CO. PAH-patients were in a relatively good functional state (NYHA class II 17 of 21; comparable 6MWD to control), presumably related to intensive treatment (multiple therapy: 16 of 21).

We further used the single-beat method to calculate RV diastolic stiffness in PAH patients and controls (Fig. 6A). Compared to the control curve, the steeper PAH-curve indicates increased stiffness of the myocardium. On average, PAH-patients had an almost two-fold increase in RV diastolic stiffness parameter β (Fig. 6B), and a reduced curve constant α (Table 3). After controlling for the covariance of α and β, RV diastolic stiffness remained significant in PAH-patients in comparison to control (V_{20ml}; Table 3).

Table 3 – Exponential curve parameters

Parameters	PAH (n=21)	Controls (n=7)	p-value
Alpha (α)	0.003 ± 0.001	0.007 ± 0.002	0.048
Beta (β)	0.050 ± 0.005	0.029 ± 0.003	0.034
V_{20} (ml)	281 ± 7	308 ± 3	0.028

Data presented as mean ± SEM. Alpha, curve-fitting constant; beta, diastolic stiffness constant; V20, calculated volume at a common pressure of 20 mmHg based on individual derived α and β.

Non-invasive assessment of diastolic dysfunction by measures of MRI-obtained E/A ratio confirmed the observed increase in RV diastolic stiffness in PAH-patients (Fig. 6C). In addition, RV diastolic stiffness measurements β and V_{20ml} were both modestly correlated to E/A ratio (r E/A vs. β = -0.41; r E/A vs. V20 = 0.48; both $p<0.05$). Increased RV diastolic stiffness coincided with increased RV Ees in the same PAH patients (Fig. 6D).

To investigate whether RV diastolic stiffness is also present in other forms of pulmonary hypertension, we included an additional group of patients with chronic thrombo-embolic pulmonary hypertension (CTEPH; n=24). Similar to PAH, RV diastolic stiffness was significantly increased in CTEPH-patients in comparison to control (β CTEPH: 0.054±0.005, PAH: 0.050±0.005 vs. control: 0.029±0.003; $p<0.05$).

Figure 6 – Diastolic and systolic function

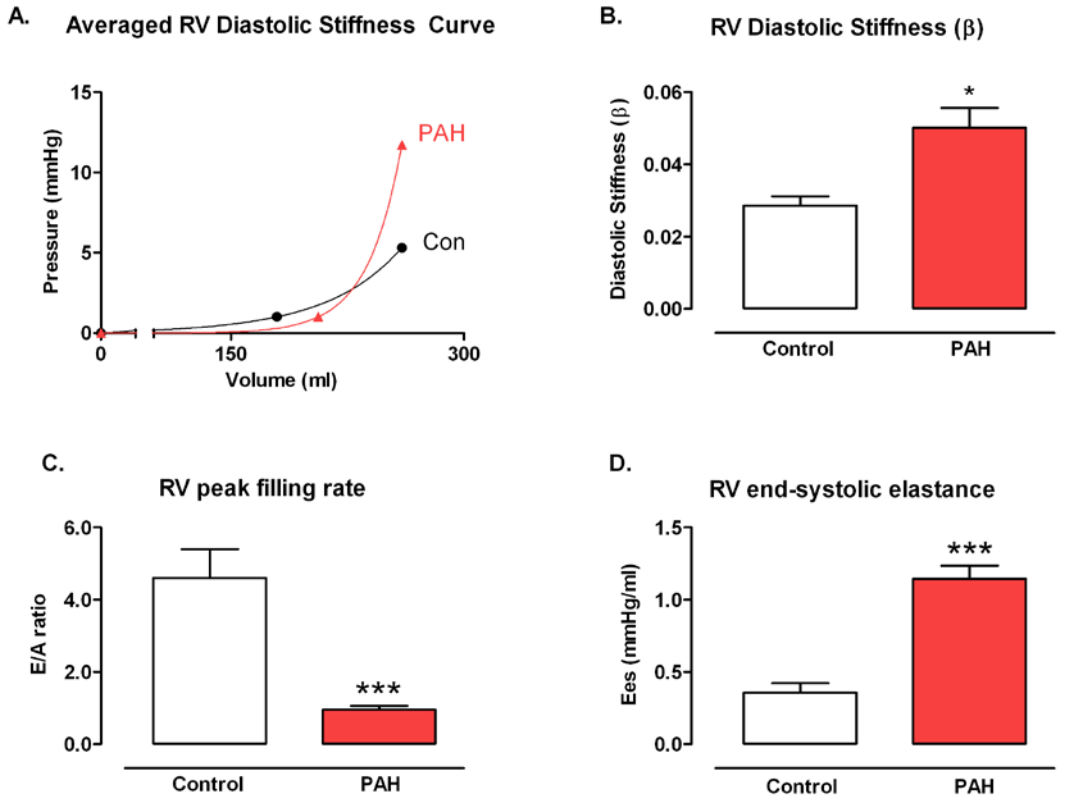

B. Average diastolic PV relations in control and PAH patients C. Diastolic stiffness coefficient (β) measured by the single-beat method D. Noninvasive assessment of RV early (E) and atrial (A) induced peak filling rate (E/A ratio) E. RV end-systolic elastance (Ees). Data presented as mean±SEM; n=21 PAH patients, n=7 control subjects. ***P<0.001.

RV diastolic stiffness, characterized by the curve constant β, significantly correlated with PAH disease severity. Stroke volume and 6MWD were significantly and inversely correlated with RV diastolic stiffness, suggesting that increased RV cardiomyocyte stiffness is associated with reduced cardiac function and exercise capacity (Fig. 7A,B). In addition, RV diastolic stiffness was closely correlated to RAP and NT-proBNP, both markers of increased RV stiffness and wall stress (Fig. 7C,D). These correlations remained significant after correction for the possible confounding effects of age, gender, body surface area, treatment duration and PVR.

Figure 7 – Diastolic stiffness and disease severity

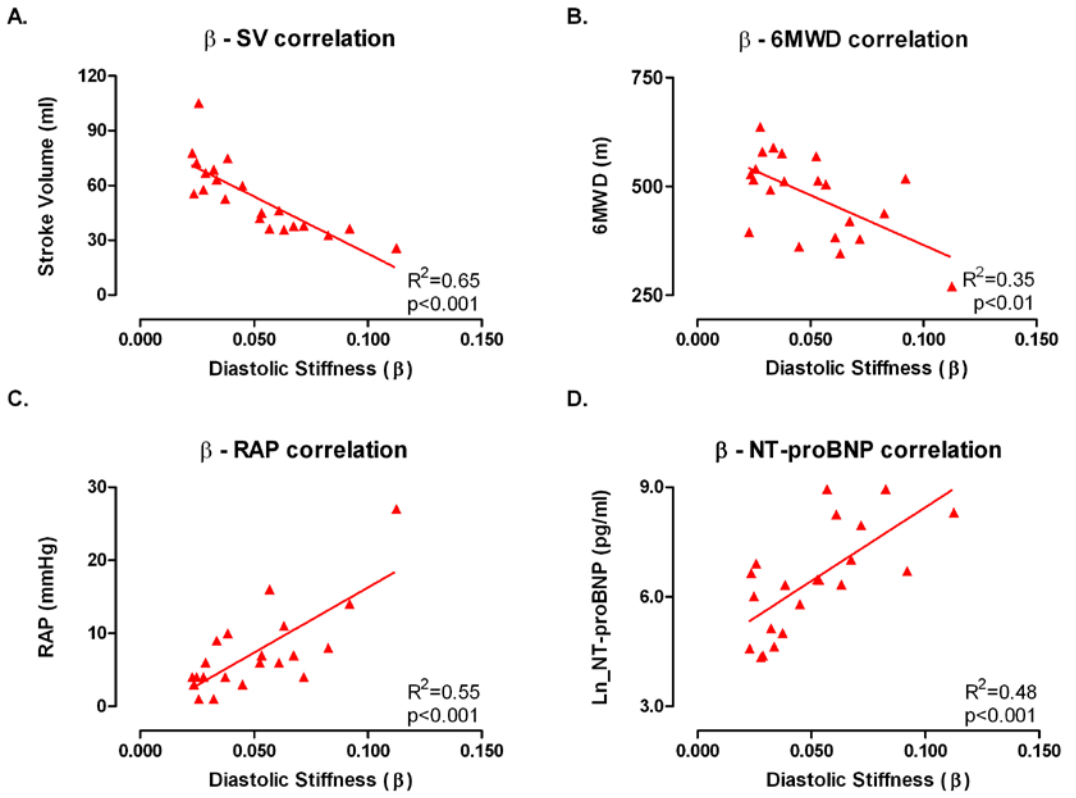

6MWD, six-minute-walk-distance; RAP, right atrial pressure; Ln_NT-proBNP, log-transformed N-terminal pro-hormone brain natriuretic peptide.

RV histology analyses

To perform histological analyses, RV tissue samples were obtained from PAH-patients (n=10) and controls (n=9). Patient characteristics are shown in Table 4. A two-fold increase of RV cardiomyocyte cross-sectional area in PAH was found compared to control cardiomyocytes (PAH: 531±34 µm2 vs. control: 256±24 µm2, p<0.001) (Fig. 8A). In addition, a significant increase in collagen content was found in PAH tissue sections compared with controls (PAH: 9.6±0.7% vs. control: 7.2±0.6% p<0.01) (Fig. 8B).

RV cardiomyocyte force measurements

To investigate the contribution of sarcomeric stiffening on RV diastolic stiffness in PAH, we isolated and membrane-permeabilized single RV cardiomyocytes of RV tissue from PAH patients (n=7) and controls (n=7).

Figure 8 – Hypertrophy and fibrosis

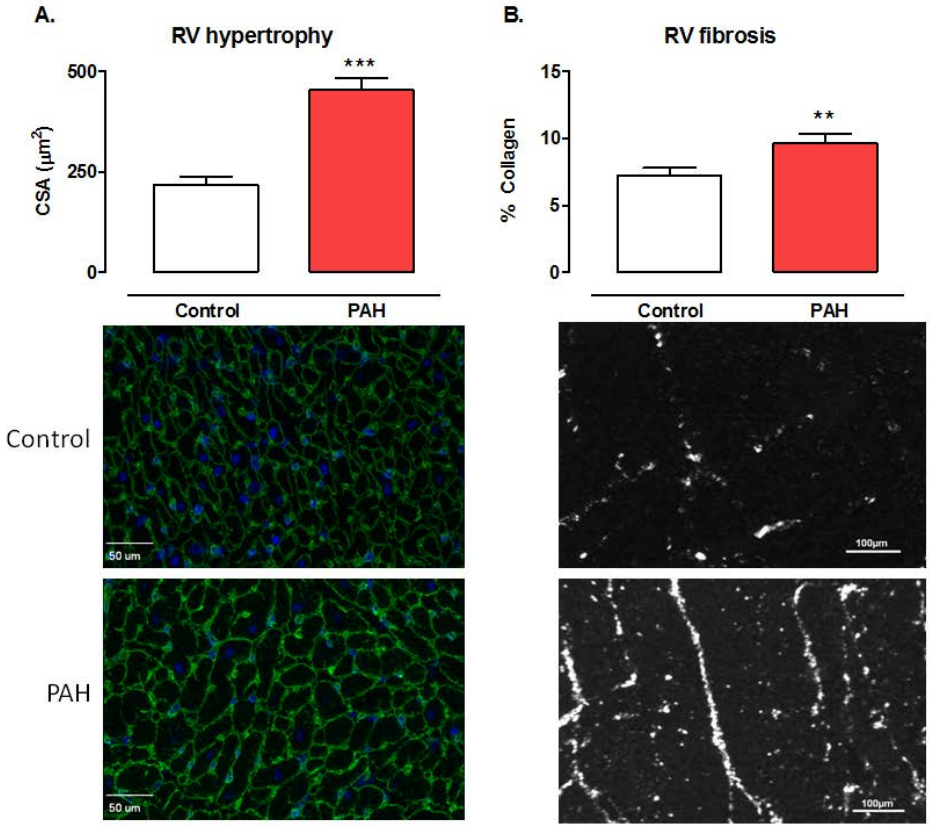

A. RV hypertrophy was significantly increased in PAH compared to controls. Laminin staining (green) and DAPI (nuclei, blue). B. A significant increase in RV fibrosis was found in PAH compared to controls. Picrosirius red staining, under double-polarized light. Data presented as mean ± SEM, n=10 PAH, n=9 controls. **: p<0.01, ***: p<0.001. CSA, cross-sectional area.

The advantage of the single RV cardiomyocyte approach is that RV sarcomeric function (the contractile apparatus of the RV cardiomyocytes) can be investigated in detail, without the confounding effects of hypertrophy, fibrosis or calcium handling. First, we investigated overall sarcomeric function in PAH and control RV cardiomyocytes. A similar length-dependent increase in F_{active} was found in both groups with increasing sarcomere lengths from 1.8 to 2.2µm. Interestingly maximal F_{active} was higher in PAH-patients compared to control cardiomyocytes at both 1.8 and 2.2µm, although the difference was only significant at 2.2 µm sarcomere length (Fig. 9A).

Normalized tension–calcium relations were constructed in order to determine myofilament Ca^{2+}-sensitivity. The length-dependent increase in myofilament Ca^{2+}-sensitivity (ΔEC_{50}, i.e. difference between EC_{50} values at 1.8 and 2.2µm) did not differ between PAH and controls, indicating preserved Frank-Starling mechanism in PAH-patients (Fig. 9B).

Figure 9 – Cardiomyocyte force measurements

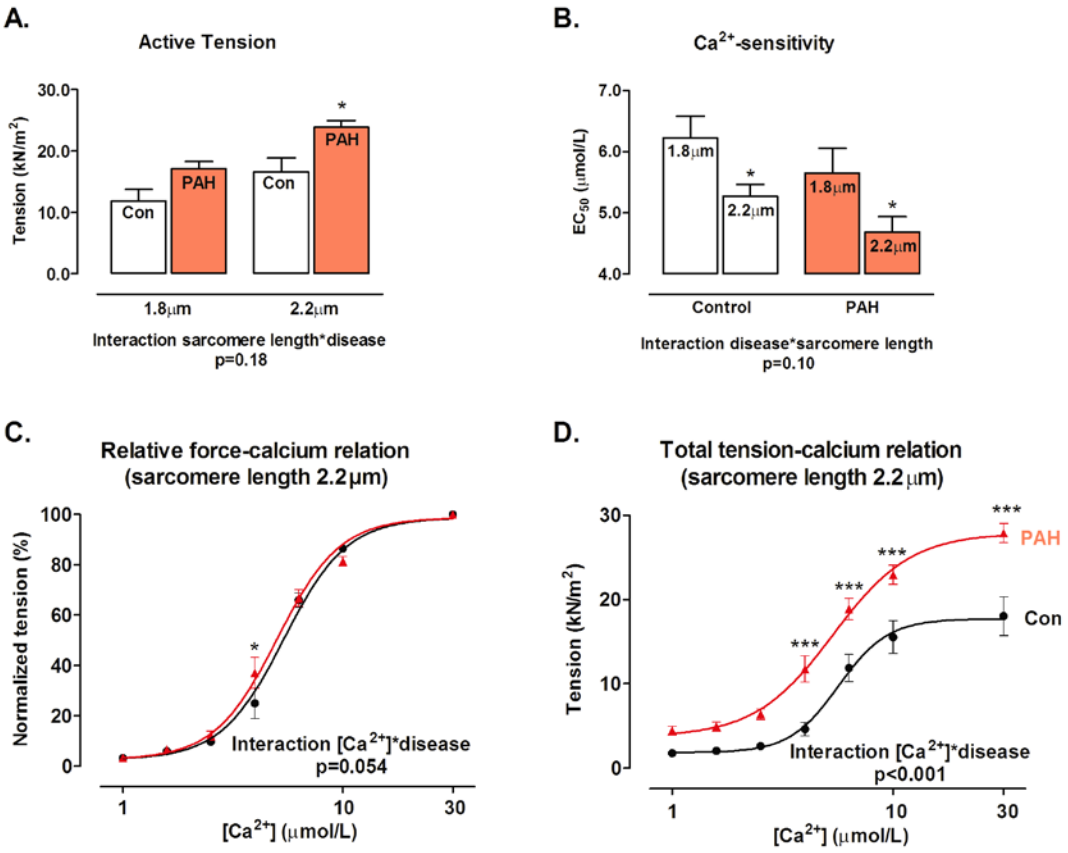

A. Active tension at maximal calcium concentration. B. C. Ca^{2+}mechanisms. D. Total tension Data presented as mean ± SEM, n=7 PAH, n=7 controls. *: p<0.05, ***: p<0.001, Bonferroni corrected.

No significant changes in Ca^{2+}-sensitivity were observed between PAH and controls, although the averaged tension-calcium curve was slightly shifted to the left in PAH (Fig. 9C). Overall, RV cardiomyocytes in PAH had a significantly higher total tension compared to control cardiomyocytes over a broad range of calcium concentrations (Fig. 9D). Second, we determined cardiomyocyte passive tension (measure of sarcomeric stiffness) in relaxing solution at increasing sarcomere lengths (1.8 to 2.6 μm).

A significantly higher cardiomyocyte passive tension at different sarcomere lengths was observed in PAH compared to control cardiomyocytes (+200%) (Fig. 10A).The relative increase in passive tension observed in PAH compared to control is shown in figure 10B.

To determine the role of the actin-myosin interaction component in generating passive tension, RV cardiomyocytes were incubated with BDM and passive tension was measured before and after incubation: no change in passive tension was observed (Fig. 11A-C), only a reduction in total tension (Fig. 11D). This indicates that the increase in

RV passive tension in PAH cardiomyocytes is not a consequence of residual actin-myosin interactions, but a consequence of increased RV sarcomeric stiffness derived from passive structures (titin).

Figure 10 - Cardiomyocyte diastolic stiffness

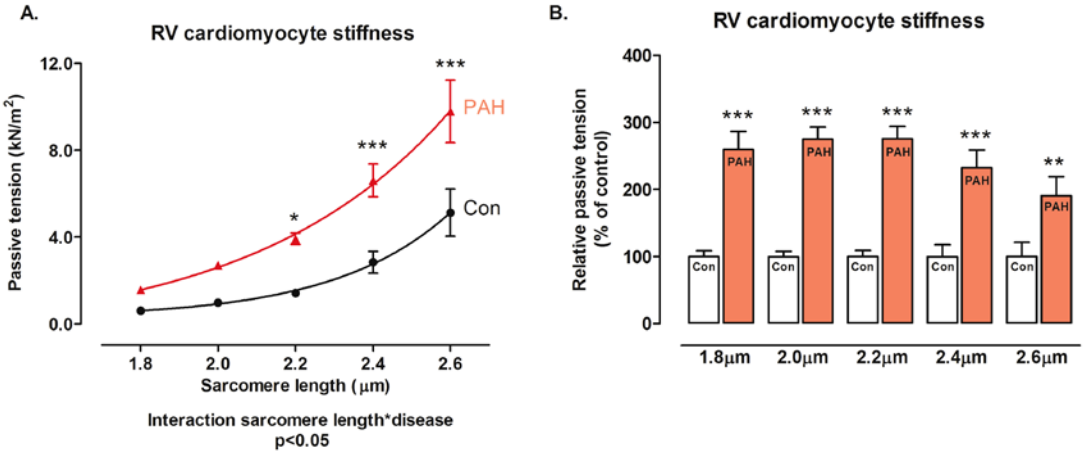

A. Passive tension at increasing sarcomere length. B. Passive tension in PAH compared to controls (set at 100%). Data presented as mean ± SEM, n=7 PAH, n=7 controls. *: p<0.05, **: p<0.01, ***: p<0.001, Bonferroni corrected.

Right ventricular cardiomyocyte resting sarcomere length

To investigate whether resting sarcomere length was different between PAH and control tissue samples, we randomly selected 10 isolated RV cardiomyocytes for each control and PAH tissue sample.[27] Resting sarcomere length was optically determined in at lease two distinct areas of the cell and the average cellular sarcomere length was calculated. No significant difference in resting sarcomere length was found between control and PAH cardiomyocytes (Fig. 12).

To investigate whether our findings of increased RV active force and cardiomyocyte stiffness differ between RV samples (iPAH vs Eisenmenger PAH) obtained from patients with idiopathic PAH or PAH secondary to congenital heart disease, we performed a subgroup analyses. The increase in RV active force and RV cardiomyocyte stiffness was comparable among the groups (Fig. 13).

Figure 11 - Role of the actin-myosin interaction in generating passive tension

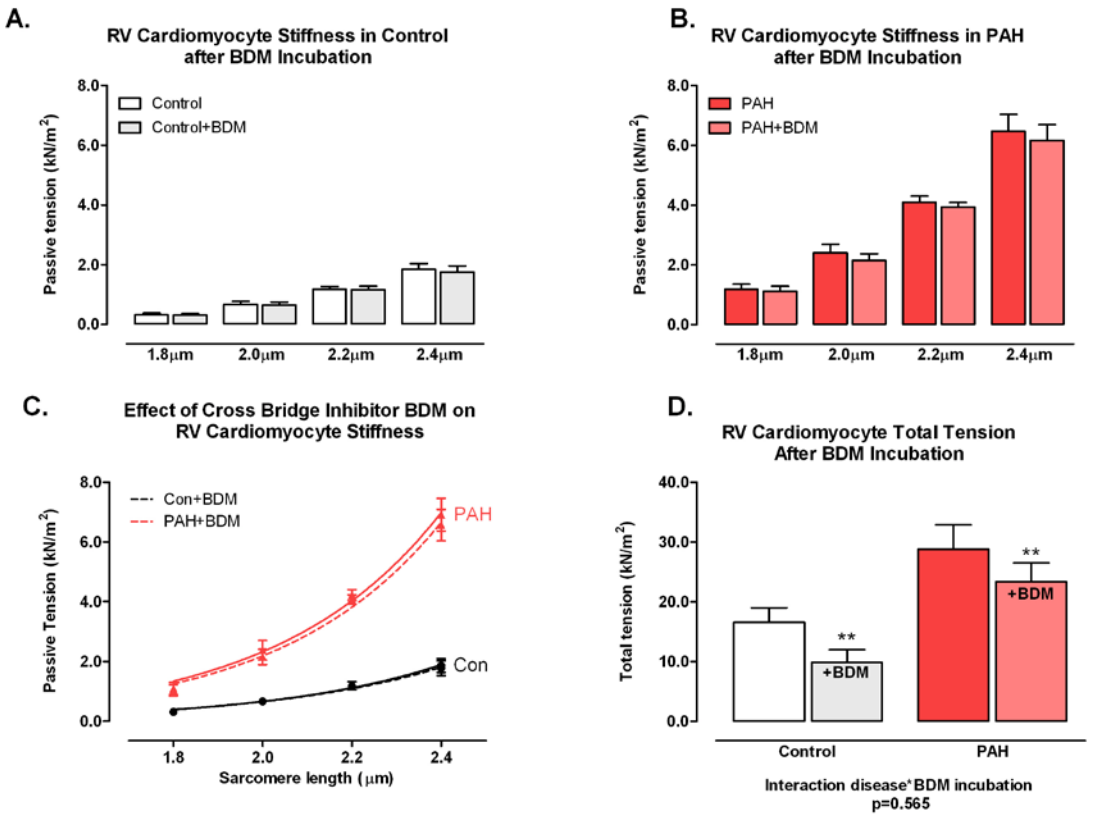

A. BDM effect in control cardiomyocytes. B. BDM effect in PAH cardiomyocytes. C. Passive tension increase in control and PAH cardiomyocyte. D. BDM effect on active tension generation

Figure 12 – Right ventricular resting sarcomere

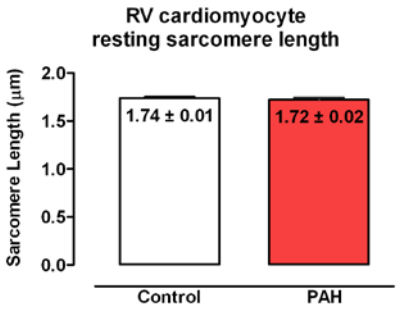

Resting sarcomere length determined in isolated skinned cardiomyocytes. p=0.56

Titin isoform expression and phosphorylation

To investigate the underlying molecular mechanism accounting for RV diastolic stiffness in PAH, we analyzed titin isoform composition and phosphorylation. Titin is a giant sarcomeric protein which regulates sarcomere compliance.[8] Titin consists of two isoforms, the stiff N2B isoform and the compliant N2BA isoform. In RV samples of PAH-patients and controls, we did not observe a difference in the ratio between N2B and

N2BA isoform expression (Fig. 14A). But, we did observe reduced titin phosphorylation in RV samples of PAH-patients (Fig. 14B), indicating that the observed RV sarcomeric stiffening was associated with reduced titin phosphorylation.

Figure 13 – Idiopathic PAH and PAH secondary to congenital heart defects.

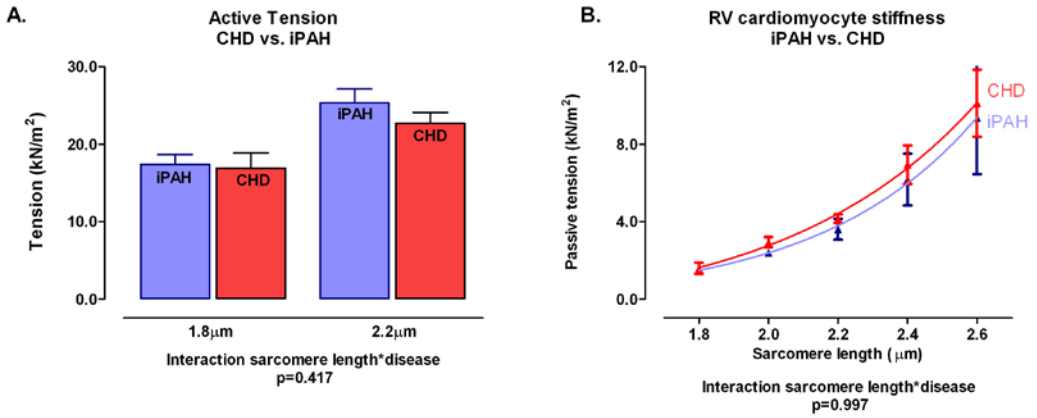

A. Active tension development in idiopathic PAH and PAH secondary to congenital heart defects. B. Diastolic stiffness in idiopathic PAH and PAH secondary to congenital heart defects. CHD: Congenital heart defect (Eisenmenger PAH) Data presented as mean ± SEM, n=3 iPAH, n=8 CHD.

Figure 14 - Titin isoform composition and phosphorylation

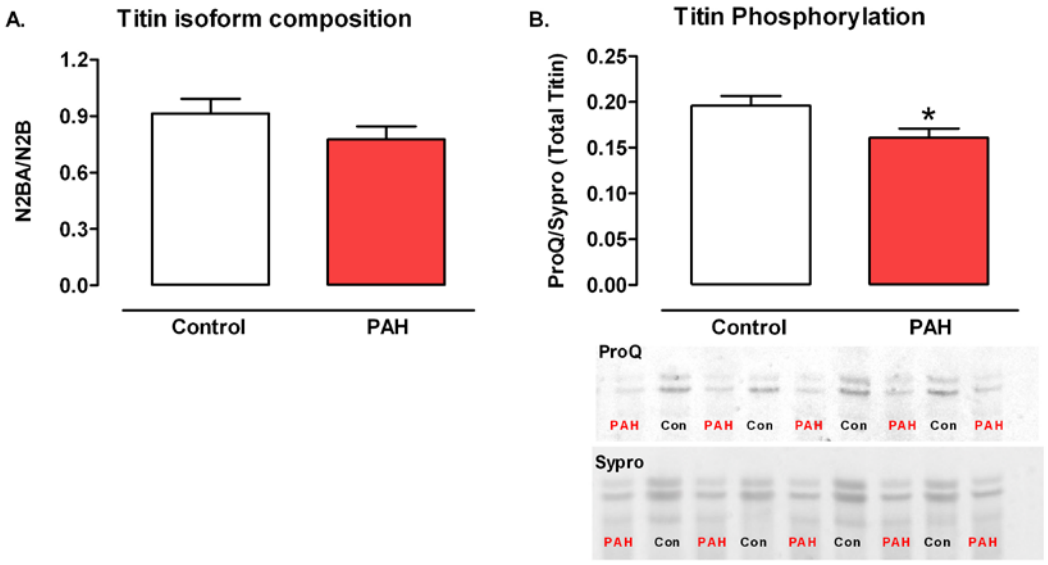

A. Titin isoform composition. B. Titin phosphorylation. Typical example of gel electrophoresis illustrating reduced titin phosphorylation in RV tissue of PAH-patients. Data presented as mean ± SEM, n=10 PAH, n=9 controls. *: $p<0.05$.

DISCUSSION

By combining in vivo measurements of RV function in PAH-patients with functional and histological analyses of RV tissue derived of PAH-patients, we were able to demonstrate that:
1. RV diastolic stiffness is increased in PAH-patients and closely associated with markers of disease severity.
2. RV hypertrophy and collagen deposition are increased in RV tissue of PAH-patients in comparison to controls.
3. RV cardiomyocyte passive tension at different sarcomere lengths was significantly higher in PAH-cardiomyocytes than in controls; RV cardiomyocytes exhibited preserved length-dependent activation and generated higher total tension in comparison to control RV cardiomyocytes over a broad range of calcium concentrations.
4. Titin phosphorylation was significantly reduced in RV tissue of PAH-patients in comparison to controls.

RV diastolic stiffness in PAH

Diastolic dysfunction is characterized by altered filling patterns, prolonged relaxation and intrinsic diastolic stiffness. Several epidemiological studies have demonstrated elevated RAP in PAH-patients.[28] In concordance, RV imaging studies revealed altered RV filling patterns characterized by increased atrial-induced filling ("atrial kick").[14] In addition, prolonged RV isovolumic relaxation time has been described in PAH-patients.[14] However, previously used measurements of diastolic function are all highly load-dependent, therefore it is still unclear whether PAH-patients suffer from true RV diastolic impairment or that the observed changes in filling and relaxation are merely a reflection of increased RV afterload.[4,29]
Therefore, we investigated the presence of RV diastolic impairment in PAH-patients both in vivo by single-beat PV analyses, as well as by measuring RV diastolic stiffness directly in RV cardiomyocytes. Diastolic stiffness is ideally quantified from the diastolic PV relationship constructed from multiple PV loops at different loading conditions. Due to cardio pulmonary compromise, this procedure is highly undesirable and considered too invasive in PAH. Therefore, we used the single-beat approach, a technique that has been used successfully in left heart failure studies.[5,6] In our experimental PAH-model, we observed an excellent correlation between RV diastolic stiffness derived by single- and multiple-beat approach, and therefore considered the single-beat approach as an appropriate, less invasive alternative for our patients. In addition, the finding of altered early and atrial induced RV peak filling rate further confirmed increased RV diastolic stiffness in PAH.

RV hypercontractility

Interestingly, RV diastolic stiffness in PAH coincided with increased RV contractility (Ees) and force generating capacity of RV cardiomyocytes (active force). This finding is somewhat unexpected, since it is well known that PAH is associated with severe RV systolic dysfunction. It is also in contrast to earlier observations of diastolic left heart failure (or heart failure with preserved ejection fraction), where increased passive stiffness was accompanied by reduced active tension.[20] In a previous study in PAH-rats,

we did observe an increase in both diastolic stiffness and RV contractility, consistent with our findings in cardiomyocytes of PAH-patients.[9,19]

However, the increase in RV contractility in rats did not result in an improved RV-arterial coupling in rats, suggesting that the increase in RV contractility was insufficient to cope with the higher increase in RV afterload.[9] Therefore the observed increase in force generating capacity may be a compensatory mechanism attempting to cope with the increased RV afterload.[30]

This compensatory mechanism might negatively affect the normal relaxation pattern. The "hypercontractile" sarcomeres, which are evident after combining the increase in maximal force generating capacity with higher myofilament Ca^{2+}-sensitivity and increased passive stiffness (Fig.5D), may limit myocardial relaxation during the diastolic phase and contribute to impaired diastolic function in PAH-induced right heart failure.

Possible mechanisms causing RV diastolic stiffness in PAH

RV diastolic stiffness was not only observed in idiopathic PAH-patients, but was also prevalent in patients with CTEPH. This indicates that RV diastolic stiffness is not specific for PAH, but could also be expected in other syndromes with increased RV pressures. Thus increased RV pressure overload could be an initial trigger for RV diastolic impairment in PAH. Nevertheless, also other factors could explain RV diastolic stiffness in PAH in vivo. We observed a 3-fold higher RV sarcomeric stiffness over the whole range of sarcomere lengths in PAH-patients compared to controls. By repeating RV sarcomeric stiffness measurements after incubation with the cross-bridge inhibitor BDM, we could rule out a contribution of remaining cross-bridge interactions on RV diastolic stiffness. A remaining factor that is likely to contribute to the high cardiomyocyte stiffness is the sarcomeric protein titin. Titin is a molecular spring that spans the half sarcomere and determines muscle stiffness in diastole.[8] Phosphorylation and isoform composition of titin determine the elasticity of the protein and thereby passive (diastolic) stiffness of the cardiomyocytes. In this study, we revealed that titin isoform composition was unaltered in PAH-cardiomyocytes, but titin phosphorylation was significantly reduced in PAH in comparison to controls. Also extracellular factors such as RV collagen deposition might contribute to diastolic impairment, though we observed only a relatively modest increase in RV collagen deposition, which is in line with previous preclinical studies.[9,10,31]

Clinical implications

RV diastolic stiffness was closely associated with markers of disease progression. This finding suggests that RV diastolic stiffness may represent a contributing factor involved in disease worsening and not a benign compensatory mechanism associated with increased afterload. Future therapeutic strategies targeting the reduced titin phosphorylation and increased RV collagen deposition will reveal the clinical implication of increased RV diastolic stiffness.

Limitations of the study

RV diastolic stiffness only weakly correlated with RV peak filling rate. This is comparable to earlier data in patients with heart failure with preserved ejection fraction where the direct comparison of E/A ratio (echo) with the diastolic stiffness

parameter β (conductance catheterization), showed a similar weak correlation.[32] A possible explanation for this finding is that E/A measurements by echo or MRI are highly sensitive to the confounding effects of increased pre- and afterload. This also indicates that other factors besides RV myocardial stiffness are associated with a reduction in E/A ratio. The majority of RV samples used in this study were from patients with PAH secondary to congenital heart disease (CHD). RV samples of patients with idiopathic PAH are difficult to procure since these patients often undergo only lung transplantation. There may be important differences in myocardial structure and function between the right ventricle of a formerly normal adult who develops idiopathic PAH and that from CHD-patients. However, both idiopathic PAH and CHD-patients were in end-stage right heart failure at time of heart/lung transplantation (NYHA IV). More importantly, subgroup analyses revealed that the increase in active force and cardiomyocyte stiffness were comparable between RV samples of idiopathic PAH and congenital heart disease.

The sample size of this study was relatively small, which may have lead to type I errors, and therefore nominal significant p-values should be interpreted with caution. However, our main finding has been confirmed by several clinical and experimental observations. Therefore, RV diastolic stiffness in PAH is not only a statistically significant finding but also physiologically plausible.

CONCLUSIONS

We demonstrated that patients with PAH have increased RV diastolic stiffness. Furthermore, we observed significant correlations between increased diastolic stiffness and disease severity. We revealed that alterations in the extracellular matrix and cardiomyocyte sarcomeres are both important contributors to increased RV diastolic stiffness in PAH patients and may represent future treatment targets.

REFERENCES

1. Humbert M *et al.* Survival in patients with idiopathic, familial, and anorexigen-associated pulmonary arterial hypertension in the modern management era. *Circulation*. 2010;122:156–163.
2. van de Veerdonk MC *et al.* Progressive right ventricular dysfunction in patients with pulmonary arterial hypertension responding to therapy. *J Am Coll Cardiol*. 2011;58:2511–2519.
3. Westerhof N *et al.* Snapshots of hemodynamics. An aid for clinical research and graduate education. Second ed. *Springer*; 2010.
4. Handoko ML *et al.* Perspectives on novel therapeutic strategies for right heart failure in pulmonary arterial hypertension: lessons from the left heart. *Eur Respir Rev*. 2010;19:72–82.
5. Klotz S *et al.* Single-beat estimation of end-diastolic pressure-volume relationship: a novel method with potential for noninvasive application. *Am J Physiol Heart Circ Physiol*. 2006;291:H403–412.
6. Burkhoff D *et al.* Assessment of systolic and diastolic ventricular properties via pressure-volume analysis: a guide for clinical, translational, and basic researchers. *Am J Physiol Heart Circ Physiol.* 2005;289:H501–512.
7. van Heerebeek L *et al.* Diastolic stiffness of the failing diabetic heart: importance of fibrosis, advanced glycation end products, and myocyte resting tension. *Circulation.* 2008;117:43–51.
8. LeWinter MM *et al.* Cardiac titin: a multifunctional giant. *Circulation* 2010;121:2137-2145.
9. de Man FS *et al.* Bisoprolol delays progression towards right heart failure in experimental pulmonary hypertension. *Circ Heart Fail*. 2012;5:97–105.
10. Handoko ML *et al.* Opposite effects of training in rats with stable and progressive pulmonary hypertension. *Circulation.* 2009;120:42–49.
11. Handoko ML *et al.* A refined radio-telemetry technique to monitor right ventricle or pulmonary artery pressures in rats: a useful tool in pulmonary hypertension research. *Pflugers Arch*. 2008;455:951-959.
12. Gan CTJ *et al.* NT-proBNP reflects right ventricular structure and function in pulmonary hypertension. *Eur Respir J*. 2006;28:1190–1194.
13. Galiè N *et al.* Guidelines for the diagnosis and treatment of pulmonary hypertension: the Task Force for the Diagnosis and Treatment of Pulmonary Hypertension of the European Society of Cardiology (ESC) and the European Respiratory Society (ERS), endorsed by the International Society of Heart and Lung Transplantation (ISHLT). *Eur Heart J*. 2009;30:2493–2537.
14. Gan CTJ *et al.* A. Right ventricular diastolic dysfunction and the acute effects of sildenafil in pulmonary hypertension patients. *Chest.* 2007;132:11–17.
15. Lam CSP *et al.* Cardiac structure and ventricular-vascular function in persons with heart failure and preserved ejection fraction from Olmsted County, Minnesota. *Circulation.* 2007;115:1982–1990.
16. Trip P *et al.* Accurate assessment of load-independent right ventricular systolic function in patients with pulmonary hypertension. *J Heart Lung Transplant*. 2013;32:50-55.
17. Sunagawa K *et al.* Estimation of the hydromotive source pressure form ejecting beats of the left ventricle. *IEEE Trans Biomed Eng*. 1980;27:299-305.
18. de Man FS *et al.* Effects of exercise training in patients with idiopathic pulmonary arterial hypertension. *Eur Respir J.* 2009;34:669–675.
19. de Man FS *et al.* Dysregulated Renin-Angiotensin-Aldosterone System Contributes to Pulmonary Arterial Hypertension. *Am J Respir Crit Care Med*. 2012;186:780-789.
20. Borbély A *et al.* Cardiomyocyte stiffness in diastolic heart failure. *Circulation*. 2005;111:774–781.
21. van der Velden J *et al.* Effects of calcium, inorganic phosphate, and pH on isometric force in single skinned cardiomyocytes from donor and failing human hearts. *Circulation.* 2001;104:1140–1146.
22. King NMP *et al.* Mouse intact cardiac myocyte mechanics: cross-bridge and titin-based stress in unactivated cells. *J Gen Physiol*. 2011;137:81–91.
23. Borbély A *et al.* Hypophosphorylation of the Stiff N2B Titin Isoform Raises Cardiomyocyte Resting Tension in Failing Human Myocardium. *Circ Res.* 2009;104:780–786.
24. Manders E *et al.* Diaphragm weakness in pulmonary arterial hypertension: role of sarcomeric dysfunction. *Am J Physiol Lung Cell Mol Physiol*. 2012;303:L1070-L1078.
25. Brimioulle S *et al.* Single-beat estimation of right ventricular end-systolic pressure-volume relationship. *Am J Physiol Heart Circ Physiol*. 2003;284:H1625-H1630.
26. Klotz S *et al.* A computational method of prediction of the end-diastolic pressure-volume relationship by single beat. *Nat Protoc*. 2007;2:2152-2158.
27. Bub G *et al.* Measurement and analysis of sarcomere length in rat cardiomyocytes in situ and in vitro. *Am J Physiol Heart Circ Physiol*. 2010;298:H1616-H1625.

28. D'Alonzo GE *et al.* Survival in patients with primary pulmonary hypertension. Results from a national prospective registry. *Ann Intern Med*. 1991;115:343–349.
29. Mauritz GJ *et al.* Prolonged right ventricular post-systolic isovolumic period in pulmonary arterial hypertension is not a reflection of diastolic dysfunction. *Heart.* 2011;97:473–478.
30. de Man FS *et al.* Neurohormonal axis in patients with pulmonary arterial hypertension: friend or foe? *Am J Resp Crit Care Med*. 2013;187:14-19.
31. Bogaard HJ *et al.* Adrenergic receptor blockade reverses right heart remodeling and dysfunction in pulmonary hypertensive rats. *Am J Respir Crit Care Med*. 2010;182:652–660.
32. Kasner M *et al.* Utility of Doppler echocardiography and tissue Doppler imaging in the estimation of diastolic function in heart failure with normal ejection fraction: a comparative Doppler-conductance catheterization study. *Circulation* 2007;116:637-647.

Chapter 3

Protein changes contributing to right ventricular cardiomyocyte diastolic dysfunction

Rain S, Bos Dda S, Handoko ML, Westerhof N, Stienen G, Ottenheijm C, Goebel M, Dorfmüller P, Guignabert C, Humbert M, Bogaard HJ, Remedios CD, Saripalli C, Hidalgo CG, Granzier HL, Vonk-Noordegraaf A, van der Velden J, de Man FS.

J Am Heart Assoc. 2014
doi: **10.1161/JAHA.113.000716**

ABSTRACT

Background – Right ventricular (RV) diastolic function is impaired in patients with pulmonary arterial hypertension (PAH). Our previous study showed that elevated cardiomyocyte stiffness and myofilament Ca^{2+}-sensitivity underlie diastolic dysfunction in PAH. This study investigates protein modifications contributing to cellular diastolic dysfunction in PAH.

Methods and Results – RV samples from PAH patients undergoing heart-lung transplantation were compared to non-failing donors (Don). *Titin stiffness* contribution to RV diastolic dysfunction was determined by Western-blot analyses using antibodies to protein-kinase-A (PKA), Cα (PKCα) and Ca^{2+}/Calmoduling-dependent-kinase (CaMKIIδ) titin and phospholamban (PLN) phosphorylation sites: N2B (Ser469), PEVK (Ser170 and Ser26) and PLN (Thr17) respectively. PKA and PKCα sites were significantly less phosphorylated in PAH compared to donors ($p<0.0001$). To test the functional relevance of PKA-, PKCα-and CaMKIIδ-mediated titin phosphorylation, we measured the stiffness of single RV cardiomyocytes before and after kinase incubation. PKA significantly decreased PAH RV cardiomyocyte diastolic stiffness, PKCα further increased stiffness while CaMKIIδ had no major effect. CaMKIIδ activation was determined indirectly by measuring PLN Thr17phosphorylation level. No significant changes were found between the groups. Myofilament Ca^{2+}-sensitivity is mediated by sarcomeric *troponin I* (cTnI) phosphorylation. We observed increased unphosphorylated cTnI in PAH compared with donors ($p<0.05$) and reduced PKA-mediated cTnI phosphorylation (Ser22/23) ($p<0.001$). Finally, altered in *Ca^{2+}-handling proteins* contribute to RV diastolic dysfunction due to insufficient diastolic Ca^{2+}-clearance. PAH SERCA2a levels and PLN phosphorylation were significantly reduced compared to donors ($p<0.05$).

Conclusions – Increased titin stiffness, reduced cTnI phosphorylation and altered levels of phosphorylation of Ca^{2+}-handling proteins contribute to RV diastolic dysfunction in PAH.

INTRODUCTION

Patients with pulmonary arterial hypertension (PAH) develop severe right ventricular (RV) failure with impaired diastolic function.[1] In a previous study we showed that collagen deposition, increased cardiomyocyte stiffness and myofilament Ca^{2+}-sensitivity contribute to compromising RV diastolic function.[1] In the present study we investigate protein changes that underlie RV cardiomyocyte diastolic dysfunction.

Diastolic dysfunction of the left ventricle (LV) was shown to be related to increased cardiomyocyte stiffness as a consequence to functional modifications of the sarcomeric protein titin. By folding during contraction and stretching during relaxation, titin acts as a sarcomeric molecular spring and represents the major determinant of cardiomyocyte stiffness at physiological sarcomere legths.[2] Titin spans half of the sarcomere, from the Z line to the M band, and consists of a linear array of proximal and distal Ig-like domains, together with N2B and PEVK segments.[3] Its stiffness is modulated by complex mechanisms involving both fast post-translational modification (phosphorylation) and slower changes in isoform expression.[4] The effect of titin phosphorylation depends on the domain targeted. Phosphorylation of the N2B domain has been shown to lower cardiomyocyte stiffness, while PEVK domain phosphorylation exerts the opposite effect.[5-7]

We have previously shown that, unlike LV diastolic dysfunction, titin isoform composition is not changed in the RV of PAH patients. However, there is an overall decrease in titin phosphorylation in these patients.[1] Therefore, the first aim of this study was to determine the particular titin phosphorylation changes specific to the RV which could explain the increase in RV cardiomyocyte stiffness in PAH patients.

In addition to titin-derived stiffness, RV cardiomyocytes of PAH patients are characterized by increased myofilament Ca^{2+}-sensitivity, which may in turn influence cardiomyocyte lusiothropy.[8] Cardiac Troponin I (cTnI) and cardiac myosin binding protein C (MyBPC) are two important regulators of myofilament Ca^{2+}-sensitivity.[8-12] The second aim of this study was to determine whether changes in cTnI and MyBPC phosphorylation are related to the previously observed increase in RV myofilament Ca^{2+}-sensitivity.

Furthermore, fast cytoplasmic Ca^{2+}-clearance during diastole is crucial for a normal relaxation pattern.[13] The speed of diastolic Ca^{2+}-reuptake into the sarcoplasmic reticulum is determined by the activity of the sarcoplasmic reticulum Ca^{2+}-ATPase-2a (SERCA2a).[14,15] The rate at which SERCA2a transfers $[Ca^{2+}]$ across the sarcoplasmic reticulum membrane is enhanced by PKA-mediated phospholamban (PLN) phosphorylation during β-AR stimulation.[16] The inhibitory coupling-protein PLN is removed from SERCA2a secondary to PLN phosphorylation (pPLN). Ca^{2+}-clearance is also regulated by the sodium-calcium exchanger 1 (NCX1) that is responsible for extracellular extrusion of one Ca^{2+} ion in exchange for three imported Na^{+} ions.[17] Previous animal model studies show the relation between altered Ca^{2+}-clearance proteins and impaired cardiac relaxation.[14,15] However, the expression and function of Ca^{2+}-clearance proteins in the failing human RV is not known. Therefore, the third aim of this study was to determine whether Ca^{2+}-clearance protein expression and phosphorylation is altered in the RV of PAH patients.

To summarize, the present study investigated the protein changes involved in altering RV cardiomyocyte diastolic function in patients with PAH. Our findings reveal that

increased titin stiffness, reduced cTnI phosphorylation and altered expression levels of the Ca^{2+}-handling proteins contribute to RV diastolic dysfunction in PAH patients.

METHODS

Tissue samples

Explanted RV tissue samples were collected from PAH patients undergoing heart transplantation (n = 11) and compared to RV tissue obtained from non-failing donors (n = 9) (Table 1). There were no significant differences in gender and age between the two groups (Age_{PAH} = 36.6±3.9, Age_{Don}=41.1±4.7, p=0.47, $Gender(F/M)_{PAH}$ = 11/1, $Gender(F/M)_{Don}$ = 6/3 p=0.28). Human cardiac tissue collection and use by collaborating universities (VU Medical Center, Amsterdam) was approved by the Human Research Ethics Committee of The University of Sydney (AU/1/961515) and the Université Paris-Sud - Inserm U999 (ID RBC 2008-A00485-50). All patients received treatment previous to cardiac transplantation corresponding to the clinical protocols present at the time of the intervention. Various treatments (acute dobutamine administration) may be associated with the differences observed between patients. After transplantation, RV tissue samples were immediately frozen and stored in liquid nitrogen, preserving the expression and phosphorylation level of the cardiomyocytes.

Titin phosphorylation

To determine kinase-specific titin phosphorylation, donor (n = 7) and PAH (n = 5) frozen RV tissue samples were weighed and pulverized in liquid nitrogen using a mortar and a pestle. Tissue powder was solubilized in 8M urea buffer with DTT and 50% glycerol solution with protease inhibitors (0.16 mmol/L Leupeptin, 0.04 mmol/L E-64 and 0.2 mmol/L PMSF). Samples were loaded on 1% agarose gels stained with Coomassie Blue for protein identification. Equal titin sample dilutions were calculated derived from Myosin Heavy Chain (MHC) protein content and applied for isoform ratio determination.[18]

Table 1 – Clinical and demographic characteristics

RV sample	Diagnosis	NYHAclass	Gender	Age
1	Idiopathic PAH	IV	Female	38
2	Idiopathic PAH	IV	Female	44
3	Idiopathic PAH	IV	Female	51
4	PAH-Eisenmenger	IV	Female	46
5	PAH-Eisenmenger	IV	Female	14
6	PAH-Eisenmenger	IV	Female	20
7	PAH-Eisenmenger	IV	Female	31
8	PAH-Eisenmenger	IV	Female	21
9	PAH-Eisenmenger	IV	Male	46
10	PAH-Eisenmenger	IV	Female	50
11	PAH-Eisenmenger	IV	Female	41
12	Donor		Female	41
13	Donor		Female	23
14	Donor		Female	19
15	Donor		Female	53
16	Donor		Male	65
17	Donor		Female	49
18	Donor		Male	45
19	Donor		Female	38
20	Donor		Male	37

PAH: pulmonary arterial hypertension. NYHA: New York Heart Association

Titin phosphorylation of PKA and PKCα sites was assessed using Western blots with specific antibodies against serine 469 (Ser4185, titin N2B cardiac, UnitprotKB: Q8WZ42) on the N2B domain (PKA phosphorylation site) and serine 26 and 170 (Ser11878, UnitprotKB:Q8WZ42 and Ser12022, UnitprotKB:Q8WZ42) on the PEVK domain (PKCα phosphorylation sites). Equal sample loadings were separated on 0.8% agarose gels, transferred to PVDF membranes (Immobilon®-FL, Cat.No.IPFL00010, 045µm) and probed with the relevant antibodies. Membranes were scanned and analyzed using Odyssey Infrared Imaging System (Li-COR Biosciences). N2B and N2BA protein content was determined on Ponceau-S-stained membranes and used to normalize for phosphorylation level.[5]

RV cardiomyocyte diastolic stiffness

RV free wall tissue samples (between 20 and 40mg) were defrosted in relaxing solution then sectioned in smaller pieces with a fine dissection scissors. Subsequently, single cardiomyocytes were isolated from these tissue pieces by manual mechanical homogenization. The single cells were then membrane-permeabilized by adding Triton (1%) to the relaxing solution in order to wash out the lipid cellular membranes. The cell solution was repeatedly washed with relaxing solution in order to remove Triton. The cell yield is somewhat variable, depending on the initial amount of tissue, the release of cardiomyocyte from the tissue bulk during mechanical homogenization and the loss of cells during Triton washing. Cells for force measurements were chosen based on length and width (length: 50-100μm, width 15-30μm at rest in relaxing solutions).[1] A minimum of three cells per sample were used to determine diastolic stiffness and their average was used for further statistic analysis. A single cell was attached with silicone adhesive between a force transducer and a piezoelectric motor. To determine cardiomyocyte stiffness a 25% shortening was performed in the relaxing solution and steady-state stiffness measurements were recorded at increasing sarcomere lengths (1.8 – 2.4 μm).[1]

Cardiomyocytes were further incubated in relaxing solution with PKA (100U/ml) (Protein Kinase A Catalytic subunit from bovine heart, P2645, Sigma Aldrich) (Donor n = 4, PAH n = 4), CaMKIIδ (50U/ml) or PKC-subunit α (10U/ml) (Protein Kinase C α human isozyme, P1782, Sigma Aldrich) (Donor n = 3, PAH n = 3) at 20°C for one hour. PKC α also requires Ca^{2+}, therefore the relaxing solution was mixed in a 1:1 concentration ratio with a Ca^{2+} containing solution of pCa 5.8, obtaining therefore an end pCa of 5.9 in which the cardiomyocytes were incubated. Diastolic stiffness was recorded after PKA, PKCα or CaMKIIδ incubation.[19] Individual force values were normalized by the cardiomyocyte cross-sectional area recorded at 2.2 μm sarcomere length.

Sarcomeric protein phosphorylation

Sarcomeric protein phosphorylation was determined for each tissue sample (Donor n = 9, PAH n = 11). RV tissue samples were homogenized and separated on gradient gels (NuPAGE® Bis-Tris Gels, Life Technologies). ProQ Diamond Phosphoprotein Stain was used to determine the amount of protein phosphorylation. Gels were further fixed, washed, destained and stained with SYPRO Ruby to determine the total amount of protein. Myofilament protein phosphorylation ratio (ProQ) was calculated relative to the corresponding SYPRO staining (ProQ/SYPRO).[20]

Cardiac troponin I phosphorylation

Proteins were separated on one-dimensional gel electrophoresis on NuPAGE® Bis-Tris gels (Donor n = 9, PAH = 11). The XCell II™ Blot Module (Life Technologies) was used for wet protein transfer from mini-gels to ECL membranes (Hybond ECL Nitrocellulose Membrane, GE Healthcare). Blots were incubated with the following primary antibodies against specific protein or protein phosphorylation sites: cTnI dephosphorylated form (4T46, mouse monoclonal antibody, HyTest), cTnI PKA-specific serine 22/23 site phosphorylation (4004, rabbit polyclonal antibody, Cell Signaling

Technology).[9,10] The amount of protein expression or phosphorylation was normalized to the concentration of Ponceau-S stained actin.
The distribution of cTnI phosphorylation (unphosphorylated (P_0), mono-phosphorylated (P_1), bis-phosphorylated (P_2)) was determined on acrylamide Phos-Tag™ gels.[10]

Ca^{2+}-handling proteins expression and phosphorylation
To determine SERCA2a expression, monoclonal rabbit antibody was used (courtesy of Warner S. Simonides, VU University Medical Center, Amsterdam) (Donor n = 9, PAH = 11). PLN binds to and inhibits SERCA2a, while phosphorylation of PLN (pPLN) removes the inhibitory binding of PLN and promotes SERCA2a activity. PLN and pPLN were determined with the following antibodies: total PLN (L15, sc21923, Santa Cruz Biotechnology, Inc), PKA-specific PLN phosphorylation site (Ser16, sc12963, Santa Cruz Biotechnology, Inc) and CaMKIIδ-specific PLN phosphorylation (Thr17, A010-13AP, Badrilla). NCX1 expression was quantified using NCX1-C2C12 antibody (ab2869, Abcam). Cardiac specific Ryanodine Receptor 2 expression was also quantified (C3-33, ThermoFisher Scientific). The amount of protein expression or phosphorylation was normalized to the concentration of Ponceau-S-stained actin.

Statistical analyses
Statistical analyses were performed using Prism 5 for Windows (GraphPad Software Inc, San Diego, CA and IBM® SPSS® Statistics 20.0, IBM Corporation, Somers, NY). P-values lower than 0.05 were considered significant. All data are presented as mean ± SEM.
Age differences between patients were tested for significance by a non-paired t-test. Gender differences were tested by a Fisher's exact test. Changes in protein expression were tested for significance by a non-paired non-parametric Mann Whitney u-test. Phos-Tag™ analysis was tested for significance by repeated two-way ANOVA followed by the Bonferroni post-hoc test.
The effects of PKA, PKCα and CaMKIIδ incubation in PAH patients and donors at increasing sarcomere lengths were tested by using a mixed-design ANOVA with disease as between-group measure, sarcomere length and PKA/PKCα/CaMKIIδ -incubation as repeated measures. The green-house Geisser correction was used, because sphericity could not be assumed.

RESULTS

PKA-mediated titin phosphorylation in PAH RV cardiomyocytes
Cardiomyocyte stiffness is modulated by titin isoform composition and phosphorylation. In our previous study we showed that titin isoform ratio (N2BA/N2B) is not significantly changed in PAH compared to donors ($N2BA/N2B_{Don}$=0.91±0.08, $N2BA/N2B_{PAH}$=0.77±0.07, p=0.20).[1] Therefore, the overall increase in cardiomyocyte stiffness may be a consequence of titin N2B or PEVK domain phosphorylation.

Titin phosphorylation was determined using phospho-specific antibodies for PKA and PKCα phosphorylation sites. We found significantly reduced levels of PKA-dependent phosphorylation of N2B serine 469 site and PKCα-dependent phosphorylation of PEVK

serine 170 site (PKA_{Don}= 1.00 ± 0.03, PKA_{PAH}= 0.44 ± 0.04, p=0.002) (Fig. 1A1) and ($PKC\alpha\text{-}S170_{Don}$= 1.00 ± 0.06, $PKC\alpha\text{-}S170_{PAH}$= 0.46 ± 0.06, p=0.002) (Fig. 1B1). No significant difference was found in PKCα-dependent phosphorylation of PEVK serine 26 ($PKC\alpha\text{-}S26_{Don}$= 1.00 ± 0.12, $PKC\alpha\text{-}S26_{PAH}$= 0.96 ± 0.12, p=0.53) (Fig. 1B2).

Activation of CaMKIIδ determined indirectly by assessing the level of PLN CaMKIIδ-dependent phosphorylation of the residue threonine at position 17, which is an exclusive specific site for CaMKIIδ.[25] We found no statistical significant difference between the two groups ($CaMKII\delta_{Don}$= 1.00 ± 0.19, $CaMKII\delta_{PAH}$= 1.42 ± 0.29, p=0.41) (Fig. 1C1).

PKA incubation partially restores RV cardiomyocyte stiffness

Subsequently, we tested in a subgroup of samples the functional relevance titin PKA PKCα and CaMKIIδ-mediated phosphorylation. For this purpose, membrane-permeabilized cardiomyocytes in relaxing solution were used to minimize the influence of additional determinants of cardiomyocyte stiffness such as membrane and sarcoplasmic reticulum Ca^{2+}-handling. Therefore, cardiomyocyte stiffness is attributed solely to the sarcomeric protein titin.

RV cardiomyocyte stiffness was measured at increasing sarcomere lengths, starting at 1.8μm and stretched to 2.0, 2.2 and 2.4 μm.

After PKA incubation we recorded a significant decrease in PAH cardiomyocyte stiffness. Donor cardiomyocyte stiffness was minimally affected by PKA incubation ($p_{interaction}$PKA*disease = 0.01) (Fig. 1A2). PKCα incubation significantly increased cardiomyocyte stiffness in PAH samples and had little effect on donor cardiomyocyte stiffness ($p_{interaction}$ PKCα*disease = 0.09) (Fig. 1B3). CaMKIIδ incubation decreased cardiomyocyte stiffness of both Don and PAH samples ($p_{interaction}$CaMKIIδ*disease = 0.08) (Fig. 1C2). Similar stretch or incubation in relaxing solutions without kinases would not modify baseline cardiomyocyte stiffness.

Figure 1 – PKA, PKCα and CaMKIIδ treatment effect on diastolic stiffness mediated by titin phosphorylation

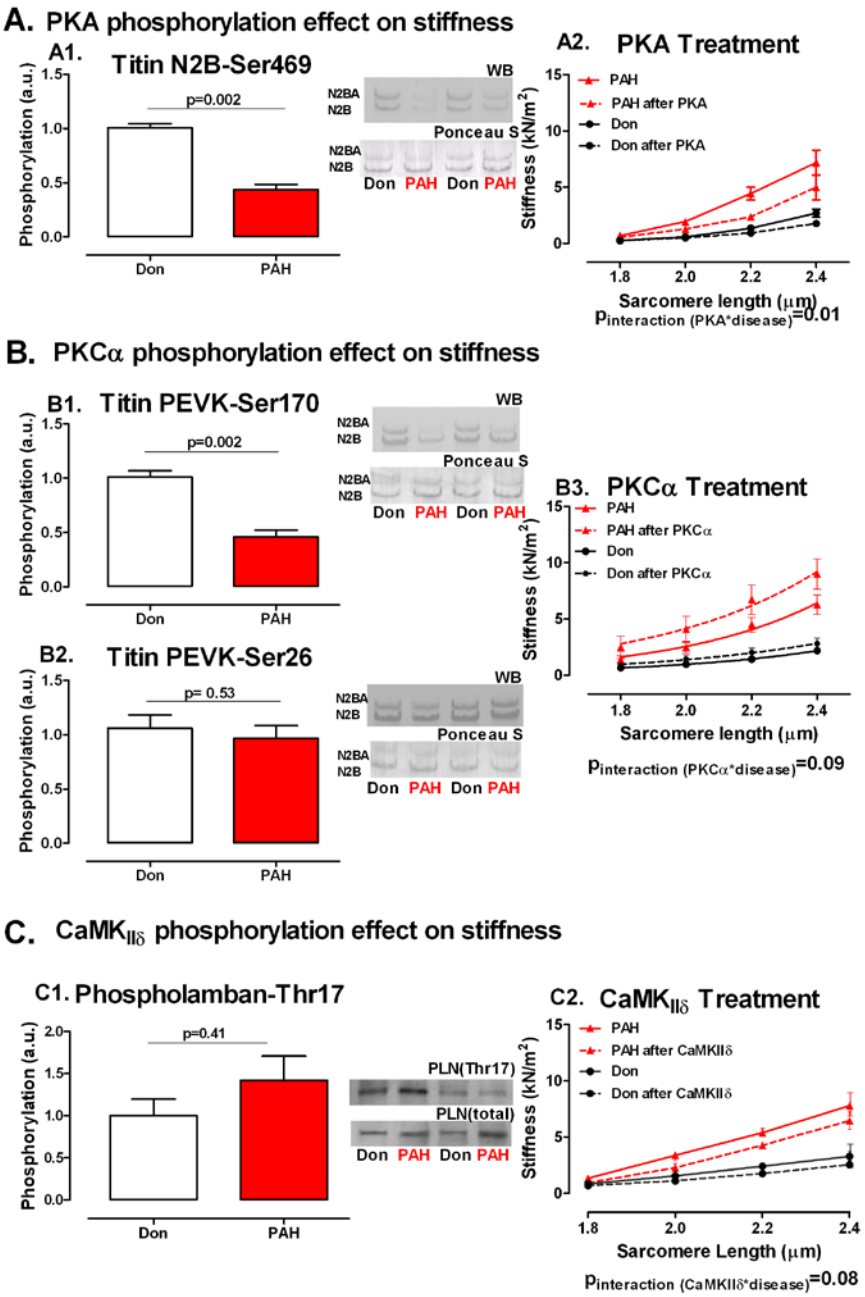

A. Titin N2B domain serine 469 PKA-dependent phosphorylation. B. Titin PEVK domain serine 170 PKCα-dependent phosphorylation. C. Phospholamban Threonine 17 CaMKIIδ-dependent phosphorylation was used as an indirect measurement of titin CaMKIIδ phosphorylation. Data presented as mean ± SEM

Figure 2 – Sarcomeric protein phosphorylation

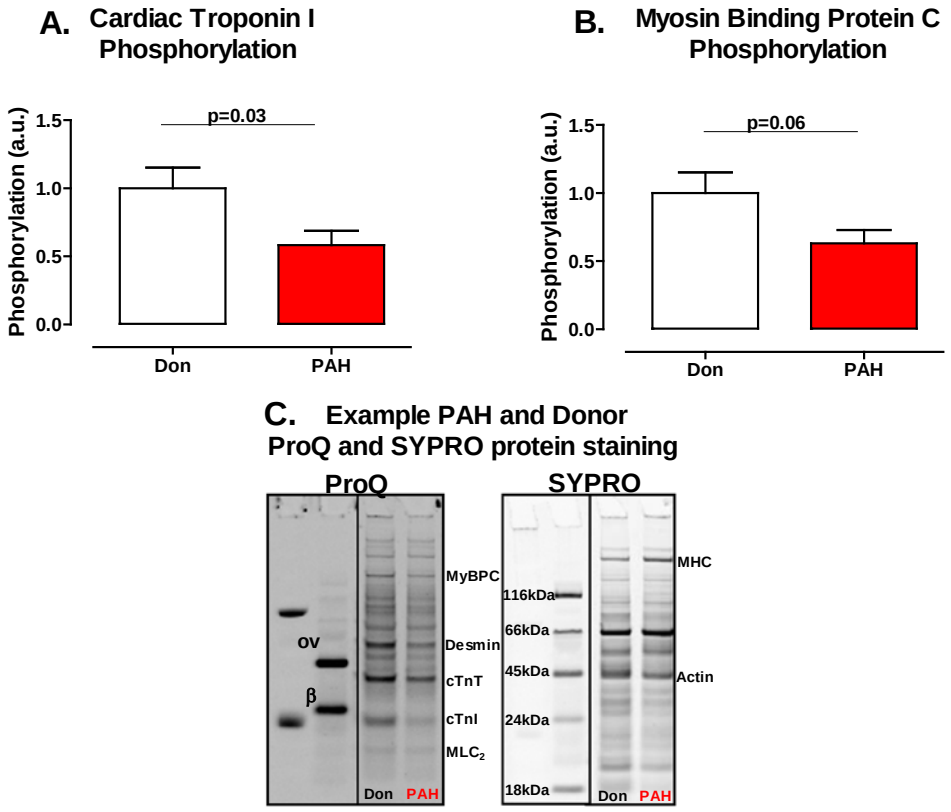

A. cTnI phosphorylation. B. MyBPC phosphorylation Typical example of donor and PAH phosphorylation. ov: ovalbumin; β: β-casein; MyBPC: myosin binding protein C; cTnT: cardiac troponin T; cTnI: cardiac troponin I; MLC_2: myosin light chain MHC: myosin heavy chain. Data presented as mean ± SEM

Reduced phosphorylation of sarcomeric cTnI

Measurements of myofilament Ca^{2+}-sensitivity revealed a higher sensitivity in PAH compared to donor samples. To investigate whether reduced phosphorylation of the sarcomeric protein cTnI could play a role in determining high myofilament Ca^{2+}-sensitivity and contribute to RV diastolic dysfunction in PAH, overall sarcomeric protein phosphorylation was determined. A significant decrease in cTnI and MyBPC phosphorylation was found in PAH compared with donors ($cTnI_{Don}$= 1.00 ± 0.15, $cTnI_{PAH}$= 0.58 ± 0.11, p=0.03; $MyBPC_{Don}$= 1.00 ± 0.15, $MyBPC_{PAH}$= 0.63 ±0 .09, p = 0.06) (Fig. 2). Cardiac troponin T (cTnT) phosphorylation appeared to be higher in PAH compared to donors, however this not statistically significant ($cTnT_{Don}$= 1.00 ± 0.07, $cTnT_{PAH}$= 1.29 ± 0.13, p = 0.07). No difference was found in desmin phosphorylation ($Desmin_{Don}$= 1.00 ± 0.07, $Desmin_{PAH}$= 0.93 ± 0.06, p = 0.4).

Figure 3 – cTnI phosphorylation

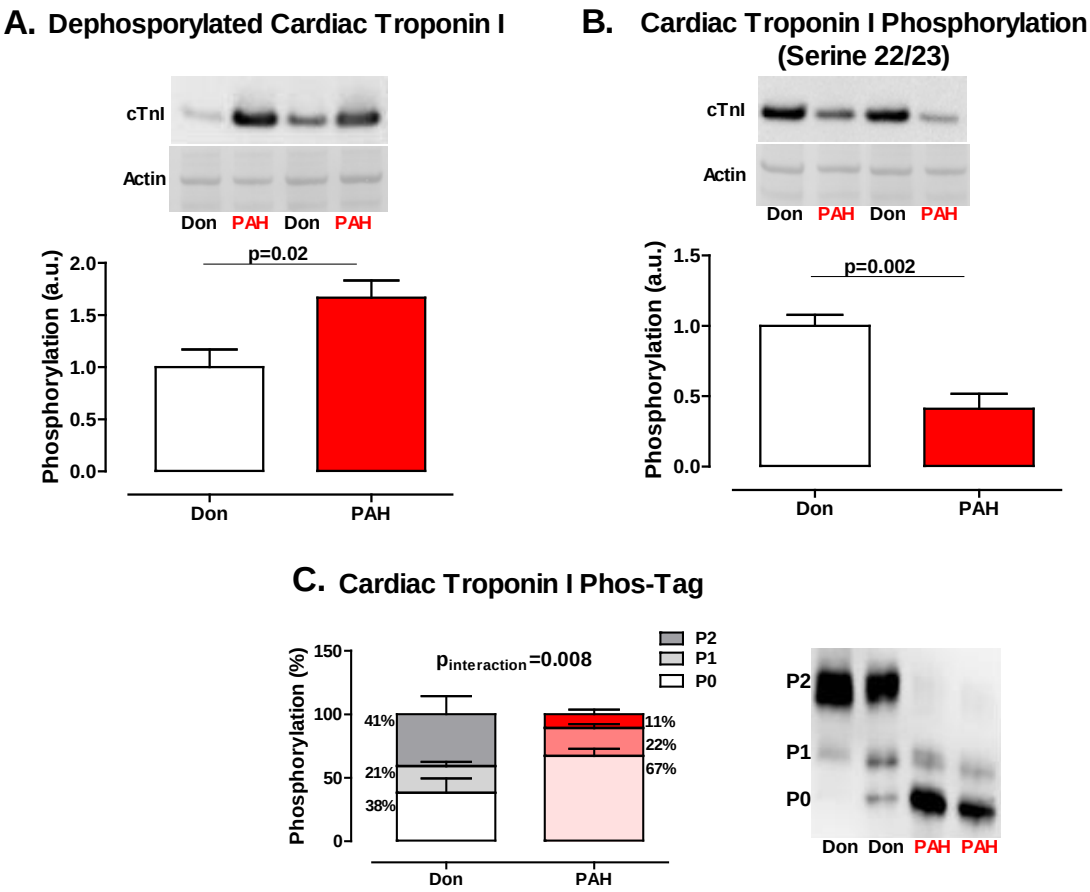

A. Unphosphorylated cTnI B. cTnI serine 22/23 phsophorylation C. TnI: unphosphorylated (P_0) cTnI, mono-phosphorylated (P_1) cTnI and bis-phosphorylated (P_2) (Phos-Tag analysis). Data presented as mean ± SEM

Reduced cTnI phosphorylation was further confirmed by Western blot and Phos-Tag™ analyses. The amount of dephosphorylated cTnI was significantly higher in PAH compared to donors (dephos-$cTnI_{Don}$= 1.00 ± 0.17, dephos-$cTnI_{PAH}$= 1.67 ± 0.17, p = 0.02) (Fig. 3A). The cTnI PKA specific phosphorylation site (serine 22/23) showed significantly lower phosphorylation in PAH samples compared with donors (cTnI-$S22/23_{Don}$= 1.00 ± 0.08, cTnI-$S22/23_{PAH}$= 0.41 ±0.11, p = 0.002) (Fig. 3B).

Phos-Tag™ analysis demonstrated that the distribution of cTnI phosphorylation (unphosphorylated (P_0), mono-phosphorylated (P_1), and bis-phosphorylated (P_2)) in PAH-cardiomyocytes was shifted to more unphosphorylated cTnI in comparison to donors, evident from higher levels of unphosphorylated cTnI and lower levels of bis-phosphorylated cTnI (P_{Don} 0/1/2 = 38.38 ± 11.55% / 20.78 ± 3.57% / 40.84 ± 14.21%, P_{PAH} 0/1/2 = 67.28 ± 5.86%,/ 21.55 ± 3.12% / 11.17 ± 3.69%, $p_{interaction}$ = 0.008) (Fig. 3C).

Figure 4 – Ca^{2+}-handling proteins expression and phosphorylation

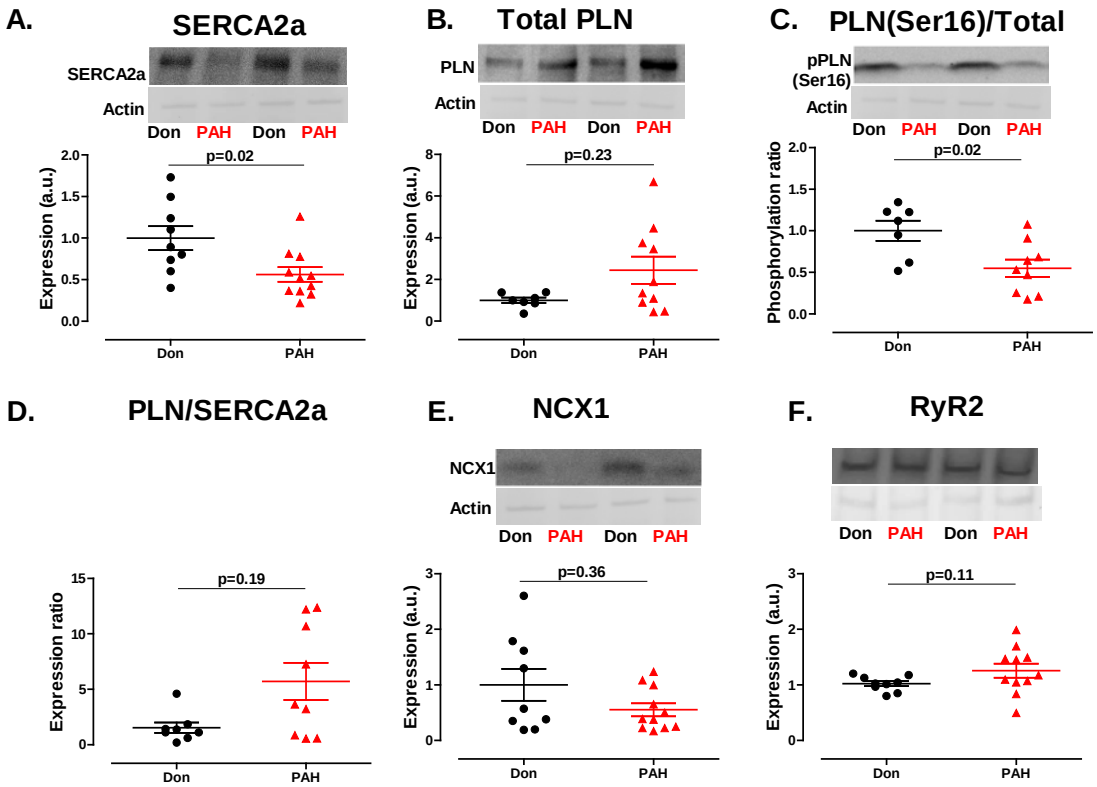

A. SERCA2a expression. B. PLN expression. C. PLN PKA-dependent phosphorylation. D. PLN/SERCA2a ratio. E. NCX1 expression. F. Ryr2 expression. Data presented as mean ± SEM

Altered expression of Ca^{2+}-handling proteins

SERCA2a expression was significantly lower in PAH cardiomyocytes ($SERCA2a_{Don}$= 1.00 ± 0.14, $SERCA2a_{PAH}$= 0.56 ± 0.09, p = 0.02) (Fig. 4A).

Total PLN protein levels were higher in PAH, however the difference failed to reach statistical significance (PLN_{Don}= 1.00 ± 0.13, PLN_{PAH}= 2.44 ± 0.65, p = 0.23) (Fig. 4B).

PLN phosphorylation was determined as a ratio calculated from total PLN protein level in relation to the amount of phosphorylated PLN. pPLN was significantly lower in PAH compared with donors ($pPLN/PLN_{Don}$= 1.00 ± 0.12, $pPLN/PLN_{PAH}$= 0.55 ± 0.10, p = 0.02) (Fig. 4C).

The inhibitory effect of PLN on SERCA2a was determined by the PLN/SERCA2a ratio, which was higher in PAH compared with donors ($PLN/SERCA2a_{Don}$= 1.5 ± 0.47, $PLN/SERCA2a_{PAH}$= 5.71 ± 1.67, p=0.19) (Fig. 4D).

In addition, the lower level of NCX1 protein level in PAH was not statistically significant ($NCX1_{Don}$= 1.00 ± 0.28, $NCX1_{PAH}$= 0.55 ± 0.12, p = 0.36) (Fig. 4E). The expression level of RyR2, responsible for systolic Ca^{2+} release from the sarcoplasmic reticulum was not significantly different in the two groups (RyR_{2Don}= 1.00 ± 0.05, RyR_{2PAH}= 1.26 ± 0.13, p=0.11) (Fig. 4F).

DISCUSSION

This study demonstrates that cellular RV diastolic function in PAH is altered as a consequence of:

1) Reduced PKA-mediated titin phosphorylation resulting in increased RV cardiomyocyte stiffness.
2) Decreased cTnI phosphorylation, increasing Ca^{2+}-sensitivity.
3) Decreased levels of SERCA2a and PLN phosphorylation, suggesting reduced diastolic Ca^{2+}-clearance.

1) Titin determined cardiomyocyte stiffness

This is the first human study to show altered titin phosphorylation and its functional consequence in the failing right ventricle. We demonstrate that in RV tissue from PAH patients, titin serine 469 (PKA site) and serine 170 (PKCα site) phosphorylation are significantly reduced. No change was observed in titin serine 26 (PKCα site) phosphorylation between PAH and donor. Interestingly, these findings differ from those previously observed in LV pressure overload animal models. Hudson *et al.* investigated titin phosphorylation in a mouse model of hypertensive left heart failure induced by transverse aortic constriction.[21] They concluded that increased PKCα-mediated phosphorylation of serine 26 in the PEVK domain was the main contributor to left ventricular cardiomyocyte stiffness. No significant change in PKA-mediated phosphorylation of the N2B domain was found in this animal model of left heart failure. Kötter *et al.* used end-stage human LV tissue obtained during heart transplantation from hypertrophic cardiomyopathy (HCM) and idiopathic dilated cardiomyopathy (iDCM) patients and concluded that the significant increase in PEVK domain serine 26 (PKCα site) phosphorylation, together with altered titin N2B domain phosphorylation, determine the increase cardiomyocyte stiffness in LV failure.[22] This suggest that while in LV failure PKCα-dependent *hyper*phosphorylation of titin PEVK domain serine 26 plays a key role in increasing stiffness, in RV failure secondary to pressure overload, PKA-dependent *hypo*phosphorylation of N2B domain serine 469 in central in increasing cardiomyocyte stiffness.

To demonstrate the functional relevance of altered serine 469 and serine 170 phosphorylation, we incubated RV cardiomyocytes with the catalytic subunits of PKA and PKCα and measured the effects on RV cardiomyocyte stiffness. We observed that PKA incubation lowered stiffness only in PAH and largely restored RV cardiomyocyte stiffness to values observed in donors. In contrast, PKCα incubation increased cardiomyocyte stiffness in both PAH but far less in donor. At sarcomere lengths longer than physiological (>2.2μm), PKCα incubation resulted in a large increase in RV cardiomyocyte stiffness in PAH patients. These findings suggest that titin serine 469 (PKA site) hypophosphorylation is the main contributor to RV diastolic stiffness in PAH, rather than titin serine 170 (PKCα site) hypophosphorylation. The latter may be a compensatory mechanism to prevent further increase in titin stiffness in RV cardiomyocytes in PAH patients.

In addition to PKA-, PKCα- and CaMKIIδ- dependent phosphorylation, titin stiffness is subject to the fine tuning of a number of different kinases with opposite or

complementary effects. In humans, protein kinase G (PKG) was shown to phosphorylate N2B serine 469 with same functional effect as PKA.[23] In addition to PKA and PKG, recent data show that extracellular-signal-regulated kinase 2 (ERK2) can decrease titin stiffness. However, the phosphorylation site is still to be resolved.[24] Furthermore CaMKIIδ was shown to phosphorylate N2B (other sites than PKA) and PEVK domains and overlap with PKCα phosphorylation sites on the PEVK domain.[25,26] However, the functional role of these novel phosphorylation pathways was not yet shown in human.[27]

2) cTnI modulated Ca^{2+}-sensitivity

An increase in sarcomere Ca^{2+}-sensitivity can lead to incomplete actin-myosin detachment, despite low [Ca^{2+}] levels, impairing the relaxation phase.[28] Previously it was demonstrated that sarcomeric protein phosphorylation plays an important role in determining Ca^{2+}-sensitivity.[10-12] In our study, we observed reduced cTnI and MyBPC phosphorylation. Site-specific analysis further revealed that PKA-mediated cTnI phosphorylation of serine 22/23 was less phosphorylated in PAH. This was further confirmed by Phos-Tag™ analyses showing a higher level of un-phosphorylated (P0) cTnI and reduced level of bis-phosphorylated (P2) cTnI. Although in our previous study only a small increase in Ca^{2+}-sensitivity was observed, this could further contribute to the RV diastolic impairment in PAH patients.

3) Diastolic Ca^{2+}-clearance

For proper cardiomyocyte relaxation, cytosolic [Ca^{2+}] must promptly drop, followed by myofilament detachment and sarcomere elongation to diastolic length.[13] Therefore, perturbations in diastolic Ca^{2+}-clearance are central to the development of diastolic dysfunction.[28,29] Substantial decrease in SERCA2a protein levels and PKA-mediated PLN phosphorylation would imply that cellular relaxation pattern is altered in PAH patients, due to increased residual diastolic [Ca^{2+}]. However, the actual correlation between altered protein expression or phosphorylation and their functional relevance could not be determined in the present study.

PAH and excessive neurohormonal activation

Although the three mechanisms discussed here clearly affect diastolic function in a distinct way and therefore may have different relevance *in vivo*, we observe a common factor to all three mechanisms: reduced PKA-mediated phosphorylation. Decreased PKA phosphorylation determined increased titin-derived RV cardiomyocyte stiffness, increased myofilament cTnI dependent Ca^{2+}-sensitivity and altered Ca^{2+}-clearance due to reduced PLN phosphorylation. In the setting of heart failure, disturbed PKA phosphorylation is attributed to impaired β-AR signaling as a consequence of increased neurohormonal stimulation and compensatory receptor β-AR downregulation.[28] In PAH, however, the consequences of increased neurohormonal activation are less well understood.[30] Bristow *et al*. observed decreased β-AR density in failing RV myocardium.[31] In addition, reducing neurohormonal activity in an experimental model of PAH resulted in improved RV diastolic function and partially restored sarcomeric protein phosphorylation (cTnI and cMyBPC).[32] Therefore, we propose that in PAH patients the reduced PKA-mediated phosphorylation of titin, cTnI and PLN are at least partially caused by increased neurohormonal activation.

Clinical implications

Beta-blocker therapy is known to counteract the loss of function of β-AR signaling by restoring β-AR density, followed by the restoration of PKA-mediated phosphorylation.[32,33] In a previous experimental PAH model, rats receiving beta-blocker therapy showed a significant reduction in RV diastolic stiffness and increase in cTnI and cMyBPC phsophorylation compared with PAH rats receiving placebo. These effects are likely due to reduced neurohormonal activation in PAH rats receiving beta-blockers, normalization of β-adrenergic stimulation and increased PKA-mediated titin, cTnI and MyBPC phosphorylation. Although well tolerated in PAH rats, beta-blockers are currently not recommended in PAH due to possible negative inotropic effects. Nevertheless, based on the beneficial effects of beta-blockers in PAH experimental models, we have initiated a phase II clinical study to investigate the safety and efficacy of beta-blocker (Bisoprolol) in patients with PAH (Clinicaltrails.gov identifier: NCT01246037).[32] The future results of this study will reveal whether indeed, β-AR /PKA signaling pathway is a novel therapeutic target for RV diastolic impairment in PAH patients.

Limitations of the study

Efficient diastolic Ca^{2+}-clearance is vital for ensuring proper relaxation for the sarcomere, therefore in this study we quantified the expression level of the most important proteins involved in Ca^{2+}-handling. However, the functional relevance of these changes was not assessed. Functional relevance can only be determined in freshly harvested myocardial tissue/ whole hearts, usually from animal models where changes in protein levels are consequently related to the functional data. In our study we used human myocardial tissue preserved by freezing, which did not alter the protein level and phosphorylation status, however made functional assessments impossible. Nevertheless, previous animal model studies show a clear relation between expression levels and function of Ca^{2+}-handling proteins, therefore we speculate that this is also the case in our study.[13]

There are several other mechanisms which regulate diastolic dysfunction such as: increased radical oxygen species production, T-tubules loss or disorganization of cardiomyocyte cytoarhitecture. Although important for diastolic function, this study only focused on the cardiomyocyte stiffness, myofilament Ca^{2+}-sensitivity and altered Ca^{2+}-clearance protein levels.[34]

CONCLUSIONS

The present study provides novel insight in the molecular mechanism underlying RV diastolic impairment in patients with PAH. We observed that reduced PKA-mediated phosphorylation of the giant sarcomeric protein titin contributed significantly to RV cardiomyocyte stiffness. In addition, phosphorylation of the sarcomeric protein cTnI was significantly reduced in PAH. Finally, reduced PLN phosphorylation and SERCA2a protein levels may indicate altered diastolic Ca^{2+}-clearance.

REFERENCES

1. Rain S *et al.* Right ventricular diastolic impairment in patients with pulmonary arterial hypertension. *Circulation*. 2013; 128:2016–2025.
2. De Tombe PP *et al.* The cytoskeleton and the cellular transduction of mechanical strain in the heart: a special issue. *Pflugers Arch.* 2011; 462:1–2.
3. Fukuda N *et al.* Physiological functions of the giant elastic protein titin in mammalian striated muscle. *J Physiol Sci*. 2008; 58:151–159.
4. Li S *et al.* Comprehensive analysis of titin protein isoform and alternative splicing in normal and mutant rats. *J. Cell. Biochem.* 2012; 113:1265–1273.
5. Hidalgo CG *et al.* PKCA phosphorylation of titin's PEVK element: a novel and conserved pathway for modulating myocardial stiffness. *Circ. Res.* 2009; 105:631–638, 17 p following 638.
6. Yamasaki R *et al.* Protein kinase A phosphorylates titin's cardiac-specific N2B domain and reduces passive tension in rat cardiac myocytes. *Circ. Res.* 2002; 90:1181–1188.
7. Borbély A *et al.* Hypophosphorylation of the Stiff N2B titin isoform raises cardiomyocyte resting tension in failing human myocardium. *Circ. Res.* 2009; 104:780–786.
8. Boontje NM *et al.* Enhanced myofilament responsiveness upon β-adrenergic stimulation in post-infarct remodeled myocardium. *J. Mol. Cell. Cardiol.* 2011; 50:487–499.
9. Wijnker PJM *et al.* Protein phosphatase 2A affects myofilament contractility in non-failing but not in failing human myocardium. *J. Muscle Res. Cell. Motil.* 2011; 32:221–233.
10. Kooij V *et al.* Effect of troponin I Ser23/24 phosphorylation on Ca2+-sensitivity in human myocardium depends on the phosphorylation background. *J. Mol. Cell. Cardiol.* 2010; 48:954–963.
11. Solaro RJ *et al.* Phosphorylation of troponin I and the inotropic effect of adrenaline in the perfused rabbit heart. *Nature*. 1976; 262:615–617.
12. Solaro RJ *et al.* The unique functions of cardiac troponin I in the donor of cardiac muscle contraction and relaxation. *Biochem Biophys Res Commun*. 2008; 369:82–87.
13. Moon MR *et al.* Differential calcium handling in two canine models of right ventricular pressure overload. *J. Surg. Res.* 2012; 178:554–562.
14. Hadri L *et al.* Therapeutic Efficacy of AAV1. SERCA2a in Monocrotaline-Induced Pulmonary Arterial Hypertension. *Circulation*. 2013; 128:512–523.
15. Quaile MP *et al.* Reduced sarcoplasmic reticulum Ca(2+) load mediates impaired contractile reserve in right ventricular pressure overload. *J. Mol. Cell. Cardiol.* 2007; 43:552–563.
16. Sande JB *et al.* Reduced level of serine(16) phosphorylated phospholamban in the failing rat myocardium: a major contributor to reduced SERCA2 activity. *Cardiovasc. Res.* 2002; 53:382–391.
17. Wang Z *et al.* Na+-Ca2+ exchanger remodeling in pressure overload cardiac hypertrophy. *J. Biol. Chem.* 2001; 276:17706–17711.
18. Lahmers S *et al.* Developmental donor of titin isoform expression and passive stiffness in fetal and neonatal myocardium. *Circ. Res.* 2004; 94:505–513.
19. Van der Velden J *et al.* Effect of protein kinase A on calcium sensitivity of force and its sarcomere length dependence in human cardiomyocytes. *Cardiovasc. Res.* 2000; 46:487–495.
20. Hamdani N *et al.* Distinct myocardial effects of beta-blocker therapy in heart failure with normal and reduced left ventricular ejection fraction. *Eur. Heart J.* 2009; 30:1863–1872.
21. Hudson B *et al.* Hyperphosphorylation of mouse cardiac titin contributes to transverse aortic constriction-induced diastolic dysfunction. *Circ. Res.* 2011; 109:858–866.
22. Kötter S *et al.* Differential changes in titin domain phosphorylation increase myofilament stiffness in failing human hearts. *Cardiovasc. Res.* 2013; 99:648–656.
23. Krüger M *et al.* Protein kinase G modulates human myocardial passive stiffness by phosphorylation of the titin springs. *Circ. Res.* 2009; 104:87–94.
24. Raskin A *et al.* A novel mechanism involving four-and-a-half LIM domain protein-1 and extracellular signal-regulated kinase-2 regulates titin phosphorylation and mechanics. *J. Biol. Chem.* 2012; 287:29273–29284.
25. Hidalgo CG *et al.* The multifunctional Ca(2+)/calmodulin-dependent protein kinase II delta (CaMKIIδ) phosphorylates cardiac titin's spring elements. *J. Mol. Cell. Cardiol.* 2013; 54:90–97.
26. Hamdani N *et al.* Crucial role for Ca2(+)/calmodulin-dependent protein kinase-II in regulating diastolic stress of normal and failing hearts via titin phosphorylation. *Circ. Res.* 2013; 112:664–674.
27. Hidalgo C *et al.* Tuning the molecular giant titin through phosphorylation: role in health and disease. *Trends Cardiovasc. Med.* 2013; 23:165–171.

28. Van der Velden J. Diastolic myofilament dysfunction in the failing human heart. *Pflugers Arch.* 2011; 462:155–163.
29. Bers DM. Cardiac excitation-contraction coupling. *Nature*. 2002; 415:198–205.
30. De Man FS *et al.* Neurohormonal axis in patients with pulmonary arterial hypertension: friend or foe? *Am. J. Respir. Crit. Care Med.* 2013; 187:14–19.
31. Bristow MR *et al.* Beta 1- and beta 2-adrenergic-receptor subpopulations in nonfailing and failing human ventricular myocardium: coupling of both receptor subtypes to muscle contraction and selective beta 1-receptor down-regulation in heart failure. *Circ. Res.* 1986; 59:297–309.
32. De Man FS *et al.* Bisoprolol delays progression towards right heart failure in experimental pulmonary hypertension. *Circ Heart Fail*. 2012; 5:97–105.
33. Bogaard HJ *et al.* Adrenergic receptor blockade reverses right heart remodeling and dysfunction in pulmonary hypertensive rats. *Am. J. Respir. Crit. Care Med.* 2010; 182:652–660.
34. McCain ML *et al.* Mechanotransduction: the role of mechanical stress, myocyte shape, and cytoskeletal architecture on cardiac function. *Pflugers Arch*. 2011; 462:89–104.

Chapter 4

Fibrosis- and cardiomyocyte-mediated stiffness in pulmonary arterial hypertension

Rain S, Andersen S, Schultz JG, da Silva Gonçalves Bos D, Handoko ML, Westerhof N, Bogaard HJ, Vonk-Noordegraaf A, Andersen A, van der Velden J, Ottenheijm CA, de Man FS.

Circulation Heart Failure – in revision

ABSTRACT

Background – The purpose of this study was to determine the relative contribution of fibrosis-mediated and cardiomyocyte-mediated stiffness in rats with mild and severe right ventricular (RV) dysfunction.

Methods and Results – By performing pulmonary artery banding of different diameters for 7 weeks, mild RV dysfunction (Ø=0.6mm) and severe RV dysfunction (Ø=0.5mm) was induced in rats.
The relative contribution of fibrosis- and cardiomyocyte-mediated RV stiffness was determined in RV trabecular strips. Total myocardial stiffness was increased in trabeculae from both mild and severe RV dysfunction in comparison to controls. In severe RV dysfunction, increased RV myocardial stiffness was explained by both increased fibrosis- and cardiomyocyte-mediated stiffness, whereas in mild RV dysfunction only cardiomyocyte-mediated stiffness was increased in comparison to control. Histological analyses revealed that RV fibrosis gradually increased with severity of RV dysfunction, whereas the ratio of collagen I/III expression was only elevated in severe RV dysfunction. Stiffness measurements in single demembranated RV cardiomyocytes demonstrated a gradual increase in RV cardiomyocyte stiffness, which was partially restored by protein kinase A in both mild and severe RV dysfunction. Increased expression of compliant titin isoforms was observed only in mild RV dysfunction, whereas titin phosphorylation was reduced in both mild and severe RV dysfunction.

Conclusions – RV myocardial stiffness is increased in rats with mild and severe RV dysfunction. In mild RV dysfunction, stiffness is mainly determined by increased cardiomyocyte stiffness. In severe RV dysfunction, both cardiomyocyte and fibrosis-mediated stiffness contribute to increased RV myocardial stiffness.

INTRODUCTION

Pulmonary arterial hypertension (PAH) patients develop right heart failure (RHF) due to a progressive increase in right ventricular (RV) pressure overload.[1] Although it is known for some years that RV systolic adaptation is of clinical importance, it just recently became clear that RV diastolic stiffness increases and may contribute to disease progression in PAH.[2] In addition, we have previously shown that RV diastolic stiffness was closely associated with a doubling in sarcomere-derived cardiomyocyte stiffness and increased myocardial fibrosis in end-stage PAH-patients.[2,3]

Changes in cardiomyocyte stiffness are closely regulated by the giant elastic protein titin.[4] Titin stiffness can be regulated via both post-transcriptional and post-translational modifications. Post-transcriptional modification includes a shift from the compliant N2BA isoform to the stiffer N2B isoform.[5] Post-translational modification is mainly regulated via phosphorylation of titin by the protein kinases A, G and C (PKA, PKG, PKC, respectively). Titin phosphorylation by PKA and PKG reduce cardiomyocyte stiffness, whereas PKC-mediated titin phosphorylation results in increased RV diastolic stiffness.[6-10] We have previously demonstrated that in end-stage PAH, no alterations in titin isoform composition are observed, whereas PKA-mediated titin phosphorylation was significantly reduced.[2-3]

Changes in fibrosis could also contribute to diastolic stiffness, and involve differences in collagen fiber type secretion, collagen type I/III ratio, cross-linking or degradation.[11-13] Previous studies found a positive correlation between markers of collagen degradation measured in the serum of PAH patients and the severity of the disease.[14] In addition, late gadolinium enhancement studies in PAH patients further indicate a positive association between RV fibrosis and worsening of RV function.[15-16]

However, the functional relevance of increased fibrosis and cardiomyocyte stiffness to RV diastolic stiffness remains to be elucidated. Moreover, it is currently unclear whether diastolic stiffening of the RV already occurs at earlier stages of PAH-induced right heart failure, because obtaining human RV tissue is only limited to end-stage PAH due to the risks of performing RV biopsies in vivo.

To mimic disease severity observed in PAH patients, a novel rat model of pressure-overload-induced RV remodeling was developed.[17] By performing pulmonary artery banding (PAB) of different diameters 2 phenotypes were created:

1. mild RV dysfunction, induced by a moderate increase in RV afterload / RV systolic pressure (RVSP) resulting in reduced RV ejection fraction (RVEF) but without extra-cardiac signs of right heart failure;
2. severe RV dysfunction, induced by a further increase in RV afterload resulting in a severe reduction in RVEF.[17]

Thus, the aim of this study was to determine the relative contribution of fibrosis-mediated and cardiomyocyte-mediated RV myocardial stiffness in rats with mild and severe RV dysfunction.

METHODS

Study design

We used rat RV trabecular tissue obtained from a previous study protocol (Andersen S et al. J Card Fail, 2014).[17] 15 male Wistar Galas rats were used for this study (M&B

Taconic, Ry, Denmark). The rats were handled according to the Danish national guidelines and experiments were accepted in agreement with the Danish law for animal research (authorization number 2012-15-2934-00384 Danish Ministry of Justice). Rats weighting 105±30g at start of the study protocol underwent pulmonary artery banding (n=10), where a lateral thoracotomy was performed in previously sedated, intubated and mechanically ventilated state (Abbot Scandinavia AB, Solona, Sweden – induction 7% 2:1 O2/N2O, maintenance 3.5% 2:1 O2/N2O) and a titanium clip of different diameters (0.5mm or 0.6mm) was introduced and closed around the pulmonary trunk. All rats received buprenophine (Termgesic, RB Pharmaceuticals, Berkshire) in order to relieve postoperative pain. Control rats were sham operated (n=5). The 0.6 mm clip led to mild RV dysfunction (n=5) and the 0.5mm clip led to severe RV dysfunction (n=5). After 7 weeks of pulmonary artery banding, all animals underwent hemodynamic assessment as described previously and RV tissue was harvested for further analyses.[17] RV trabecular samples were dissected from the RV free wall and immediately transferred to a 50% relax-glycerol solution containing of 50% (vol/vol) Glycerol, relaxing solution (pCa = 9.0; 100 mM BES; 6.97 mM EGTA; 6.48 mM $MgCl_2$; 5.89 mM Na_2-ATP; 40.76 mM K-propionate14.50 mM creatine phosphate) and protease and phosphatase inhibitors (0.5 mM E64, 2.0 mM Leupeptine, 1 mM DTT and 0.5 mM PMSF) and placed for 12h on a roller bank at 4 ^{o}C. Subsequently, RV trabecular tissue was stored at -20 ^{o}C in a 50% relax-glycerol solution containing low concentrations of protease and phosphatase inhibitors (0.05 mM E64, 0.2 mM Leupeptine, 1 mM DTT and 0.5 mM PMSF). The rest of the RV was snap-frozen in liquid nitrogen and stored at -80^{o}C.

Force measurements on skinned muscle strips

Thin muscle strips with an average length of 1mm and diameter of ~ 0.2mm were dissected respecting the longitudinal orientation of the fibers.[18-21] The ends of the strips were attached to aluminum T clips and membrane-permeabilized in a relaxing solution containing 1% Triton X-100. The strips were mounted between a length motor (ASI 403A, Aurora Scientific Inc, Ontario, Canada) and a force transducer (ASI 315C-I, Aurora Scientific Inc) in the set-up (ASI 802D, Aurora Scientific Inc) and viewed on an inverted microscope (Zeiss Axio Observer A1).

The solutions used during the experiments were:
1) relaxing solution: pCa = 9.0 (100 mM BES; 6.97 mM EGTA; 6.48 mM $MgCl_2$; 5.89 mM Na_2-ATP; 40.76 mM K-propionate14.50 mM creatine phosphate);
2) pre-activating solution with low EGTA concentration (100 mM BES; 0.1 mM EGTA; 6.42 mM $MgCl_2$; 5.87 mM Na_2-ATP; 41.14mM K-propionate; 14.50 mM creatine phosphate; 6.9 mM HDTA);
3) activating solution: pCa = 4.5 (100 mM BES; 7.0 mM Ca-EGTA; 6.28 mM $MgCl_2$; 5.97 mM Na_2-ATP; 40.64 mM K-propionate; 14.5 mM creatine phosphate).

The integrity of the trabecular muscle strip was checked prior to the stiffness determination by activating the preparation. Thereafter the trabecular strip was transferred to a relaxing solution where it was stretched by 20% from the initial slack-length with a speed of stretch of 10% preparation length per second. Passive force was recorded at the end of stretch and divided by the corresponding strip cross-sectional

area to normalize for variation in trabecular strip diameters (passive tension (kN/m^2) = *total RV myocardial stiffness*). In order to determine the relative contribution of fibrosis and cardiomyocytes to total RV myocardial stiffness, thick and thin filaments were extracted by immersing the muscle strips in relaxing solution containing 0.6M KCl (60 minutes at 20°C) followed by a relaxation solution containing 1M KI (60 minutes at 20°C).refs Subsequently, the muscle strips were transferred to fresh relaxing solutions and passive force development was measured again at the end of the 20% stretch and was assumed to represent *fibrosis-mediated stiffness*. *Cardiomyocyte-mediated stiffness* was determined as total RV myocardial stiffness minus fibrosis-mediated stiffness.[18-21]

RV fibrosis

Absolute RV myocardial fibrosis content was determined on histological sections as previously described.[2,17,22-23] Collagen I and III mRNA levels were quantified by real-time PCR (7900 HT Applied Biosystem) using 5µL of gene expression master mix, 1µL cDNA and 0.5µL of the gene expression assay for CollagenIA1 (Rn0143848-m1) and CollagenIIIA1 (Rn01437683-m1) in a final volume of 10 µL. The house keeping gene GAPDH (Rn99999916-s1) was used as an internal control. Collagen I/III ratio was calculated for each sample.

Force measurements on skinned cardiomyocyte

Small RV myocardial pieces were defrosted in relaxing solution and single cardiac cells were isolated mechanically as previously described (Control n=3, mild RV dysfunction n=3 and severe RV dysfunction n=3 samples).[2] A minimum of 3 cells per sample were used to determine cardiomyocyte stiffness and their averages were used for further statistical analysis. Cardiomyocytes were incubated for 5 minutes in relaxing solution containing 0.5% Triton X-100 in order to permeabilize the cellular membrane. To remove Triton, cardiomyocytes were washed six times with relaxing solution.

A single cardiomyocyte was attached with silicone adhesive between a force transducer and a piezoelectric motor. Diastolic stiffness was determined in the relaxing solution at increasing sarcomere lengths (1.8 – 2.4 µm). Cardiomyocytes were further incubated in relaxing solution with PKA (Protein-Kinase-A Catalytic subunit from bovine heart, P2645, Sigma Aldrich) at 20°C for 40 minutes and passive tension was again recorded after PKA treatment.

Individual force values were normalized for the cardiomyocyte width and depth recorded at 2.2µm sarcomere length.

Titin isoform and phosphorylation

To determine titin isoform expression and phosphorylation, frozen RV free-wall tissue samples of control rats, rats with mild RV dysfunction and rats with severe RV dysfunction were weighed and pulverized in liquid nitrogen using a mortar and a pestle. Tissue powder was solubilized using a 8M urea buffer with DTT and 50% glycerol solution and protease inhibitors (0.16 mmol/L Leupeptin, 0.04 mmol/L E-64 and 0.2 mmol/L PMSF).[2-3]

Increasing sample volumes (3 - 4.5 -6 – 7.5 - 9µL) were loaded on 1% agarose gels and stained with Coomassie Blue. The slope of the protein band intensity – volume loading was used for titin isoforms quantification. The N2BA/Total Titin ratio was calculated.[2]

ProQ Diamond Phosphoprotein Stain was used to determine titin phosphorylation. Gels were fixed, washed, distained and stained with SYPRO Ruby to determine total protein amount. The ratio between phosphorylation (ProQ) and total protein content (Sypro) was used to quantify differences in titin phosphorylation.[2]

Statistical analyses

Statistical analyses were performed using Prism 5 for Windows (GraphPad Software Inc, San Diego, CA). P-values lower than 0.05 were considered significant. All data are presented as mean ± SEM.

All analyses were performed using one-way ANOVA with Bonferroni post-hoc comparison between control, mild and severe RV dysfunction, unless stated otherwise. The effects of PKA incubation on single RV cardiomyocytes of rats with mild RV dysfunction and severe RV dysfunction were tested at a sarcomere length of 2.2 using a two-way repeated measures ANOVA followed by Bonferroni post-hoc test.

RESULTS

Figure 1 – RV myocardial stiffness in skinned trabecular strips

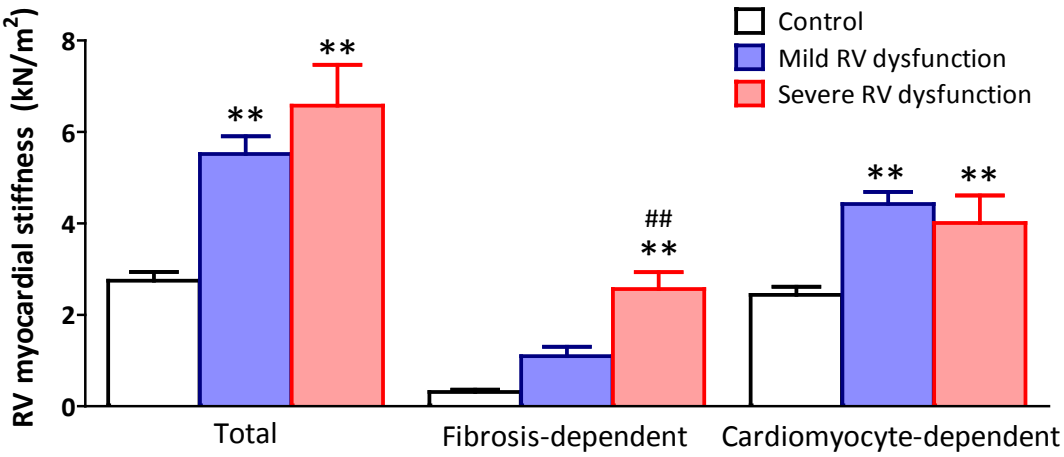

Total RV myocardial stiffness was significantly increased in both mild RV dysfunction and severe RV dysfunction in comparison to controls. In severe RV dysfunction, increased RV myocardial stiffness could be explained by both increased fibrosis- and cardiomyocyte-mediated stiffness, whereas in mild RV dysfunction only cardiomyocyte-mediated stiffness was increased in comparison to control.
Data presented as mean ± SEM, Controls: n=5, mild RV dysfunction: n=5 and severe RV dysfunction: n=5. **: $p<0.01$ vs. control; ##: $p<0.01$ vs. mild RV dysfunction, Bonferroni corrected.

Relative contribution of fibrosis- and cardiomyocyte-mediated stiffness

RV diastolic stiffness was measured on small RV muscle strips of control rats (n=5; RVSP: 30±1 mmHg; RVEF: 74±1%), rats with mild RV dysfunction (n=5; RVSP: 84±8 mmHg; RVEF: 55±2%; both $p<0.01$ vs. control) and rats with severe RV dysfunction (n=5; RVSP: 115±8 mmHg; RVEF: 45±3%; both $p<0.001$ vs. control, $p<0.05$ vs. mild RV dysfunction).

As can be observed in Figure 1, RV myocardial stiffness was significantly increased in both rats with mild and rats with severe RV dysfunction in comparison to controls ($p<0.05$).

To determine the separate contribution of fibrosis on RV myocardial stiffness, the sarcomeric component of the tissue was extracted by KI/KCl treatment. This treatment disrupts titin anchoring to the thick filament and thereby eliminates the contribution of sarcomeric stiffness to the overall muscle strip stiffness, the residual stiffness being attributed to the fibrotic component. We found a stepwise increase in fibrosis-mediated stiffness with a moderate increase in fibrosis-mediated stiffness in rats with mild RV dysfunction, and a further significant increase in fibrosis-mediated stiffness in rats with severe RV dysfunction. Subsequently, cardiomyocyte-derived stiffness was calculated by subtracting fibrosis stiffness from total stiffness. RV cardiomyocyte-derived stiffness was increased in all rats with RV dysfunction independent of the severity of the RV dysfunction.
These data suggests that RV myocardial stiffness is closely associated with RV dysfunction. RV cardiomyocyte stiffness contributes to RV myocardial stiffness in both mild and severe RV dysfunction, whereas fibrosis-mediated stiffness led to a further increase in RV myocardial stiffness in rats with severe RV dysfunction only.

RV fibrosis
To explain the increasing contribution of fibrosis-mediated stiffness with the severity of RV dysfunction, we further investigated the presence of fibrotic areas in the RV free wall. As observed previously, the percentage of fibrosis gradually increased with the severity of RV dysfunction (Fig. 2A).[17]

Figure 2 – RV fibrosis and collagen I/III ratio

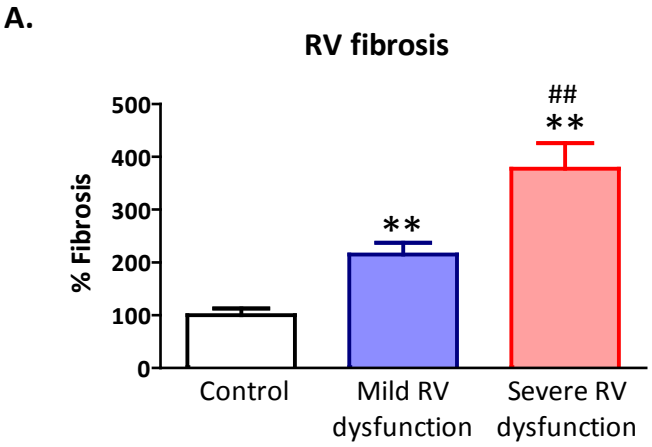

A. (Results from Andersen et al, J Card Fail, 2014) RV histology sections were stained for collagen using a Picrosirius red staining and analyzed under double-polarized light. A gradual increase in RV fibrosis was found in mild and severe RV dysfunction in comparison to control. Data presented as % of controls.

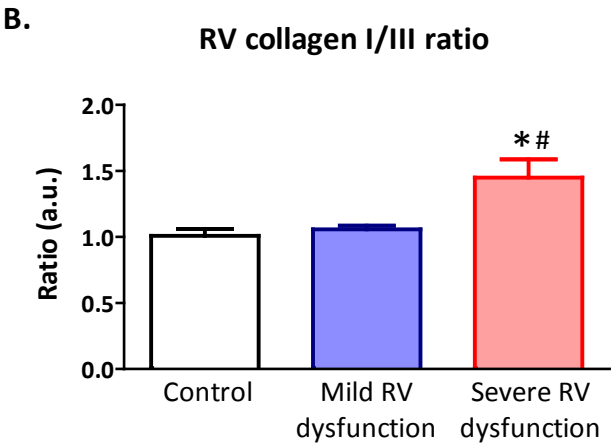

B. Collagen type I and III mRNA expression was determined by qPCR and the collagen I/III ratio was calculated. Collagen I/III expression was significantly increased in severe RV dysfunction.
Data presented as mean ± SEM, Controls: n=5, mild RV dysfunction: n=5 and severe RV dysfunction: n=5. *: $p<0.05$, **: $p<0.01$ vs. control, #: $p<0.05$, ##: $p<0.01$ vs. mild RV dysfunction, Bonferroni corrected.

Fibrosis-mediated RV myocardial stiffness can further be influenced by the predominant type of collagen fibers expressed, where increased collagen I/III ratio is known to be associated with increased myocardial stiffness.[12] Interestingly, RV collagen I/III ratio was only increased in rats with severe RV dysfunction (Fig.2B). These data suggest that the increased fibrosis-mediated stiffness is a consequence of increased fibrosis and increased collagen I/III expression in the right ventricle of rats with severe RV dysfunction.

RV cardiomyocyte-mediated stiffness

To investigate in more detail the cardiomyocyte-derived stiffness, we subsequently determined cardiomyocyte stiffness in single membrane-permeabilized RV cardiomyocytes from control rats, rats with mild RV dysfunction and rats with severe RV dysfunction. As can be observed in Figure 3A, RV cardiomyocyte mediated stiffness gradually increased with the severity of RV dysfunction. Especially at sarcomere length 2.2 and 2.4 µm, RV cardiomyocyte stiffness was increased in rats with severe RV dysfunction in comparison to rats with mild RV dysfunction (Fig. 3A,B). To investigate whether reduced PKA-mediated phosphorylation of the giant elastic filament titin may contribute to the observed increased RV cardiomyocyte stiffness, measurements of RV cardiomyocyte stiffness were repeated after PKA-incubation. As can be observed in Figure 3C, PKA-incubation resulted in a reduction in RV cardiomyocyte stiffness, but it remained elevated in comparison to control. In addition, the effect of PKA-incubation in rats with severe RV dysfunction was larger than in mild RV dysfunction or controls ($p_{interaction}<0.01$; Fig. 3D), suggesting that PKA-mediated phosphorylation of sarcomeric proteins is more hampered in RV cardiomyocytes of rats with severe RV dysfunction.

Figure 3 – Skinned cardiomyocytes

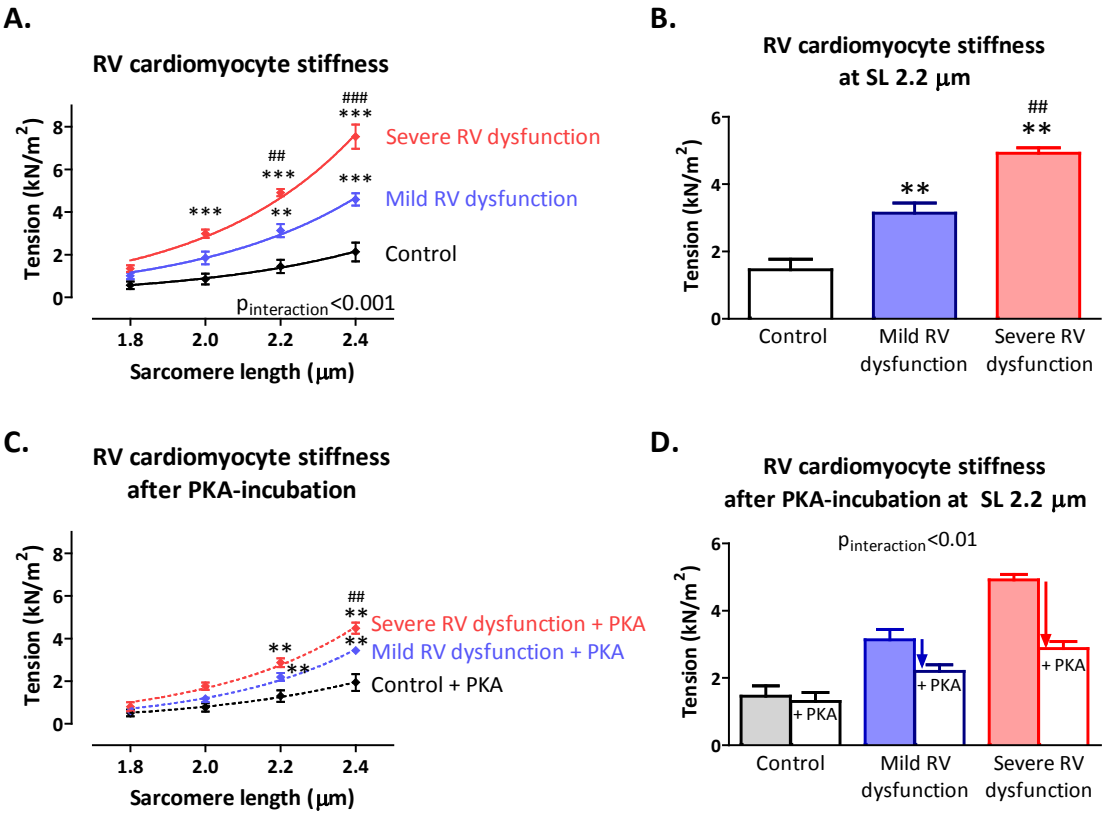

A, B. RV cardiomyocyte stiffness was gradually increased in mild and severe RV dysfunction in comparison to control.
C, D. Protein kinase A incubation significantly decreased cardiomyocyte stiffness in mild and severe RV dysfunction, but remained significantly elevated in comparison to controls.
Data presented as mean ± SEM, Controls: n=3, mild RV dysfunction: n=3 and severe RV dysfunction: n=3. **: p<0.01, ***: p<0.001 vs. control; ##: p<0.01, ###: p<0.001 vs. mild RV dysfunction, Bonferroni corrected.

Titin isoform and phosphorylation

To further explain the findings of RV cardiomyocyte stiffness we investigated whether titin isoform composition or titin phosphorylation was altered in RV dysfunction. We observed an increase in expression of the compliant titin isoform (N2BA) in rats with mild RV dysfunction, whereas titin isoform composition was unaltered in rats with severe RV dysfunction (Fig. 4A). Subsequently, we determined overall phosphorylation levels of titin (ProQ Diamond staining) normalized to total protein content (Sypro Ruby staining). Titin phosphorylation was lower in both rats with mild or severe RV dysfunction (Fig. 4B). These data suggests that although more compliant titin isoform was expressed in rats with mild RV dysfunction, this compensatory mechanism was insufficient to prevent an increase in RV cardiomyocyte stiffness, probably due to a reduced phosphorylation of titin.

Figure 4 – RV titin isoform composition and titin phosphorylation

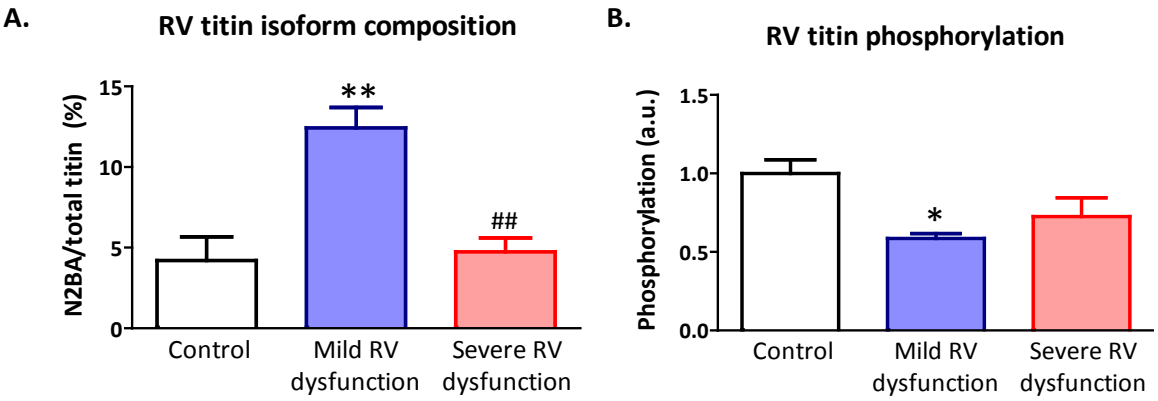

A. Titin isoform ratio determined on 1% agarose gels stained with Comassie Blue by dividing the N2BA isoform content to the more abundant N2B isoform and expressed in percentages. N2BA/Total Titin ratio was similar in Control and severe RV dysfunction, whereas elevated in mild RV dysfunction.
B. Total titin phosphorylation was determined by ProQ staining for phosphorylation divided by Sypro staining for total protein content. Titin phosphorylation was significantly lower both in mild and severe RV dysfunction.
Data presented as mean ± SEM, Controls: n=5, mild RV dysfunction: n=5 and severe RV dysfunction: n=5. *: $p<0.05$, **: $p<0.01$ vs. controls; ##: $p<0.01$ vs. mild RV dysfunction, Bonferroni corrected.

DISCUSSION

By combining RV cardiomyocyte mechanics with protein and histological analyses, we demonstrated that:

- RV myocardial stiffness is increased in both mild and severe RV dysfunction; cardiomyocyte-derived stiffness contributes to both mild and severe RV dysfunction, whereas fibrosis-mediated stiffness plays an additional role in severe RV dysfunction.
- RV fibrosis-mediated stiffness is associated with gradually increased fibrosis deposition in mild and severe RV dysfunction, and increased collagen I/III ratio in rats with severe RV dysfunction.
- RV cardiomyocyte-mediated stiffness gradually increases with severity of RV dysfunction. Probably explained by the finding that phosphorylation of titin was reduced in both mild and severe RV dysfunction, whereas titin isoform composition was only changed in mild RV dysfunction towards more compliant titin.

Fibrosis-mediated stiffness

The role of fibrosis in RV remodeling in PAH is inconclusive. With imaging techniques, fibrotic areas are only observed in the insertion points between the septum and right ventricular wall.[15-16] Whereas in tissue of PAH-patients with end-stage right heart failure and in several PAH animal models, RV fibrosis is either absent or mildly increased in the RV free wall.[2,22-28] However, until now it was unclear whether the observed increase in RV fibrosis had any functional consequence. We demonstrate in this study for the first time that increased RV fibrosis, especially in rats with severe RV dysfunction, significantly impairs RV diastolic function. Besides histologically observed

increase in RV fibrosis, we could also demonstrate that a shift in collagen isoform expression occurred. Because increased fibrosis-mediated stiffness, increased fibrosis and collagen I/III isoform shift occurred mainly in rats with severe RV dysfunction, the presence of RV fibrosis may be used as a tool to predict deterioration of RV function in PAH-patients. This suggestion is further supported by the recent finding of Safdar et al, that a biological marker of collagen metabolism (N-terminal pro-peptide of type III procollagen) could be used to predict prognosis and disease progression in PAH-patients.[14] In addition, the development of more advanced imaging modalities may further improve the sensitivity to detect RV fibrosis in PAH-patients which may be used to predict RV dysfunction in future.[29]
The underlying mechanism of increased RV fibrosis in RV dysfunction remains elusive. One may speculate that increased neurohormonal activity could play a role.[30] Previously, we have shown increased activation of the renin-angiotensin-aldosterone system, which was closely associated with disease progression.[31] Increased levels of angiotensin II could lead to the activation of TGF-β and increased collagen production by RV fibroblasts.[13, 32-33] Furthermore, overactive RAAS could also increase RV fibrosis via aldosterone signaling pathways via the activation of mitogen-activated protein kinases (MAPKs), including extracellular signal-regulated kinases (ERK1/2) with a net effect of increased mRNA levels of types I, III, and IV collagen.[13,33] But further studies are needed to determine the exact underlying mechanism of RV fibrosis in PAH which could further be used as therapeutic target.

Cardiomyocyte mediated stiffness
In the present study, we determined the contribution of cardiomyocyte-derived stiffness in two ways: 1. By subtracting fibrosis-mediated stiffness from total RV myocardial stiffness of RV trabecular muscle strips; 2. By measuring cardiomyocyte stiffness in single demembranated single RV cardiomyocytes. Interestingly, no difference in cardiomyocyte-derived RV diastolic stiffness was observed in trabecular muscle strips of mild versus severe RV dysfunction, whereas on single cardiomyocyte level we observed a further increase in RV myocardial stiffness in severe RV dysfunction compared to mild RV dysfunction. The cardiomyocyte stiffness derived from the trabecular stiffness may be underestimated due to the normalization of the stiffness to the trabecular cross-sectional area, which includes not only cardiomyocytes, but also the fibrotic component. Since the collagen fraction is increased in severe RV dysfunction, we expect that the area of the total cross-sectional area occupied by cardiomyocytes is smaller, leading to an underestimation of the overall cardiomyocyte stiffness (Fig. 5).

The giant sarcomeric protein titin is an important regulator of cardiomyocyte-mediated stiffness.[4] Changes in titin phosphorylation or titin isoform composition contributes closely to stiffening of cardiomyocytes. In this study, we observed that overall titin phosphorylation was reduced in both mild and severe RV dysfunction. Although PKA-mediated titin phosphorylation could not be specifically measured in rat RV tissue, the reduction observed in RV diastolic stiffness after PKA-incubation suggests that the reduced titin phosphorylation is partly mediated by reduced PKA-activity in both mild and severe RV dysfunction. A decreased intracellular PKA-mediated phosphorylation of titin could be a direct consequence of the downregulation

and desensitization of the β-adrenergic receptor pathway.[6,34] However, PKA-incubation could not fully restore RV myocardial stiffness indicating that other kinases and/or post-translational modifications may play an additional role.

Figure 5 – Components of trabecular stiffness

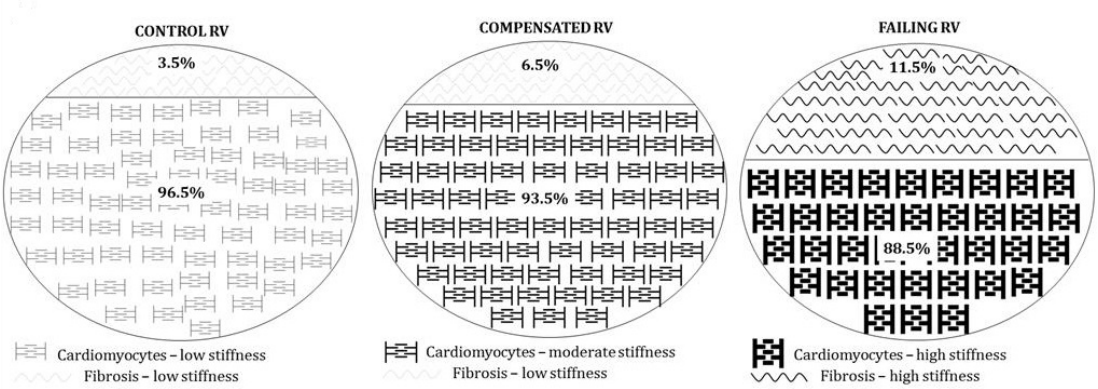

Schematic representation of the relative contribution of fibrosis and cardiomyocytes to trabecular stiffness.

While titin phosphorylation was reduced in both mild and severe RV dysfunction, increased expression of the compliant titin isoform was observed only in rats with mild RV dysfunction and unaltered in rats with severe RV dysfunction. This is in line with our previous data from tissue of patients with end-stage right heart failure, in which we did not observe any change in titin isoform expression compared to control samples.[2] This may suggest that titin isoform switch is a dynamic process, which in mild RV dysfunction may play a protective role maintaining cardiomyocyte stiffness relatively low by enhancing the expression of the compliant N2BA isoform, whereas in later stages of RV dysfunction titin isoform composition reverses toward a N2BA/N2B ratios that are similar to those in controls.
In addition to a role in cardiomyocyte stiffness, important mechano-sensing properties and hypertrophy inducing signals have been associated with titin.[35-36] Therefore, changes in titin isoform and phosphorylation may not only increase cardiomyocyte stiffness, but also alter the capacity of the cardiomyocytes to correctly sense the afterload and stop the hypertrophic signaling triggered by the increase in RV wall stress. At this point the transition from a hypertrophic compensated RV phenotype to a dilative failing RV phenotype may occur.

Right ventricular versus left ventricular pressure overload

In PAH-patients, the right ventricle is exposed to an up to 4-fold increase in pressure.[34] This magnitude of pressure overload in PAH is much higher than observed in left ventricular pressure overload induced by, for example, hypertension or aortic stenosis. This may explain why some of our findings are not in line with previously published results on LV pressure overload. First of all, RV myocardial stiffness is increased in all severities of PAH, whereas in LV pressure overload increased myocardial stiffness is only observed in patients with hypertension and heart failure.[37-38] Secondly, increased expression of the more compliant titin isoform (N2BA) is frequently observed in

patients with decompensated LV pressure overload, whereas our study only observed a shift to the more compliant titin isoform in mild RV dysfunction and not in end-stage disease.[37,39-40]
Besides the magnitude of pressure overload, also embryological differences between the RV and LV may underlie the differential response to pressure overload.

Limitations
In order to determine the relative contributions of cardiomyocyte stiffness and fibrosis to RV myocardial stiffness, we isolated RV trabecular tissue, which we considered representative for the overall RV free wall morphological and molecular changes than papillary muscle strips. However, in contrast to strips of papillary muscles, trabecular muscle strips have a more heterogeneous fiber orientation with unevenly distributed sarcomeres, limiting accurate sarcomere length determination.[20] Therefore we performed our experiments at a 20% increase in slack length. As a consequence, it is possible that the sarcomere length may have been unevenly distributed between the experiments, with variable influence on the cardiomyocyte stiffness. Therefore, to accurately determine cardiomyocyte stiffness in relation to sarcomere length, we also isolated cardiomyocytes from the free wall and measured stiffness at increasing sarcomere lengths (from 1.8μm to 2.4μm).

Clinical implications
Although an abnormally high fibrotic response in severe RV dysfunction may imply that treatment should be directed toward reducing fibrosis, it is important to point out that cardiomyocyte stiffness is already increased in rats with mild RV dysfunction. Therefore, efforts should be directed toward improving lusitropy by targeting both the fibrotic component and cardiomyocyte stiffness. Restoring the neurohormonal-dependent cellular and extracellular signaling pathways by for instance beta-blocker therapy or RAAS-inhibitors has already been shown to be effective in reducing overall RV diastolic stiffness in PAH-animal models.[23,31] Whether this effect is mediated by reduction of both fibrosis and cardiomyocyte stiffness should be further investigated.

CONCLUSIONS

RV myocardial stiffness is increased in rats with mild and severe RV dysfunction. However, the underlying mechanism differs between the groups. RV myocardial stiffness in mild RV dysfunction is mainly contributed to cardiomyocyte-mediated stiffness as a consequence of hypophosphorylation of the giant elastic titin filament. In contrast, in severe RV dysfunction, RV myocardial stiffness is mediated by both cardiomyocyte- and fibrosis-mediated stiffness as a consequence of hypophosphorylation of titin and increased ratio of collagen I/III expression.

REFERENCES

1. Vonk-Noordegraaf A *et al.* Right heart adaptation to pulmonary arterial hypertension: physiology and pathobiology. *J Am Coll Cardiol.* 2013; 62:D22–33.
2. Rain S *et al.* Right ventricular diastolic impairment in patients with pulmonary arterial hypertension. *Circulation.* 2013; 128:2016–25, 1–10.
3. Rain S *et al.* Protein changes contributing to right ventricular cardiomyocyte diastolic dysfunction in pulmonary arterial hypertension. *J Am Heart Assoc.* 2014; 3:e000716.
4. LeWinter MM *et al. Circulation.* 2010; 121:2137–45.
5. Trombitás K *et al.* Cardiac titin isoforms are coexpressed in the half-sarcomere and extend independently. *Am J Physiol Heart Circ Physiol.* 2001; 281:H1793–9.
6. Yamasaki R *et al.* Protein kinase A phosphorylates titin's cardiac-specific N2B domain and reduces passive tension in rat cardiac myocytes. *Circ Res.* 2002; 90:1181–8.
7. Krüger M *et al.* Protein kinase G modulates human myocardial passive stiffness by phosphorylation of the titin springs. *Circ Res.* 2009; 104:87–94.
8. Anderson BR *et al.* The effects of PKCalpha phosphorylation on the extensibility of titin's PEVK element. *J Struct Biol.* 2010; 170:270–7.
9. Hidalgo C *et al.* PKC phosphorylation of titin's PEVK element: a novel and conserved pathway for modulating myocardial stiffness. *Circ Res.* 2009; 105:631–8, 17 p following 638.
10. Hudson BD *et al.* Excision of titin's cardiac PEVK spring element abolishes PKCalpha-induced increases in myocardial stiffness. *J Mol Cell Cardiol.* 2010; 48:972–8.
11. Chapman D *et al.* Regulation of fibrillar collagen types I and III and basement membrane type IV collagen gene expression in pressure overloaded rat myocardium. *Circ Res.* 1990; 67:787–94.
12. Cleutjens JP *et al.* Collagen remodeling after myocardial infarction in the rat heart. *Am J Pathol.* 1995; 147:325–38.
13. Weber KT *et al.* Cardiac interstitium in health and disease: the fibrillar collagen network. *J Am Coll Cardiol.* 1989; 13:1637–52.
14. Safdar Z *et al.* Circulating collagen biomarkers as indicators of disease severity in pulmonary arterial hypertension. *JACC Heart Fail.* 2014; 2:412–21.
15. Blyth KG *et al.* Contrast enhanced-cardiovascular magnetic resonance imaging in patients with pulmonary hypertension. *Eur Heart J.* 2005; 26:1993–9.
16. Freed BH *et al.* Late gadolinium enhancement cardiovascular magnetic resonance predicts clinical worsening in patients with pulmonary hypertension. *J Cardiovasc Magn Reson.* 2012; 14:11.
17. Andersen S *et al.* Effects of bisoprolol and losartan treatment in the hypertrophic and failing right heart. *J Card Fail.* 2014; 20:864–73.
18. Hudson B *et al.* Hyperphosphorylation of mouse cardiac titin contributes to transverse aortic constriction-induced diastolic dysfunction. *Circ Res.* 2011; 109:858–66.
19. Wu Y *et al.* Changes in titin and collagen underlie diastolic stiffness diversity of cardiac muscle. *J Mol Cell Cardiol.* 2000; 32:2151–62.
20. Granzier HL *et al.* Passive tension in cardiac muscle: contribution of collagen, titin, microtubules, and intermediate filaments. *Biophys J.* 1995; 68:1027–44.
21. Hamdani N *et al.* Myocardial titin hypophosphorylation importantly contributes to heart failure with preserved ejection fraction in a rat metabolic risk model. *Circ Heart Fail.* 2013; 6:1239–49.
22. Handoko ML *et al.* Opposite effects of training in rats with stable and progressive pulmonary hypertension. *Circulation.* 2009; 120:42–9.
23. De Man FS *et al.* Bisoprolol delays progression towards right heart failure in experimental pulmonary hypertension. *Circ Heart Fail.* 2012; 5:97–105.
24. Overbeek MJ *et al.* Characteristics of interstitial fibrosis and inflammatory cell infiltration in right ventricles of systemic sclerosis-associated pulmonary arterial hypertension. *Int J Rheumatol*. 2010; pii: 604615.
25. Bogaard HJ *et al.* Adrenergic receptor blockade reverses right heart remodeling and dysfunction in pulmonary hypertensive rats. *Am J Respir Crit Care Med.* 2010; 182:652–60.
26. Bogaard HJ *et al.* Suppression of histone deacetylases worsens right ventricular dysfunction after pulmonary artery banding in rats. *Am J Respir Crit Care Med*. 2011; 183:1402–10.
27. Drake JI *et al.* Molecular signature of a right heart failure program in chronic severe pulmonary hypertension. *Am J Respir Cell Mol Biol.* 2011; 45:1239–47.

28. Bogaard HJ *et al.* Chronic Pulmonary Artery Pressure Elevation Is Insufficient to Explain Right Heart Failure. *Circulation.* 2009; 120:1951–60.
29. García-Álvarez A *et al.* Association of Myocardial T1-Mapping CMR With Hemodynamics and RV Performance in Pulmonary Hypertension. *JACC Cardiovasc Imaging.* 2015; 8:76–82.
30. De Man FS *et al.* Neurohormonal axis in patients with pulmonary arterial hypertension: friend or foe? *Am J Respir Crit Care Med.* 2013; 187:14–9.
31. De Man FS *et al.* Dysregulated Renin-Angiotensin-Aldosterone System Contributes to Pulmonary Arterial Hypertension. Am J Respir Crit Care Med. 2012; 186:780-9.
32. Horiguchi M *et al.* Matrix control of transforming growth factor-β function. *J Biochem* (Tokyo). 2012; 152:321–9.
33. Lijnen PJ *et al.* Stimulation of reactive oxygen species and collagen synthesis by angiotensin II in cardiac fibroblasts. *Cardiovasc Ther*. 2012; 30:e1–8.
34. Rain S *et al.* Pressure-overload-induced right heart failure. *Pflüg Arch Eur J Physiol*. 2014; 466:1055–63.
35. Linke WA *et al.* The giant protein titin as an integrator of myocyte signaling pathways. *Physiol Bethesda Md*. 2010; 25:186–98.
36. Granzier HL *et al.* Deleting titin's I-band/A-band junction reveals critical roles for titin in biomechanical sensing and cardiac function. *Proc Natl Acad Sci USA.* 2014; 111:14589–94.
37. Zile MR *et al.* Myocardial Stiffness in Patients with Heart Failure and a Preserved Ejection Fraction: Contributions of Collagen and Titin. *Circulation.* 2015; 114:013215.
38. Falcão-Pires I *et al.* Diabetes mellitus worsens diastolic left ventricular dysfunction in aortic stenosis through altered myocardial structure and cardiomyocyte stiffness. *Circulation.* 2011; 124:1151–9.
39. Borbély A *et al.* Cardiomyocyte stiffness in diastolic heart failure. *Circulation*. 2005; 111:774–81.
40. Van Heerebeek L *et al.* Myocardial structure and function differ in systolic and diastolic heart failure. *Circulation.* 2006; 113:1966–73.

Chapter 5

Pressure-overload induced right heart failure

Rain S[1,2], Handoko ML[1,3], Vonk Noordegraaf A[2], Bogaard HJ[2], van der Velden J[1], de Man FS[1,2]

Pflugers Arch. 2014
doi: **10.1007/s00424-014-1450-1**

ABSTRACT

Although pulmonary arterial hypertension originates in the lung and is caused by progressive remodeling of the small pulmonary arterioles, patients die from the consequences of pressure-overload-induced right heart failure. Prognosis is poor, and currently there are no selective treatments targeting the failing right ventricle. Therefore, it is of utmost importance to obtain more insights into the mechanisms of right ventricular adaptation and the transition toward right heart failure. In this review, we propose that the same adaptive mechanisms, which initially preserve right ventricular systolic function and maintain cardiac output, eventually initiate the transition toward right heart failure.

INTRODUCTION

Right heart failure can develop as a complication of numerous diseases, such as left-sided heart failure, congenital heart disease, and pulmonary arterial hypertension (PAH).[22] Although the origin of right heart failure in these conditions is distinctly different, the presence of right heart failure is the main determinant of prognosis in all patients.[22] Because selective treatments for the right ventricle are currently not available, it is essential to obtain more insights into the pathophysiology of right heart failure. This review will focus on right heart failure as a consequence of severe pressure overload as seen in patients with PAH. Several reviews are already available on the clinical aspects of PAH-induced right heart failure.[2,4,15,19,22,24,28,53,57,58,67-69] In the present review, we provide a perspective on how right ventricular (RV) adaptation is regulated in PAH and which mechanisms may be responsible for the transition from RV adaptation toward right heart failure.

Figure 1 – Relative increase in pressure overload, ventricular mass and wall stress

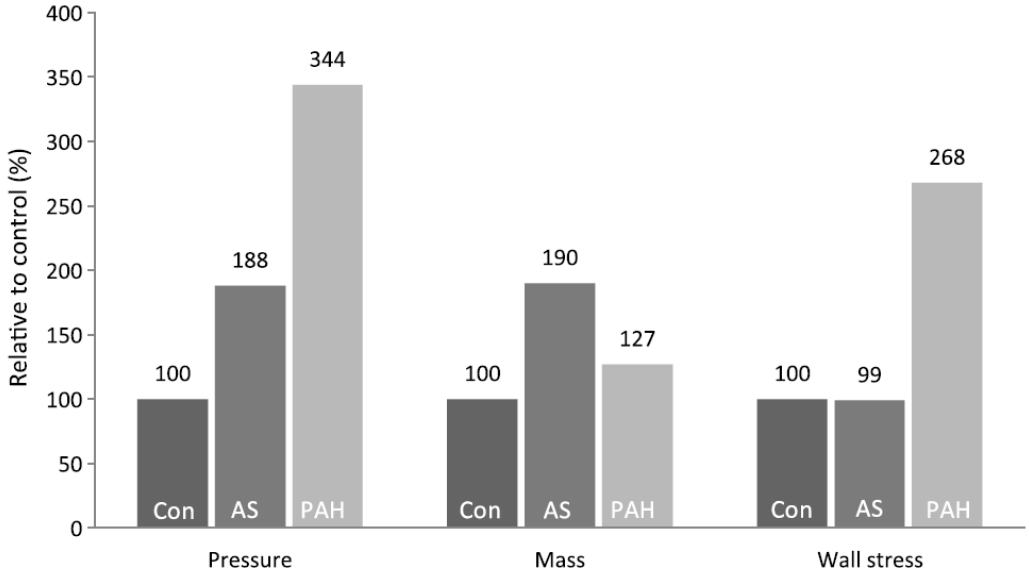

The magnitude of pressure overload for the right ventricle due to pulmonary arterial hypertension is of different order than the previously described pressure overload in the left ventricle due to aortic stenosis. Unless in both conditions, ventricular mass increases, this does not lead to a normalization of wall tension in right ventricular pressure overload in contrast to left ventricular pressure overload. This suggests that the response to pressure overload may differ between the right and left ventricle. Con control, AS aortic stenosis, PAH pulmonary arterial hypertension.[20,21]

Recent findings give us the opportunity to connect different molecular changes together and provide a novel-integrated physiological concept.

The right ventricle in normal physiology

The right ventricle originates from the anterior or secondary heart field, in contrast to the left ventricle, which originates from the primary heart field.[4,67] During fetal life, the right and left ventricles are equal with respect to free wall thickness and force development. After birth, and because of the drop in
pulmonary vascular resistance, the right ventricle regresses in size and becomes more crescent-like in shape.[23] The left ventricle remains a high-pressure pump and is therefore elliptic in shape with a thick wall. Shape importantly determines the differences in contraction patterns of both ventricles, which occur via lateral torsion and shortening in the left ventricle, as opposed to the longitudinal shortening of the right ventricle.[70]

Pulmonary arterial hypertension

PAH is a fatal disease characterized by abnormal remodeling of the pulmonary vessels resulting in a progressive increase in pulmonary artery pressures. The disease typically affects young women (female to male ratio of 2:1) with a median age at a diagnosis of 36 years.[29] Although PAH is primarily a lung disease, PAH almost invariably leads to right heart failure and death. Despite the wide range of therapeutic options, the prognosis of PAH patients is still unsatisfactorily low with an average life expectancy of only 3–5 years.[29] The only curative treatment currently available is lung transplantation. Lung transplantation can normalize RV afterload leading even to a total restoration of RV morphology and function.[33,42,47] Partial reductions in pulmonary vascular resistance, as achieved by currently available vascular-dilating treatment, are unfortunately insufficient to prevent progression of right heart failure in PAH patients.[66] More importantly, among patients, there is a wide heterogeneous response to pressure overload, which is independent to the load itself. This indicates that the right ventricle is a key player in the clinical outcome of PAH and a potential treatment target. As can be observed in Fig. 1, the magnitude of pressure overload is much higher in PAH (~340 %) compared with that of LV pressure overload induced by, for example, aortic stenosis (180 %).[20,21] In contrast, mass index, as a surrogate marker of hypertrophy, is higher in LV pressure overload than in RV pressure overload, resulting in an almost normalization of wall stress in LV pressure overload, whereas RV wall stress remains increased. These data illustrate the distinct differences in LVand RV pressure overload and infer that the mechanisms known to play a role in LV failure do not necessarily extrapolate to right heart failure. Load-independent right ventricular function RV function is closely related to the pulmonary vascular resistance in PAH patients. Indirect measures for systolic (RV ejection fraction, RVEF) and diastolic (right atrial pressure) RV function are widely used in the clinic and have proven their prognostic value.[16,48,49,72] However, for better understanding of the pathophysiology of right heart failure, these parameters are less accurate because of their high load dependency.[24] Pressure-volume analyses are the gold standard to measure cardiac function in a load independent manner.[71] In origin, pressure-volume analyses were performed on multiple pressure-volume loops obtained via vena cava occlusion to reduce preload.[13] Unfortunately, maneuvers to decrease ventricular blood supply cannot be performed without substantial risk in PAH patients who are already hemodynamically compromised. Therefore, single beat pressure-volume analysis methods were developed in order to circumvent the issue of preload reduction in

patients, yet quantifying RV function in a load-independent manner.[61,63] By combining RV pressure tracings with stroke volume (SV) measurements, end-systolic elastance (Ees, (Ees=Piso−RV end-systolic pressure)/SV) as a measure for RV systolic function, diastolic elastance (Ed (β), P=α(eVβ−1)) as a measure of RV diastolic function, and arterial elastance (Ea, Ea=RVSP/SV) as a measure of RV afterload can be quantified. In addition, by calculating the ratio of end-systolic elastance to arterial elastance (Ees/Ea), one can obtain insights into the adaptation of RV systolic function to its afterload.[10,52,65]

Animal models for right heart failure

Because RV tissue of PAH patients is scarce, the current pathophysiologic knowledge of PAH-induced right heart failure is mainly based on studies with animal models representing the clinical features of clinical RV hypertrophy and right heart failure. Moderate pulmonary artery banding, hypoxia, and low-dose monocrotaline (30/40 mg/kg) induce the characteristics of RV hypertrophy without the development of overt right heart failure.[1,6,25] High-dose monocrotaline (60–80 mg/kg), hypoxia in combination with Sugen 5416 (vascular endothelial growth factor (VEGF) receptor inhibitor), and severe pulmonary artery banding induce overt right heart failure. The advantage of pulmonary artery banding is that the effect of pressure overload on the right ventricle can be selectively investigated without the confounding systemic effects of toxins. While some animal models may be more suitable than others for the study of right heart failure, there is not an animal model which perfectly represents clinical PAH.[59] Therefore, it should be noted that part of the pathophysiological mechanisms described below still has to be confirmed in clinical PAH patients.

Right ventricular adaptation in pulmonary arterial hypertension

The adaptation of the right ventricle in PAH patients is mainly directed toward preserving systolic function to maintain cardiac output. This is demonstrated by pressure-volume analyses showing that end-systolic elastance as a measure of RVsystolic function is increased in PAH patients.[34,52] To maintain RV-arterial coupling (Ees/Ea ratio), the increase of end-systolic elastance has to be sufficient to adapt to the increased RVafterload (arterial elastance). To accomplish this, two important molecular regulatory mechanisms are activated:
(1) a glycolytic shift and an associated upregulation of hypoxia-inducible factor α (HIF-1α) mediated signaling resulting in increased RV capillarization (2) neurohormonal activation resulting in increased RV hypertrophy and RV contractility (Fig. 2).

RV capillarization

The right ventricle adapts to an increase in pressure overload by reducing the amount of energy needed to generate force. This is mainly accompanied by a reduced expression of alphamyosin heavy chain and overexpression of beta-myosin heavy chain.[37] In addition, a metabolic shift is observed preferring glycolysis to fatty acid oxidation, which requires less oxygen.[69] As a consequence of the mitochondrial suppression, pseudohypoxic signaling is activated. Thereby, HIF-1α axis is upregulated promoting RV capillarization by increasing VEGF expression and activity.[62] This angiogenic adaptation is essential to maintain the equilibrium between oxygen supply

and demand.[64] An increase in cell size due to hypertrophy will increase oxygen demand and diffusion distance, which should be adjusted for by increased oxygen supply.[55,73]

Figure 2 – Proposed mechanisms of right ventricular adaptation and maladaptation in pulmonary arterial hypertension

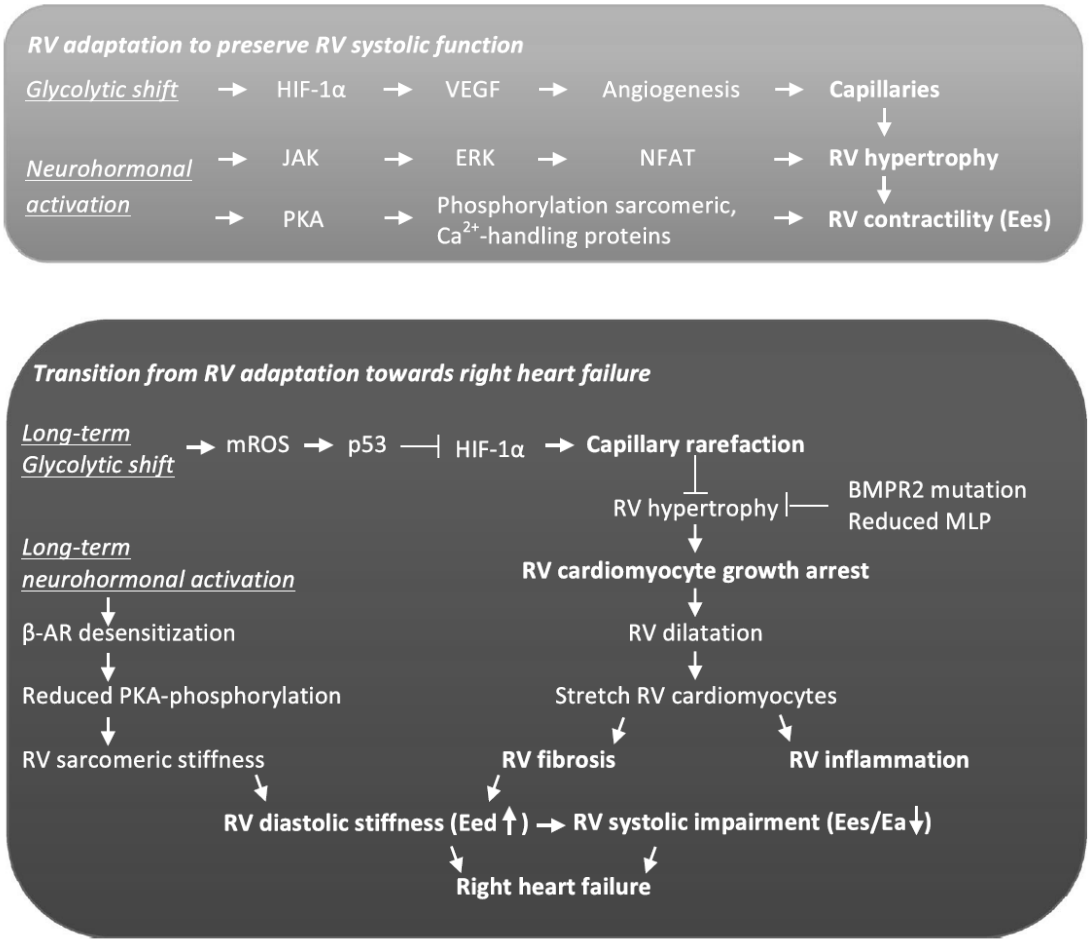

Right ventricular hypertrophy

RV pressure overload results in an increased RV wall stress, as described earlier. RV wall stress is an important trigger to induce hypertrophy.[21] Following Laplace's law, wall stress is dependent on pressure, radius, and thickness of the ventricle.[71] An increase in RV wall thickness by RV hypertrophy is an important adaptation mechanism in PAH. Both at the histological level as with noninvasive imaging techniques, it was demonstrated that RV mass is substantially increased in PAH patients.[48,52,55,72] There are two important mechanisms to induce hypertrophy as a consequence of increased wall stress (Fig. 3). First, cardiomyocytes facing increased wall stress release neurohormones such as angiotensin II, endothelin, and norepinephrine to induce hypertrophy via activation of the janus kinase 2 (JAK) and extracellular signal-regulated kinase (ERK).[26]

As a consequence, the transcription factor nuclear factor of activated T-cells (NFAT) is translocated from the cytosol to the nucleus initiating hypertrophy. Nagendran et al. recently provided evidence for neurohormone release by RV cardiomyocytes of PAH patients by demonstrating that endothelin-1 protein and receptor expression were increased and closely associated to RV hypertrophy in the RV tissue of PAH patients and a PAH animal model.[44]

Second, mechanosensing of the heart also plays an important role.[26] Increased stress is sensed by the extracellular matrix and transduced to the cytoskeleton via the integrin receptor.[40] The integrin receptor is coupled to alpha actinin via talin and vinculin. Genetic models have demonstrated that titin subsequently binds to alpha actinin via its capture protein telethonin (T-cap) and muscle LIM protein.[32] Elevated wall stress can lead to extension of the elastic I-band of titin, thereby revealing binding places for several signaling molecules, as for instance a four-and-a-half LIM (FHL) protein.[51] Recently, a novel binding protein was identified — melusin.[9] Melusin binds to the cytoplasmic tail of integrin β1 and is associated with hypertrophy via inactivation of GSK3 beta by AKT phosphorylation thereby inducing translocation of NFAT and GATA4 to the nucleus.[8] Only little is known about the role of mechanosensing mechanisms in PAH-induced hypertrophy. However, it was previously demonstrated that GATA4 expression indeed plays an important role in RV hypertrophy.[46] For an extensive review on the mechanosensing pathways, see the review of Knöll et al.

Figure 3 – Proposed mechanism of the induction of right ventricular hypertrophy by neurohormonal activation and mechanosensing in pulmonary arterial hypertension

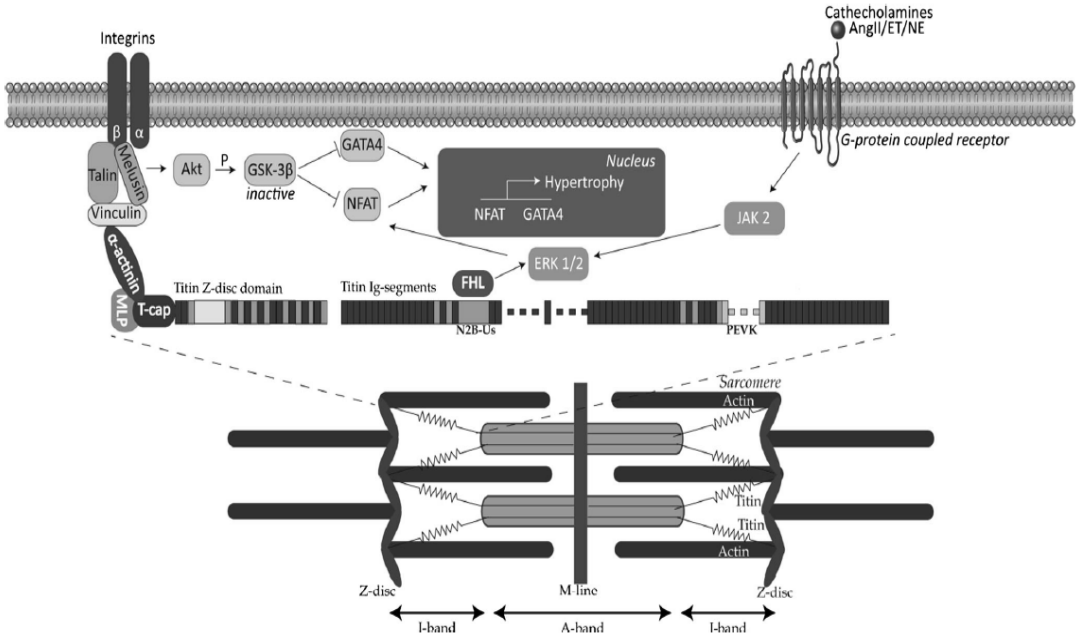

Right ventricular contractility

Activation of the neurohormonal system is not only required for the induction of RV hypertrophy but also contributes to improved contractility and relaxation of the RV cardiomyocytes. Binding of norepinephrine to the beta-adrenergic receptor will result in activation of cyclic AMP that conversely activates protein kinase A (PKA).[3] PKA plays an important role in regulating cardiomyocyte function by phosphorylating key proteins for calcium handling and myofilament function, and as such, PKA increases contraction and relaxation of the cardiomyocytes. PKA-mediated phosphorylation of the L-type Ca2+-channel and ryanodine receptor results in increased delivery of Ca2+ to the myofilaments improving contraction.[43] In addition, relaxation is also improved due to PKA-mediated phospholamban phosphorylation leading to optimal Ca2+ reuptake and desensitization of the myofilaments to Ca2+ by PKA-mediated troponin I and myosin binding protein-C phosphorylation.[31,43] Finally, stiffness of the RV cardiomyocytes is lowered by PKA-mediated phosphorylation of the giant sarcomeric protein titin enhancing both relaxation and contraction of the RV cardiomyocytes.[76]

Figure 4 – The downward spiral of pressure-overload-induced right heart failure

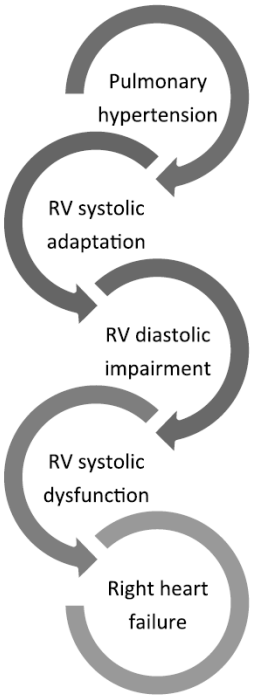

Transition from right ventricular adaptation toward right heart failure

It is unclear which cellular mechanisms are responsible for the inevitable transition from RV adaptation toward right heart failure. We do know that right heart failure is characterized by reduced RV capillarization, RV cardiomyocyte growth arrest, increased RV inflammation, and marked RV fibrosis.[4-7,17,25,38,39,52,54,55,69] However, the trigger for these events remains elusive. We propose in this review that the glycolytic shift and neurohormonal activation, which are initially beneficial, will be detrimental

for the right ventricle on the long run, leading to the transition toward right heart failure (Fig. 2).

Detrimental effects of the glycolytic shift on the long run

A recent elegant study by Sutendra and coworkers shows that the glycolytic shift can eventually result in increased mitochondrial release of reactive oxygen species (ROS).[62] By comparing compensated RV hypertrophy with decompensated RV hypertrophy in PAH rats, they were able to demonstrate two distinct adaptation patterns. On the one hand, compensated RV hypertrophy was characterized by low levels of mitochondria-derived ROS, activated HIF-1α, increased VEGF expression, and a degree of angiogenesis sufficient to maintain normal RV capillarization. On the other hand, in decompensated RV hypertrophy, increased levels were seen of mitochondria-derived ROS, along with reduced HIF-1α, VEGF expression, and capillary rarefaction. The authors propose that these divergent phenotypes were caused by ROSmediated activation of the pro-oncogenic factor p53. The p53 was shown in LV pressure overload to induce capillary rarefaction by its inhibition of HIF-1α activity and VEGF expression.[34,56] Capillary rarefaction could be an important factor in limiting further hypertrophy of RV cardiomyocytes. Capillary density and cardiomyocyte size are closely related because there is a tight equilibrium between oxygen demand and oxygen supply to prevent hypoxia.[64] By comparing stable/compensated PAH to progressive/decompensated PAH, we showed that the greater degree of pressure overload in the second group had not resulted in a greater degree of hypertrophy.[22,55] Besides capillary rarefaction, changes in mechanosensing or genetic variations could play additional roles in the growth arrest of RV cardiomyocytes. In the serial analyses of muscle LIM protein (MLP) expression in the RV tissue of the monocrotaline PAH rat, it was demonstrated that in end-stage PAH, MLP expression was severely reduced.[18] This could result in impaired mechanosensing at a later stage of the disease. Moreover, a recent paper of Hemnes et al. suggests that mutations of the bone morphogenetic protein, which occurs in a subset of PAH patients, could result in a disturbed hypertrophic response to pressure overload.[27] As a consequence of halted RV hypertrophy, the heart will first dilate to maintain RV contractility via the Frank-Starling mechanism.[75] However, excessive dilatation will result in reduced contractile force and stretch of the RV cardiomyocytes. Excessive RV dilatation is one of the important clinical hallmarks of deterioration toward right heart failure.[72] On the cellular level, stretch of cardiomyocytes can result in the release of proinflammatory cytokine tumor necrosis factor alpha (TNF-α), causing inflammatory cell infiltration and RV fibrosis.[30,60]

Detrimental effects of neurohormonal activation on the long run

Long-term neurohormonal overactivation can lead to betaadrenergic receptor desensitization.[36] Several studies in the RV tissue of PAH patients and rats have demonstrated that indeed in end-stage right heart failure, beta-adrenergic density is reduced.[11,12,50] This results in reduced PKA-mediated activation of myofilament and calcium handling proteins and may have important consequences for both systolic and diastolic function. We recently demonstrated that active force development of the RV cardiomyocytes was maintained and that Ca2+ sensitivity was somewhat increased. In contrast, we observed clear diastolic impairment of RV cardiomyocytes of PAH patients

with overt right heart failure evident from high passive stiffness.[52] High RV cardiomyocyte stiffness was partially caused by reduced PKA-mediated phosphorylation of titin in the RV tissue of PAH patients compared with that in the control tissue. In addition to the cardiomyocyte stiffness, RV fibrosis was increased as well resulting in a high diastolic elastance indicating overall stiffening of the right ventricle in PAH patients. That increased activity of the neurohormonal system could play an important role in the development of RV diastolic stiffness was demonstrated when beta-blocker treatment in rats could significantly improve PKA-mediated signaling, reduced RV fibrosis, and resulted in an overall improvement of RV diastolic function.[38] Stiffening of the right ventricle will also disturb the shortening of the cardiomyocytes and thereby contribute to systolic dysfunction. Indeed, we know from animal models that in end-stage right heart failure, RV systolic function is no longer adapted to the increased RV afterload, leading to RV-arterial uncoupling (measured by pressure-volume analyses as reduced Ees/Ea ratio).[10,38] Therefore, it is our perspective that the right ventricle in PAH patients enters a downward spiral (Fig. 4): starting off with hypertrophy and enhanced contractility, but in time, adaptation processes will no longer suffice resulting in RV diastolic impairment leading eventually to right heart failure.

Future perspective

As described above, our proposed mechanisms of right heart failure are mostly based on findings from animal models which reflect the human pathology only to a certain extent. Therefore, it is of utmost importance to validate our pathophysiological understanding of right heart failure in PAH patients prior to developing novel therapeutic interventions specific for right heart failure. Currently, it is impossible to obtain the RV tissue of PAH patients during the progression of the disease because the risk for bleeding or rupture of the RV myocardium is high.

However, novel molecular imaging techniques such as positron emission tomography (PET) may be used to translate the preclinical findings. By this technique, the preference of the right heart for glucose has been quantified, and changes in oxygen efficiency have been determined.[41,45,74] With the development of novel specific tracers, we will be able to quantify the molecular processes of a glycolytic shift and neurohormonal overactivation in much more detail.[14] In addition, the findings of PET can now be directly coupled to RV function with the introduction of PET-MRI techniques.[35] These novel technological developments will provide new opportunities to further enhance our understanding of pressure-overload-induced right heart failure.

CONCLUSIONS

In this review, we have discussed the role of the glycolytic shift and neurohormonal overactivation in RV adaptation. More importantly, we propose that these adaptation mechanisms may be initially beneficial although detrimental in the long run and initiate the transition from RV adaptation toward right heart failure. Future studies will focus on translating these pathophysiological processes to clinical PAH in the hope to find new treatment strategies specific for right heart failure in the future.

REFERENCES

1. Andersen A *et al.* Right ventricular hypertrophy and failure abolish cardioprotection by ischaemic pre-conditioning. *Eur J Heart Fail.* 2013; 15:1208–1214.
2. Banerjee D *et al.* Right ventricular failure: a novel era of targeted therapy. *Curr Heart Fail Rep.* 2010; 7:202–211.
3. Bers DM. Cardiac excitation–contraction coupling. *Nature.* 2002; 415:198–205.
4. Bogaard HJ *et al.* The right ventricle under pressure: cellular and molecular mechanisms of right-heart failure in pulmonary hypertension. *Chest.* 2009; 135:794–804.
5. Bogaard HJ *et al.* Suppression of histone deacetylases worsens right ventricular dysfunction after pulmonary artery banding in rats. *Am J Respir Crit Care Med.* 2011; 183:1402–1410.
6. Bogaard HJ *et al.* Chronic pulmonary artery pressure elevation is insufficient to explain right heart failure. *Circulation.* 2009; 120:1951–1960.
7. Bogaard HJ *et al.* Adrenergic receptor blockade reverses right heart remodeling and dysfunction in pulmonary hypertensive rats. *Am J Respir Crit Care Med.* 2010; 182:652–660.
8. Brancaccio M *et al.* Melusin, a muscle-specific integrin beta1-interacting protein, is required to prevent cardiac failure in response to chronic pressure overload. *Nat Med.* 2003;9:68–75.
9. Brancaccio M *et al.* Melusin is a new muscle-specific interactor for beta(1) integrin cytoplasmic domain. J Biol Chem. 1999; 274:29282–29288.
10. Brimioulle S *et al.* Single-beat estimation of right ventricular end-systolic pressure-volume relationship. *Am J Physiol Heart Circ Physiol.* 2003; 284:H1625–H1630.
11. Bristow MR *et al.* Beta1- and beta 2-adrenergic-receptor subpopulations in nonfailing and failing human ventricular myocardium: coupling of both receptor subtypes to muscle contraction and selective beta 1-receptor downregulation in heart failure. *Circ Res.* 1986; 59:297–309.
12. Bristow MR *et al.* Betaadrenergic neuroeffector abnormalities in the failing human heart are produced by local rather than systemic mechanisms*. J Clin Invest.* 1992; 89:803–815.
13. Burkhoff D *et al.* Assessment of systolic and diastolic ventricular properties via pressure-volume analysis: a guide for clinical, translational, and basic researchers. *Am J Physiol Heart Circ Physiol.* 2005; 289:H501–H512.
14. Chen IY *et al.* Cardiovascular molecular imaging focus on clinical translation. *Circulation.* 2011; 123:425–443.
15. Chin KM *et al.* The right ventricle in pulmonary hypertension. *Coron Artery Dis.* 2005; 16:13–18.
16. D'Alonzo GE *et al.* Survival in patients with primary pulmonary hypertension. Results from a national prospective registry. *Ann Intern Med.* 1991; 115:343–349.
17. Drake JI *et al.* Molecular signature of a right heart failure program in chronic severe pulmonary hypertension. *Am J Respir Cell Mol Biol.* 2011; 45:1239–1247.
18. Ecarnot-Laubriet A *et al.* Downregulation and nuclear relocation ofMLP during the progression of right ventricular hypertrophy induced by chronic pressure overload. *J Mol Cell Cardiol.* 2000; 32:2385–2395.
19. Franco V *et al.* Right ventricular remodeling in pulmonary hypertension. *Heart Fail Clin.* 2012; 8:403–412.
20. Gan CTJ *et al.*Impaired left ventricular filling due to right-to-left ventricular
interaction in patients with pulmonary arterial hypertension. *Am J Physiol Heart Circ Physiol.* 2006; 290:H1528–H1533.
21. GrossmanW *et al.* Wall stress and patterns of hypertrophy in the human left ventricle. *J Clin Invest.* 1975; 56:56–64.
22. Haddad F *et al.* Right ventricular function in cardiovascular disease, part II: pathophysiology, clinical importance, and management of right ventricular failure. *Circulation.* 2008; 117:1717–1731.
23. Haddad F *et al.* Right ventricular function in cardiovascular disease, part I: anatomy, physiology, aging, and functional assessment of the right ventricle. *Circulation.* 2008; 117:1436–1448.
24. Handoko ML *et al.* Perspectives on novel therapeutic strategies for right heart failure in pulmonary arterial hypertension: lessons from the left heart. *Eur Respir Rev.* 2010; 19:72–82.
25. Handoko ML *et al.* Opposite effects of training in rats with stable and progressive pulmonary hypertension. *Circulation.* 2009; 120:42–49.
26. Heineke J *et al.* Regulation of cardiac hypertrophy by intracellular signalling pathways. *Nat Rev Mol Cell Biol.* 2006; 7:589– 600.
27. Hemnes AR *et al.* Evidence for right ventricular lipotoxicity in heritable pulmonary arterial hypertension. *Am J Respir Crit CareMed.* 2014; 189:325-34.

28. Hoeper MM *et al.* Intensive care unit management of patients with severe pulmonary hypertension and right heart failure. *Am J Respir Crit Care Med.* 2011;184:1114–1124.
29. Humbert M *et al.* Survival in patients with idiopathic, familial, and anorexigen-associated pulmonary arterial hypertension in the modern management era. *Circulation.* 2010; 122:156–163.
30. Kapadia SR *et al.* Hemodynamic regulation of tumor necrosis factor-alpha gene and protein expression in adult feline myocardium. *Circ Res.* 1997; 81:187–195.
31. Kentish JC *et al.* Phosphorylation of troponin I by protein kinase A accelerates relaxation and crossbridge cycle kinetics in mouse ventricular muscle. Circ Res. 2001; 88:1059–1065.
32. Knöll R *et al.* The cardiac mechanical stretch sensor machinery involves a Z disc complex that is defective in a subset of human dilated cardiomyopathy. *Cell.* 2002; 111:943–955.
33. Kramer MR *et al.* Recovery of the right ventricle after single-lung transplantation in pulmonary hypertension. *Am J Cardiol.* 1994; 73:494–500.
34. Kuehne T *et al.* Magnetic resonance imaging analysis of right ventricular pressure-volume loops: in vivo validation and clinical application in patients with pulmonary hypertension. *Circulation.* 2004; 110:2010–2016.
35. Lee WW *et al.* PET/ MRI of inflammation inmyocardial infarction. *J Am Coll Cardiol.* 2012; 59: 153–163.
36. Lohse MJ *et al.* What is the role of beta-adrenergic signaling in heart failure? *Circ Res.* 2003; 93:896–906.
37. Lowes BD *et al.* Changes in gene expression in the intact human heart. Downregulation of alpha-myosin heavy chain in hypertrophied, failing ventricular myocardium. *J Clin Invest.* 1997; 100:2315–2324.
38. De Man FS *et al.* Bisoprolol delays progression towards right heart failure in experimental pulmonary hypertension. *Circ Heart Fail.* 2012; 5:97–105.
39. De Man FS *et al.* Dysregulated renin-angiotensinaldosterone system contributes to pulmonary arterial hypertension. *AmJ Respir Crit CareMed.* 2012; 186:780–789.
40. McCain ML *et al.* Mechanotransduction: the role of mechanical stress, myocyte shape, and cytoskeletal architecture on cardiac function. *Pflugers Arch.* 2011; 462:89–104.
41. Mielniczuk LM *et al.* Relation between right ventricular function and increased right ventricular [18F]fluorodeoxyglucose accumulation in patients with heart failure. *Circ Cardiovasc Imaging.* 2011; 4:59–66.
42. Moulton MJ *et al.* Magnetic resonance imaging provides evidence for remodeling of the right ventricle after single-lung transplantation for pulmonary hypertension. *Circulation.* 1996; 94:II312–II319
43. Mudd JO *et al.* Tackling heart failure in the twenty-first century. *Nature.* 2008; 451:919–928.
44. Nagendran J *et al.* Endothelin axis is upregulated in human and rat right ventricular hypertrophy. *Circ Res.* 2013; 112:347–354.
45. Oikawa M *et al.* Increased [18F]fluorodeoxyglucose accumulation in right ventricular free wall in patients with pulmonary hypertension and the effect of epoprostenol. *J Am Coll Cardiol.* 2005; 45:1849–1855.
46. Park AM *et al.* Pulmonary hypertension-induced GATA4 activation in the right ventricle. *Hypertension.* 2010; 56:1145–1151.
47. Pasque MK *et al.* Single lung transplantation for pulmonary hypertension. Single institution experience in 34 patients. *Circulation.* 1995; 92:2252–2258
48. Peacock AJ *et al.* Changes in right ventricular function measured by cardiac magnetic resonanceimaging in patients receiving pulmonary arterial hypertensiontargeted therapy: the EURO-MR study. *Circ Cardiovasc Imaging.* 2013; 7:107-14.
49. Peacock AJ *et al.* Cardiac magnetic resonance imaging in pulmonary arterial hypertension. *Eur Respir Rev.* 2013; 22:526–534.
50. Piao L *et al.* GRK2-mediated inhibition of adrenergic and dopaminergic signaling in right ventricular hypertrophy: therapeutic implications in pulmonary hypertension. *Circulation.* 2012; 126:2859–2869.
51. Radke MH *et al.* Targeted deletion of titin N2B region leads to diastolic dysfunction and cardiac atrophy. *Proc Natl Acad Sci USA.* 2007;104:3444–3449.
52. Rain S *et al.* Right ventricular diastolic impairment in patients with pulmonary arterial hypertension. *Circulation.* 2013; 128:1–10.
53. Rich S *et al.* Right ventricular adaptation and maladaptation in chronic pulmonary arterial hypertension. *Cardiol Clin.* 2012; 30:257–269.
54. Rondelet B *et al.* Prolonged overcirculation-induced pulmonary arterial hypertension as a cause of right ventricular failure. *Eur Heart J.* 2012; 33:1017–1026.

55. Ruiter G *et al.* Right ventricular oxygen supply parameters are decreased in human and experimental pulmonary hypertension. *J Heart Lung Transplant.* 2013; 32:231–240.
56. Sano M *et al.* p53-induced inhibition of Hif-1 causes cardiac dysfunction during pressure overload. *Nature.* 2007; 446:444–448.
57. Schrier RW *et al.* Pulmonary hypertension, right ventricular failure, and kidney: different from left ventricular failure? *Clin J Am Soc Nephrol.* 2008; 3:1232–1237.
58. Simon MA *et al.* Right ventricular adaptation to pressure overload. *Curr Opin Crit Care.* 2010; 16:237–243.
59. Stenmark KR *et al.* Animal models of pulmonary arterial hypertension: the hope for etiological discovery and pharmacological cure. *Am J Physiol Lung Cell Mol Physiol.* 2009; 297:L1013–L1032.
60. Sun M *et al.* Tumor necrosis factor-alpha mediates cardiac remodeling and ventricular dysfunction after pressure overload state. Circulation. 2007; 115:1398–1407.
61. Sunagawa K *et al.* Estimation of the hydromotive source pressure from ejecting beats of the left ventricle. *IEEE Trans Biomed Eng.* 1980; 27:299–305.
62. Sutendra G *et al.* A metabolic remodeling in right ventricular hypertrophy is associated with decreased angiogenesis and a transition from a compensated to a decompensated state in pulmonary hypertension. *J Mol Med (Berl).* 2013; 91:1315–1327.
63. Takeuchi M *et al.* Single-beat estimation of the slope of the end-systolic pressure-volume relation in the human left ventricle. *Circulation.* 1991; 83:202–212.
64. Des Tombe AL *et al.* Calibrated histochemistry applied to oxygen supply and demand in hypertrophied rat myocardium. *Microsc Res Tech.* 2002; 58:412–420.
65. Trip P *et al.* Accurate assessment of load-independent right ventricular systolic function in patients with pulmonary hypertension. *J Heart Lung Transplant.* 2013; 32:50–55.
66. Van de Veerdonk MC *et al.* Progressive right ventricular dysfunction in patients with pulmonary arterial hypertension responding to therapy. J Am Coll Cardiol. 2011; 58:2511–2519.
67. Voelkel NF *et al.* Right ventricular function and failure: report of a National Heart, Lung, and Blood Institute working group on cellular and molecular mechanisms of right heart failure. *Circulation.* 2006; 114:1883–1891.
68. Vonk Noordegraaf A *et al.* The role of the right ventricle in pulmonary arterial hypertension. *Eur Respir Rev.* 2011; 20:243–253.
69. Vonk-Noordegraaf A *et al.* Right heart adaptation to pulmonary arterial hypertension: physiology and pathobiology. *J Am Coll Cardiol.* 2013; 62:D22–D33.
70. Walker LA *et al.* Biochemical and myofilament responses of the right ventricle to severe pulmonary hypertension. *AmJ Physiol Heart Circ Physiol.* 2011; 301:H832–H840.
71. Westerhof N *et al.* Snapshots of hemodynamics. An aid for clinical research and graduate education, 2nd edn. *Springer.* 2005.
72. Van Wolferen SA *et al.* Prognostic value of right ventricular mass, volume, and function in idiopathic pulmonary arterial hypertension. Eur Heart J. 2007; 28:1250–1257.
73. Wong YY *et al.* Reduced mechanical efficiency of rat papillary muscle related to degree of hypertrophy of cardiomyocytes. *Am J Physiol Heart Circ Physiol.* 2010; 298:H1190– H1197.
74. Wong YY *et al.* Right ventricular failure in idiopathic pulmonary arterial hypertension is associated with inefficient myocardial oxygen utilization. *Circ Heart Fail.* 2011; 4:700–706.
75. Yadid M *et al.* Adaptive control of cardiac contraction to changes in loading: from theory of sarcomere dynamics to whole-heart function. *Pflugers Arch Eur J Physiol.* 2011; 462:49–60.
76. Yamasaki R *et al.* Protein kinase A phosphorylates titin's cardiac-specific N2B domain and reduces passive tension in rat cardiac myocytes. *Circ Res.* 2002; 90:1181–1188.

Chapter 6

Right ventricular-arterial coupling in patients with pulmonary arterial hypertension

Trip P, Rain S, Handoko ML, Bogaard HJ, Boonstra A, Westerhof N, de Man FS, Vonk-Noordegraaf A

Submitted

ABSTRACT

Background – An increase in cardiac load due to pulmonary vascular remodeling in idiopathic pulmonary arterial hypertension (IPAH) directly affects RV function. Pressure-volume analysis is used to distinguish changes in load and RV function. In the present study we aimed to assess whether in IPAH RV pressure-volume analysis allows for the distinction of clinical phenotypes and the effect of afterload reduction on RV function and adaptation.

Methods and Results – Using single-beat pressure-volume analyses, we determined systolic elastance (Ees), arterial elastance (Ea), diastolic elastance (Ed), and RV-arterial coupling (Ees/Ea) in controls (n=17), IPAH-patients at baseline (n=88), after treatment (n=45), and in stable (survival>5 years, n=26) and progressive disease (survival<5 years, n=28). The distribution of RV function and adaptation and superimposed effects of age and sex were determined, as well as the effects of afterload reduction. In addition, it was investigated whether a reduced RV-arterial coupling indicates clinical progression.
Ees, Ea, Ed and Ees/Ea all showed a wide range at baseline, Ees/Ea being lower in male patients. Under treatment Ea, Ees, Ed decreased (ΔEa=-30%, ΔEes=-11%, ΔEd=-23%, $p<0.01$) and Ees/Ea increased (ΔEes/Ea=30%, $p<0.01$). The increase in Ees/Ea was independent of the degree of afterload reduction. At baseline, an Ees/Ea$\leq$1.24 was associated with worse survival (age-corrected hazard-ratio 2.72, $p<0.05$). Furthermore, in treated IPAH-patients ROC-analysis revealed Ees/Ea as being discriminative for progressive disease (AUC 0.79, $p<0.01$).

Conclusions – Pressure-volume analysis in IPAH-patients allows the distinction of different clinical phenotypes and reveals that a decrease in RV afterload is not required for improvements in RV systolic adaptation.

INTRODUCTION

Pulmonary arterial hypertension (PAH) is characterized by an increased pulmonary vascular resistance imposing an increased load on the right ventricle (RV). The ability of the RV to adapt to the increased load plays an important role in PAH patient outcome.[1] The best way to obtain insight into RV adaptation in pressure overloaded conditions is with pressure-volume analysis.[2] The use of pressure-volume analysis in PAH has been limited because it requires simultaneous pressure and volume measurements under preload reduction which is not without risk in PAH-patients. Alternative methods that do not require preload reduction, the so-called singe-beat methods, have been successfully developed and were earlier used in two relatively small PAH patient studies.[3-6] With the additional development and validation of a single-beat method for determining RV diastolic elastance, a practical method has become available allowing a comprehensive analysis of systolic and diastolic RV function and adaptation.[6]

Figure 1 - Schematic presentation of pressure-volume parameters (Ea, Ees and Ed)

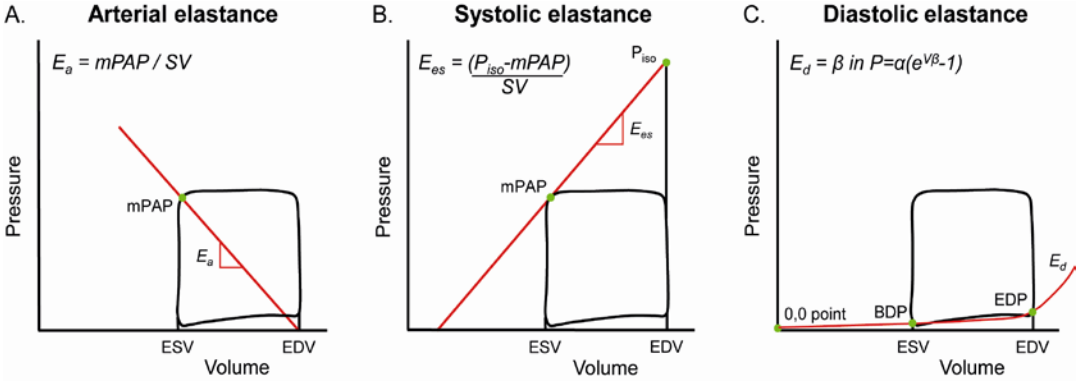

A. For the calculation of arterial elastance (Ea) mean pulmonary artery pressure (mPAP) is used as a surrogate of right ventricular end-systolic pressure. B. Systolic elastance (Ees) is calculated by dividing the difference between estimated right ventricular isovolumic pressure (Piso) and mPAP with stroke volume. C. Diastolic elastance (Ed) is calculated with an exponential curve through three pressure points: 1) end-diastolic pressure (EDP), 2) begin-diastolic pressure (BDP), and 3) zero pressure-zero volume point. End-diastolic and end-systolic volume (EDV and ESV respectively) are drawn for clarity and are not used in the calculations.

RV pressure-volume analysis allows the derivation of parameters that describe load-independent RV systolic function (end-systolic elastance, Ees), load-independent RV diastolic function (diastolic elastance or stiffness, Ed) and RV afterload (arterial elastance, Ea) (Fig. 1). The ratio of RV end-systolic elastance and arterial elastance, Ees/Ea i.e. RV-arterial coupling, quantifies the matching of RV systolic function to the increased RV load. For example, an increase in arterial elastance will reduce RV-arterial coupling unless the RV adapts by increasing its systolic function. Similarly, when arterial elastance decreases, RV-arterial coupling will increase unless the RV reduces in systolic function. Use of pressure-volume analysis may provide a tool to discriminate between stable and progressive PAH patients and to evaluate direct treatment effects on heart function.

Therefore, the aim of the current study is:
1) investigate in a large cohort of idiopathic and hereditary PAH (I/HPAH) patients:
   a) the distribution of RV function and adaptation
   b) the effects of age and sex on RV function and adaptation
2) determine the effect of a reduction in afterload on RV function and adaptation
3) assess whether a reduced RV-arterial coupling indicates clinical progression.

METHODS

Subjects

The study was conducted at the VU University Medical Center. All patients diagnosed with I/HPAH from August 10 1989 until January 15 2013 (n=254) were evaluated for inclusion in the current study. Only patients with digitally stored, good quality RV pressure recordings were selected for this study. Details regarding the selection of patients can be observed in Figure 2 and the supplemental data.

Due to the retrospective character of the study using data obtained for clinical purposes the Medical Ethics Review Committee of the VU University Medical Center did not consider this study to fall within the scope of the Medical Research Involving Human Subjects Act. Therefore, no additional approval was acquired.

Pressure-volume analyses

Right heart catheterization and pressure-volume analyses were performed as previously described.[6,7] A detailed description can be found in the online data supplement.

Statistical analysis

The data are presented as mean ± SEM unless stated otherwise. A p-value < 0.05 was considered significant. Details on the statistical analysis can be found in the online data supplement.

Figure 2 - Inclusion flowchart

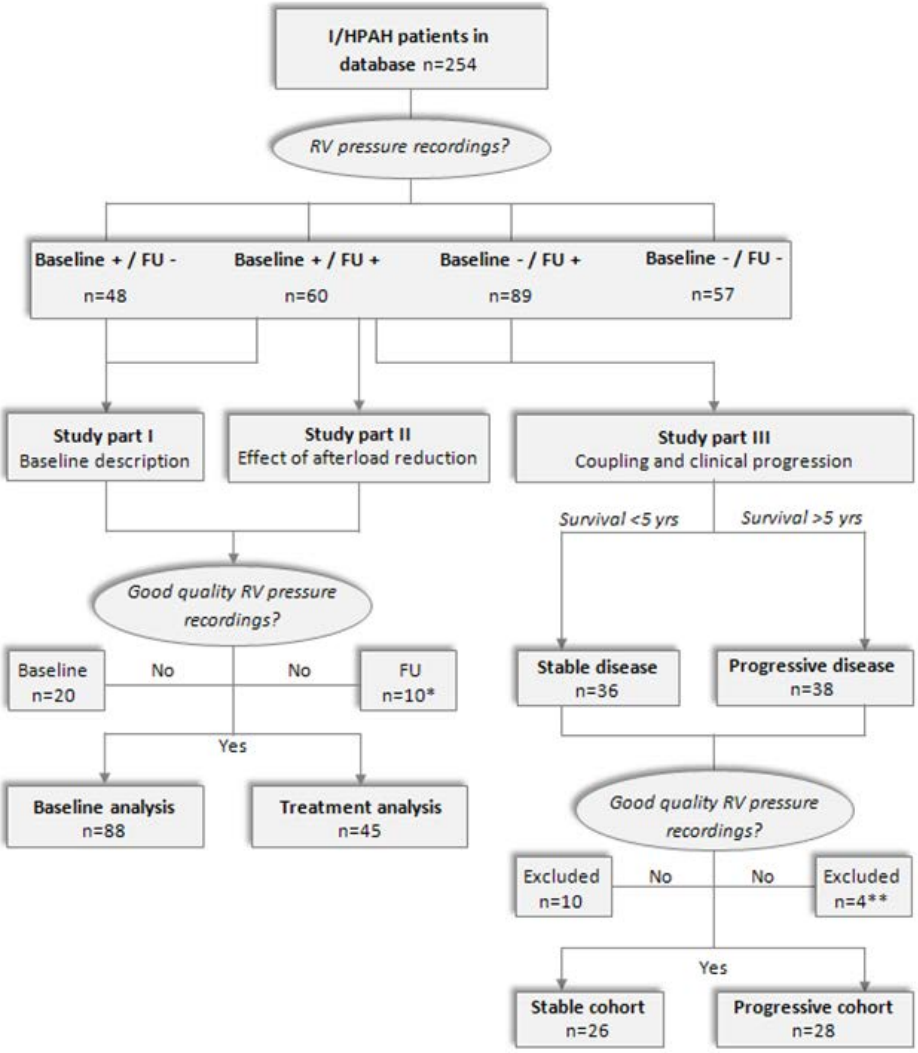

In total 254 I/HPAH-patients were assessed for inclusion for both part I, II and III of the study. *Six out of ten patients were not included in the follow-up analysis because the follow-up measurement did not fall within the time range. **Ten of these patients were not included because they were also included in the stable group (n=6) or due to poor pressure curve quality (n=4).

Table 1 - General characteristics, hemodynamics and treatment

Baseline population (n=88)		**Follow-up population (n=45)**	
General characteristics			
Age (y)	58 (38-73)	49 (30-64)	-
Sex (n, female %)	58 (66%)	35 (78%)	-
BSA (m^2)	1.9 (1.7-2.1)	1.9 (1.7-2.1)	-
Follow-up (y)	2.0 (1.0-7.2)	1.9 (1.4-3.5)	-
Hemodynamics		**Baseline**	**Follow-up**
mPAP (mmHg)	50 (42-58)	52 (44-65)	45 (37-59)#
CO (L/min/m^2)	4.4 (3.6-5.5)	4.3 (3.5-5.2)	6.2 (4.9-6.9)#
HR (bpm)	77 (68-90)	74 (69-90)	76 (68-89)
PVR(dyn•s•cm^{-5})	944 (645-1248)	964 (665-1447)	629 (454-951)#
mRAP (mmHg)	6 (4-11)	8 (5-12)	5 (4-8)*
SvO_2 (%)	64 (54-68)	62 (55-68)	69 (63-75)#
Treatment		**1st line**	**Follow-up**
ERAs	-	16 (36%)	10 (22%)
Prostanoids	-	6 (13%)	4 (9%)
PDE-5 inh.	-	11 (24%)	9 (20%)
Ca ch. blockers	-	1 (2%)	1 (2%)
Combination	-	11 (24%)	21 (47%)

Data presented as median (25-75%) or n (%). *p<0.05 vs. Follow-up population – baseline, #p<0.01 vs. Follow-up population – baseline. mPAP: mean pulmonary artery pressure; CO: cardiac output; HR: heart rate; TPVR: total pulmonary vascular resistance; mRAP: mean right atrial pressure; SvO2: mixed venous oxygen saturation; ERA: endothelin receptor antagonists; PDE-5: phosphodiesterase type-5.

RESULTS

Part I – Distribution and the effect of sex and age

To determine the distribution of pressure-volume parameters in a general I/HPAH population we included a total of 88 treatment naive I/HPAH-patients.

General characteristics and hemodynamics are shown in table 1. Figure 3 shows the frequency distributions of Ees, Ed, Ea and the coupling parameter Ees/Ea of both controls and I/HPAH-patients. All parameters show a wide range in values.

Ees, Ea, and Ed were higher and Ees/Ea was reduced in I/HPAH compared to controls (Ees, 1.26±0.07 vs. 0.26±0.02 mmHg/ml in controls; Ea, 1.01±0.06 vs. 0.15±0.01 mmHg/ml; Ed, β 0.04±0.002 vs. 0.02±0.001; Ees/Ea, 1.35±0.05 vs. 1.95±0.15, p<0.05 for all).

Table 2 - Clinical characteristics and treatment of different 396 IPAH groups

		I/HPAH	
	Controls (n=17)	**Stable (n=17)**	**Progressive (n=17)**
General characteristics			
Age (y)	49 (45-64)	42 (34-56)	53 (41-67)
Sex (n, female %)	10 (59%)	23 (89%)	17 (61%)#
BSA (m^2)	1.9 (1.7-2.0)	1.7 (1.7-2.0)	1.8 (1.7-1.9)
Hemodynamics		**Baseline**	**Follow-up**
mPAP (mmHg)	15 (13-17)	50 (38-59)	53 (42-61)*
CO ($L/min/m^2$)	7.0 (6.7-9.0)	5.2 (4.2-6.4)	6.4 (3.9-5.4)*
HR (bpm)	77 (68-89)	75 (63-88)	89 (62-88)#
PVR($dyn•s•cm^{-5}$)	156 (130-183)	721 (541-1099)	880 (672-1213)*
mRAP (mmHg)	3 (2-4)	6 (3-9)	9 (4-13)*
SvO_2 (%)	74 (71-78)	67 (60-71)	61 (55-65)*#
Treatment		**1st line**	**Follow-up**
ERAs	-	8 (31%)	4 (14%)
Prostanoids	-	6 (23%)	5 (18%)
PDE-5 inh.	-	0 (0%)	3 (11%)
Ca ch. blockers	-	4 (15%)	0 (0%)#
Combination	-	8 (31%)	16 (57%)

Data presented as median (25-75%) or n (%). *p<0.05 vs. Follow-up population – baseline, #p-value < 0.05 vs. stable I/HPAH. I/HPAH: idiopathic and hereditary pulmonary arterial hypertension patients; BSA: body surface area; mPAP: mean pulmonary artery pressure; CO: cardiac output; HR: heart rate; PVR: total pulmonary vascular resistance; mRAP: mean right atrial pressure; SvO2: mixed venous oxygen

To describe the effect of sex and age on RV function and adaptation we compared the baseline pressure-volume parameters between male and female patients and between young (<58 years) and older (>58 years) patients. Young and older patients were divided by median age. Baseline characteristics of the groups are shown in supplemental table 1 and 2, see online data supplement. I/HPAH-patients >58 years of age had a lower Ea and Ees compared to I/HPAH ≤58 years. Although Ees/Ea was not different between the two age groups, age was found to be a confounder in the analysis of sex differences. Out of the total baseline population 34% (n=30) was male. Male patients were older at presentation (64±18 vs. 50±19 years, p<0.01). No differences in hemodynamic parameters could be observed between male and female patients (see supplemental data – table 2). Among the pressure-volume parameters, only Ees/Ea was lower in male patients when corrected for age (Fig. 4).

Figure 3 - Frequency distributions of RV function and adaptation

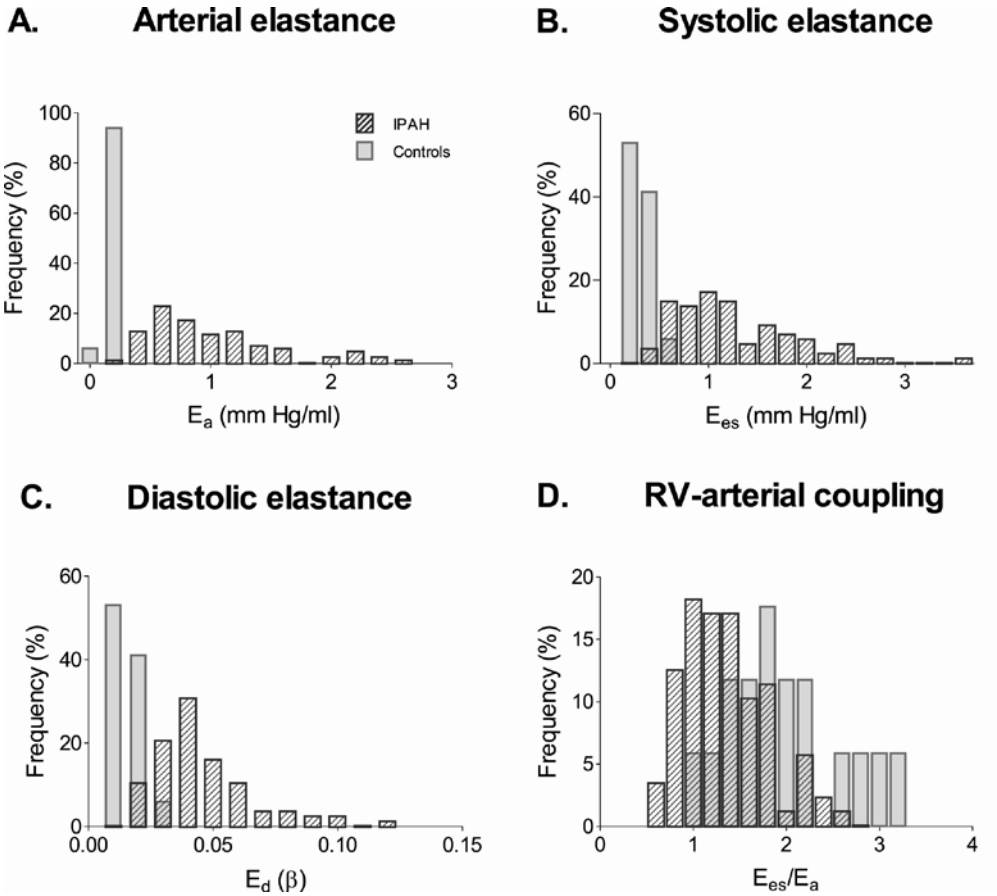

Shown are Ea, Ees, Ed, and Ees/Ea in healthy subjects (clear bars) and I/HPAH-patients (hatched bars). I/HPAH: idiopathic/hereditary pulmonary arterial hypertension.

Part II – Effect of afterload reduction

To assess the effect of a reduction in afterload on RV function and adaptation we determined pressure-volume parameters at baseline and after treatment in 45 patients. General characteristics and baseline hemodynamics were similar in the follow-up population compared to the total population (table 1).

Median follow-up time was 0.8 years (interquartile range 0.4-1.0). Ees, Ea and Ed all decreased under treatment (Fig. 5). Baseline Ees/Ea was lower compared to controls (Ees/Ea 1.95±0.63 in controls vs. 1.28±0.38 in I/HPAH, p=0.01).

Despite the decrease in Ees during follow-up, the Ees/Ea–ratio almost normalized after treatment (Ees/Ea follow-up 1.58±0.55, p=0.37 vs. controls) indicating that the decrease in Ea was larger than the decrease in Ees. Figure 6 shows the % change in Ea versus the percentage change in Ees.

Figure 4 – RV function and adaptation according to age and sex

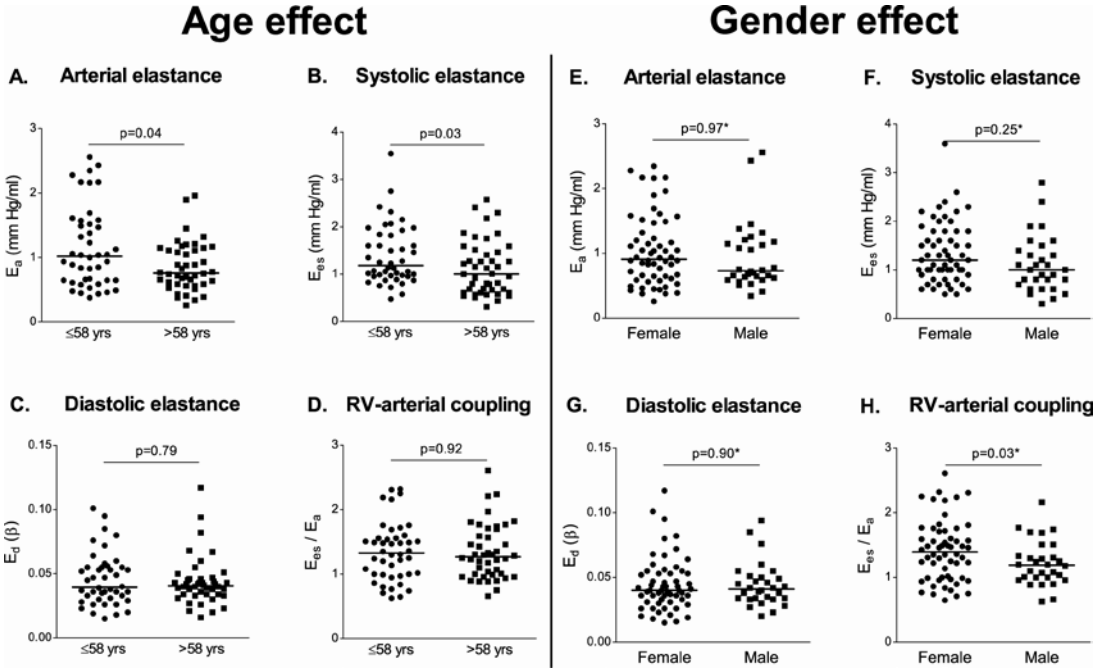

Baseline arterial elastance (A), end systolic elastance (B), diastolic stiffness (C), and RV-arterial coupling (D) in two I/HPAH age groups and according to sex. *RV-arterial coupling was lower in male patients when corrected for the confounding factor age.

In the majority of patients a reduction in Ea was observed, with an increase in RV-arterial coupling. However, an increase in RV-arterial coupling during follow-up did also occur in patients with an increase in Ea, suggesting that changes in RV arterial coupling are not only influenced by afterload changes. This lack of influence of afterload alterations on RV-arterial coupling was additionally supported by a correlation analysis between percentage change of Ea and RV-arterial coupling (Spearman's rank correlation coefficient -0.08, p>0.05).

Survival analysis

To assess whether a reduced RV-arterial coupling is an indicator of clinical progression, we performed a Kaplan-Meier analysis using baseline data. Median follow-up was 2.4 years (interquartile range 1.3-7.5). During follow-up, 27 patients died or underwent lung transplantation. Figure 7 shows the Kaplan Meier curves of I/HPAH patient groups. No differences in age-corrected survival were observed between I/HPAH patient groups when differentiated based on Ees or Ea alone. However, when the coupling parameter Ees/Ea was used to divide I/HPAH-patients, a reduced survival was observed in I/HPAH-patients with a baseline Ees/Ea≤1.24 (Fig. 7C).

Figure 5 - Changes in RV function and adaptation during follow-up

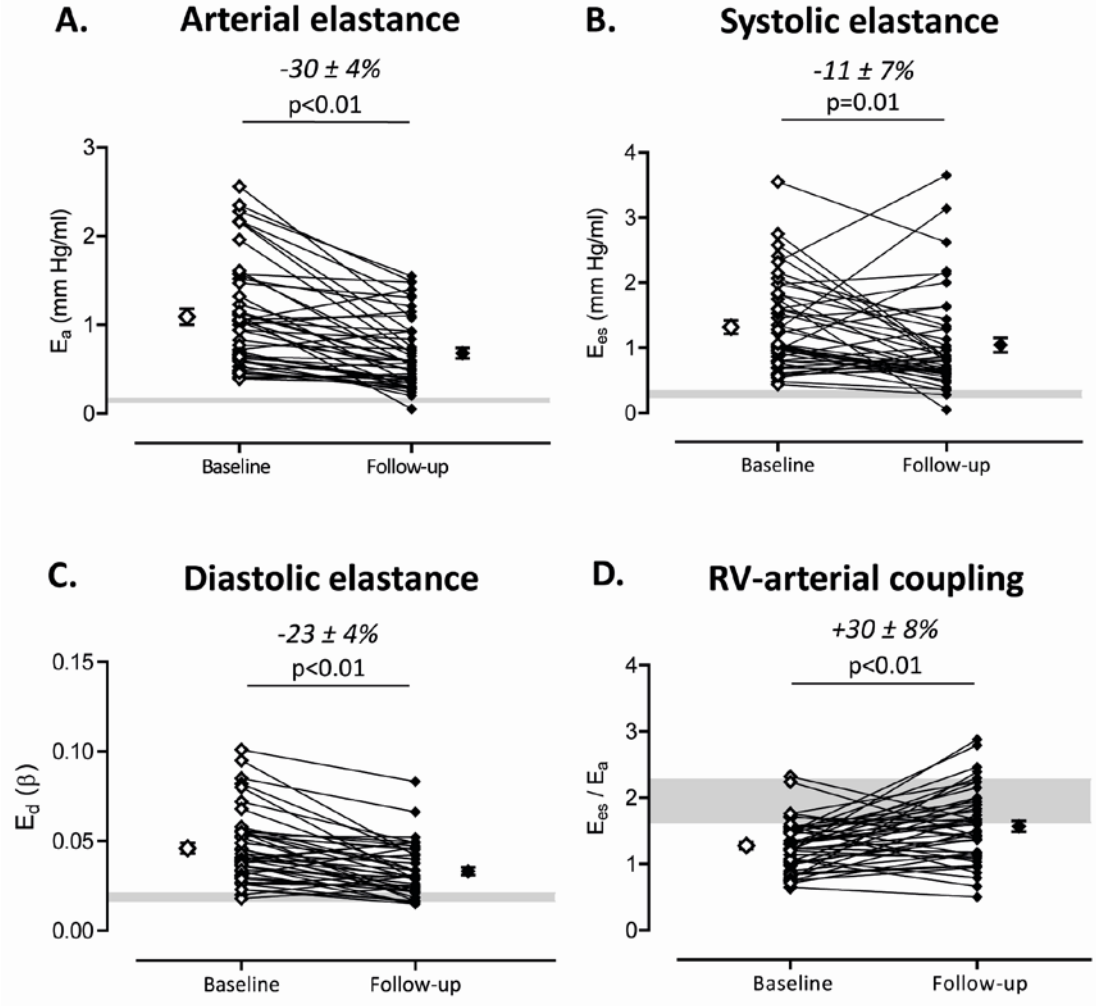

Arterial elastance (A), end systolic elastance (B), diastolic stiffness (C) and RV-arterial coupling (D) changed with treatment in a group of I/HPAH-patients. Also plotted are as mean ±SEM.

Stable vs. progressive IPAH-patients

To further assess whether a reduced RV-arterial coupling is an indicator of clinical progression we subsequently compared pressure-volume parameters of stable and progressive I/HPAH-patients. Table 2 shows general characteristics, hemodynamics and treatment of the two I/HPAH groups and controls. Ees, and Ea were significantly increased compared to controls in stable and progressive I/HPAH (Fig. 8A-B). Ees/Ea was similar to control values in stable I/HPAH, but reduced in progressive I/HPAH (Fig. 8C). Sex-corrected analysis of differencesbetween stable and progressive I/HPAH showed no difference between Ees (p=0.31) or Ea (p=0.09), but a lower Ees/Ea in progressive I/HPAH (p=0.003). ROC analysis revealed that a cut-off value of Ees/Ea 1.39 discriminated between stable and progressive I/HPAH-patients (Ees/Ea: area under the curve 0.79, p<0.001; sensitivity 92%, specificity 68%) (Fig. 8D).

Part III – RV-arterial coupling as an indicator of clinical progression

Figure 6 - Percentage change during follow-up in Ees and Ea

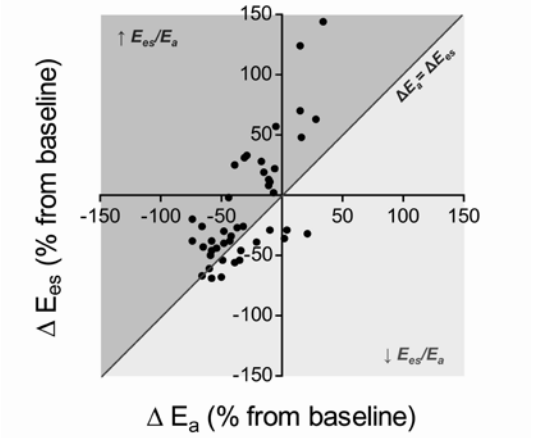

Change in arterial elastance versus RV systolic elastance under treatment in I/HPAH-patients.

This finding was not affected by age (age-adjusted Cox-regression analysis: Ees/Ea, p=0.01). Age-adjusted Cox-regression analysis based on mRAP, CO or SvO2 revealed that only mRAP and SvO2 were discriminative for survival. Patients with mRAP≤12.5 mmHg had a better survival (age-adjusted HR 0.30, CI 0.12-0.70, p=0.006) and patients with a SvO2≤65.5% had worse survival (age-adjusted HR 4.31, CI 1.28-14.45, p=0.018). No difference was observed between patients with a CO≤4.35 or CO>4.35 L/min (age-adjusted HR 1.52, CI 0.69-3.37, p=0.30).

DISCUSSION

In the present study we used pressure-volume analysis in incident and prevalent I/HPAH-patients, as well as in treated stable and progressive patients and were able to show that:

1) Baseline RV function and adaptation as measured by single (Ea, Ees, Ed) and coupled pressure volume parameters (Ees/Ea) show a wide range in I/HPAH-patients and are either increased (Ea, Ees, Ed) or reduced (Ees/Ea) compared to control values
2) Male sex is associated with a lower RV-arterial coupling ratio at baseline
3) RV systolic and diastolic elastance decrease and RV-arterial coupling increases under treatment independent of the magnitude of afterload reduction
4) Reduced RV-arterial coupling is an indicator of clinical progression

Several authors have argued that measuring RV-arterial coupling is the best way to assess RV function and adaptation in pulmonary hypertension.[8] In comparison with load-dependent measures of RV function, such as RV ejection fraction and tricuspid annular plane systolic excursion, RV-arterial coupling reflects intrinsic RV myocardial adaptation to the arterial load more closely.

Figure 7 - Survival according to pressure-volume parameters

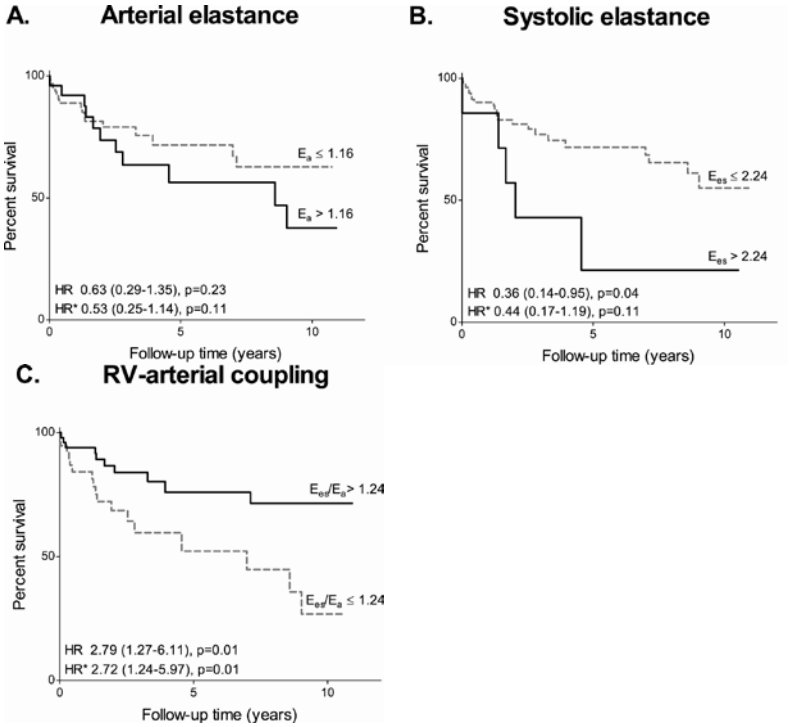

Kaplan-Meier curves of the total baseline study population (n=88) based on Ea, Ees, and Ees/Ea cut-off values determined with ROC analysis. HR, uncorrected hazard-ratio. HR*, hazard-ratio corrected for age.

However, the clinical value of RV-arterial coupling has not yet been tested in a large cohort of PAH patients. Therefore, we assessed RV-arterial coupling invasively in a large I/HPAH patient cohort and showed that RV-arterial coupling was on average reduced. This is in line with the findings of Kuehne et al. who determined RV-arterial coupling in a small subset of six IPAH-patients.[5] However, considerable overlap between controls and I/HPAH-patients was seen, suggesting that at baseline a substantial amount of patients have an RV systolic function that is well matched to the increased arterial load. This heterogeneity could explain why Tedford et al. found a normal RV-arterial coupling ratio in 5 IPAH-patients.[9] Heterogeneity in RV-arterial coupling was also observed in control subjects. The RV-arterial coupling ratio normally is between 1.5-2.0, reflecting optimal cardiac efficiency with regards to oxygen use and power output.[2] The wide range we observed in our control subjects could be caused by a selection bias. Although only control subjects without significant co-morbidities were included in the analysis, possible subtle influences on cardiac function cannot be excluded and might explain the lower RV-arterial coupling values. Another possible explanation may be the use of the single-beat analysis for the estimation of RV systolic elastance. This validated method, however, has been shown to give a good approximation of RV isovolumic pressure and thus RV systolic elastance.[3] RV systolic and diastolic elastance were both increased in the great majority of PAH-patients at

baseline. This finding could be the consequence of an increase in RV mass, an altered intrinsic RV systolic and diastolic myocardial stiffness or both.

The influence of sex on RV adaptation to its increased load in patients with PAH became also apparent in our study.[10-12] The effects of sex on RV function have been investigated by several study groups. In healthy subjects, RV ejection fraction is lower in male subjects.[10] In IPAH, the negative association between RV ejection fraction and male sex was first described by Kawut et al.[11] However, more recently a direct comparison of baseline RV ejection fraction of male and female IPAH-patients has been performed by Jacobs et al. who showed similar values at baseline for both sexes, but a smaller improvement to treatment in males.[12] Here, we demonstrate that sex differences in RV systolic adaptation to the increased arterial load are already present at baseline, RV systolic adaptation being inferior in male patients. RV-arterial coupling may thus be a more sensitive marker for differences in RV systolic adaptation in PAH.

The effect of afterload reduction

We found that a low RV-arterial coupling was associated with clinical progression. Therefore, aiming to preserve RV-arterial coupling as long as possible might be beneficial in patients with PAH. In our study, we observed an increased RV-arterial coupling under treatment in most PAH-patients. Interestingly, the improvement in RV-arterial coupling was unrelated to the degree of afterload reduction, indicating that RV adaptation does not necessarily improve when afterload is reduced or worsens when afterload increases despite of treatment. Whether PAH therapies have a direct effect on the RV cannot be determined based on our results.

RV-arterial coupling and clinical progression

We observed that in newly diagnosed and treated patients alike, RV-arterial uncoupling was associated with clinical progression. The fact that RV afterload was not indicative for clinical progression in our patient cohort is not surprising since multiple PAH studies have demonstrated that pulmonary vascular resistance is not a factor that determines disease progression, unless a high cut off value is considered.[13,14] Indeed, RV function parameters have been shown to determine prognosis instead.[15] Thus far, the RV function parameters that have been investigated were all load-dependent or were indirect reflections of RV function (right ventricular ejection fraction, mean right atrial pressure). This means that these parameters are influenced not only by RV systolic or diastolic function, but also by RV afterload or preload.[16] The present study demonstrates that load-independent RV systolic function alone is not enough to explain differences in clinical progression between I/HPAH-patients. Indeed, RV function and its relation to its load are more important, marking the relevance of good morphological and intrinsic RV adaptation in PAH-patients. Since the current study lacked power to make comparisons with known prognostic parameters such as mean right atrial pressure or cardiac output, the additive value of RV-arterial coupling remains to be established.

Figure 8 - RV function and adaptation in treated stable and progressive patients

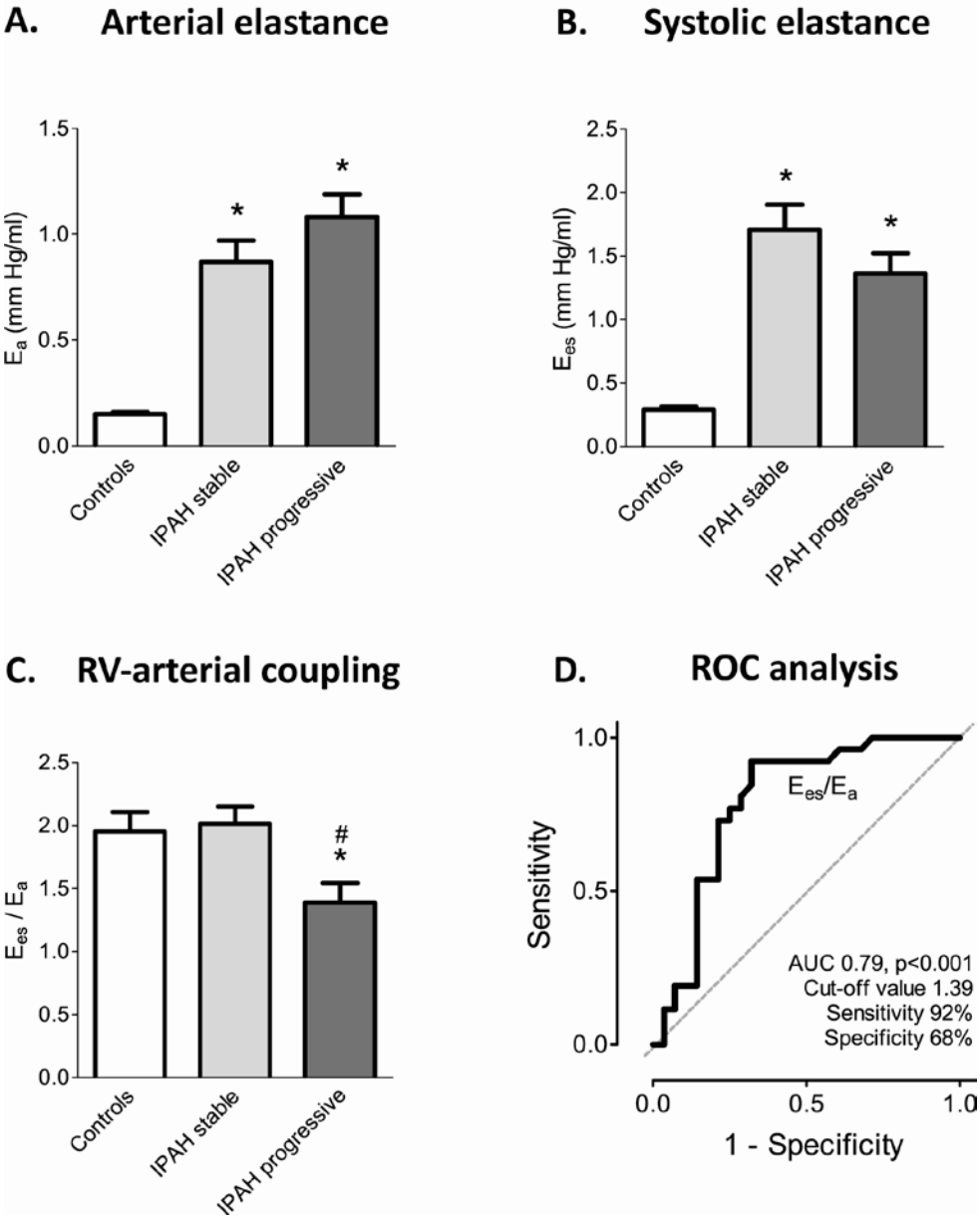

*p-value <0.05 vs. controls, #p-value <0.05 vs. stable I/HPAH. Stable I/HPAH: measurement performed at least 5 years from death/lung transplantation or end of follow-up; progressive I/HPAH: measurement performed within years from death/lung transplantation.

Limitations

In the present study we assumed that mPAP can be taken as a surrogate for RV end-systolic pressure (RVESP).[17] While true in patients with low PA pressures, in a remodeled RV, RVESP could be closer to peak systolic RV pressure, leading to an overestimation of Ees and thus overestimation of RV arterial coupling.[18,19] Despite of this possible overestimation in RV adaptation to arterial load in the more severe patient population, we were able to show that our calculation of RV-arterial coupling

can distinguish between clinical phenotypes. Furthermore, the single-beat estimation of RV Ees has not been validated in PAH-patients. However, in animals a wide range of measured maximal isovolumic pressures correlated well with predicted values, suggesting that maximal RV isovolumic pressure is acceptably predicted in overloaded right ventricles as well.[3]

In the present study, we used fluid-filled catheters to measure RV pressures. We took special care to prevent under- and over-damping of the pressure signal. Before data analysis was performed, we excluded data showing RV pressure tracings with catheter artifacts. Kuehne et al. showed that data obtained in this way is in good agreement with data obtained by catheter-tip manometers.[5]

CONCLUSIONS

Pressure-volume analysis in PAH-patients allows the distinction of different clinical phenotypes and reveals that a decrease in RV afterload is not required for improvements in RV systolic adaptation.

REFERENCES

1. van de Veerdonk MC et al. Progressive right ventricular dysfunction in patients with pulmonary arterial hypertension responding to therapy. J Am Coll Cardiol. 2011; 58:2511-9.
2. Sagawa K et al. Cardiac Contraction and the Pressure-Volume Relationships. Oxford University Press. 1988.
3. Brimioulle S et al. Single beat estimation of right ventricular end-systolic pressure-volume relationship. Am J Physiol Heart CircPhysiol. 2003; 284:H1625-30.
4. Sunagawa K et al. Estimation of the hydromotive source pressure from ejecting beats of the left ventricle. IEEE Trans Biomed Eng. 1980; 27:299-305.
5. Kuehne T et al. Magnetic resonance imaging analysis of right ventricular pressure-volume loops: in vivo validation and clinical application in patients with pulmonary hypertension. Circulation. 2004; 110:2010-6.
6. Rain S et al. Right Ventricular Diastolic Impairment in Patients with Pulmonary Arterial Hypertension. Circulation. 2013; 128:2016-25.
7. Trip P et al. Accurate assessment of load-independent right ventricular systolic function in patients with pulmonary hypertension. J Heart Lung Transplant. 2013; 32:50-5.
8. Naeije R et al. Right ventricular function in pulmonary hypertension: physiological concepts. Eur Heart J Suppl. 2007; 9((Supplement H)):H5-H9.
9. Tedford RJ et al. Right ventricular dysfunction in systemic sclerosis-associated pulmonary arterial hypertension. Circ Heart Fail. 2013; 6:953-63.
10. Ventetuolo CE et al. Sex hormones are associated with right ventricular structure and function: The MESA-right ventricle study. Am J Respir Crit Care Med. 2011; 183:659-67.
11. Kawut SM et al. Determinants of right ventricular ejection fraction in pulmonary arterial hypertension. Chest. 2009; 135:752-9.
12. Jacobs W et al. The right ventricle explains sex differences in survival in idiopathic pulmonary arterial hypertension. Chest 2013; 145:1230-6.
13. Benza RL et al. The REVEAL registry risk score calculator in patients newly diagnosed with pulmonary arterial hypertension. Chest. 2012;141(2):354-362.
14. Lee WT et al. Predicting survival in pulmonary arterial hypertension in the UK. Eur Respir J. 2012; 40:604-11.
15. Vonk Noordegraaf A et al. Right heart adaptation to pulmonary arterial hypertension – physiology and pathobiology. J Am Coll Cardiol. 2013; 62:D22-33.
16. Kass DA et al. Comparative influence of load versus inotropic states on indexes of ventricular contractility: experimental and theoretical analysis based on pressure-volume relationships. Circulation. 1987; 76:1422-36.
17. Chemla D et al. Matching dicrotic notch and mean pulmonary artery pressures: implications for effective arterial elastance. Am J Physiol. 1996; 271:H1287-95.
18. Maughan WL et al. Instantaneous pressure-volume relationship of the canine right ventricle. Circ Res. 1979; 44:309-315.
19. Redington AN et al. Changes in the pressure-volume relation of the right ventricle when its loading conditions are modified. Br Heart J. 1990; 63:45-9.

SUPPLEMENTAL METHODS

Subjects

Part I – Treatment naïve patients

For the assessment of the distribution and sex and age effect of RV systolic and diastolic function and RV-arterial coupling, patients with digitally stored good quality RV pressure recordings at baseline were included in the baseline analysis (see figure 2, n=88). Controls: Patients referred to the VU University Medical Center between 1 January 2009 and 1 January 2012 for the evaluation of pulmonary hypertension (suspicion of I/HPAH due to dyspnea (n=15), chest pain (n=1), positive family history (n=1)), but who had normal pulmonary artery pressures (mean pulmonary artery pressure (mPAP) <20 mmHg) and normal pulmonary capillary wedge pressures (PCWP <15 mmHg) were included as control subjects (n=17).

Supplemental table 1 – Clinical characteristics at baseline according to age

	I/HPAH <58 years	**I/HPAH >58 years**
	n=44	n=44
General characteristics		
Sex (n, female %)	36 (82%)	22 (50%)*
BSA (m^2)	1.95 (1.68-2.08)	1.91 (1.80-2.07)
Hemodynamics		
mPAP (mmHg)	54 (46-66)	45 (41-53)*
CO (L/min)	4.5 (3.5-5.5)	4.3 (3.8-5.5)
HR (bpm)	80 (73-92)	73 (64-86)
TPVR (dyn-sec-cm-5)	1007 (624-1482)	810 (646-1147)
mRAP (mmHg)	8 (5-12)	6 (4-9)
SvO2 (%)	65 (58-71)	62 (55-66)

Data are presented as median (25-75%) or n (%). *p<0.05 vs. I/HPAH <58 years. BSA: body surface area; mPAP: mean pulmonary artery pressure; CO: cardiac output; HR: heart rate; TPVR: total pulmonary vascular resistance; mRAP: mean right atrial pressure; SvO2: mixed venous oxygen saturation.

Part II – Follow-up patients

To determine the effect of a reduction in RV afterload on RV systolic and diastolic function and RV-arterial coupling, patients with good quality RV pressure recordings at both baseline and follow-up (between 0.2-2.5 years after baseline) were included (45 out of 88 treatment naive patients).

Part III – Treated stable and progressive patients

To assess whether a reduced RV-arterial coupling is an indicator of clinical progression, we compared stable and progressive treated patients. Stable I/HPAH was defined as survival without lung transplantation >5 years after a follow-up right heart

catheterization. Progressive I/HPAH was defined as all-cause death or lung transplantation occurring within 5 years of a follow-up right heart catheterization.

Right heart catheterization and cardiac MRI

Right heart catheterization was performed as previously described.[1,2] Under local anesthesia and constant ECG monitoring, a balloon-tipped Swan-Ganz catheter (Edwards Lifesciences, LLC, Irvine, CA) was inserted via the jugular vein and pulmonary artery, right ventricular and right atrial pressures were measured. A Powerlab data acquisition system (AD Instruments, Sydney, Australia) was used to register pressure curves alongside the standard pressure recordings. To obtain high quality pressure curves without artifacts we used shielded pressure transducers with a resistance serially connected to increase damping and flushed the catheter repeatedly with heparin to avoid potential underdamping due to blood clots. Mean PAP was averaged over at least two respiratory cycles.

Supplemental table 2 – Clinical characteristics at baseline according to age

	Male I/HPAH	**Female I/HPAH**
	n=30	n=58
General characteristics		
Age (years)	71 (56-76)	50 (30-67)*
BSA (m^2)	2.01 (1.86-2.10)	1.87 (1.66-2.03)*
Hemodynamics		
mPAP (mmHg)	47 (41-55)	50 (44-59)
CO (L/min)	44.4 (3.9-5.2)	4.3 (3.5-5.7)
HR (bpm)	74 (65-88)	78 (69-91)
TPVR (dyn-sec-cm-5)	811 (660-1182)	962 (611-1272)
mRAP (mmHg)	6 (4-11)	7 (4-11)
SvO2 (%)	61 (55-65)	65 (57-71)

Data are presented as median (25-75%) or n (%). *p<0.05 vs. male patients. BSA: body surface area; mPAP: mean pulmonary artery pressure; CO: cardiac output; HR: heart rate; TPVR: total pulmonary vascular resistance; mRAP: mean right atrial pressure; SvO2: mixed venous oxygen saturation.

Cardiac output (CO) was measured by either the direct Fick method or thermodilution. Stroke volume (SV) was calculated as CO divided by heart rate. Cardiac output and SV were indexed for body surface area (BSA). Total pulmonary vascular resistance was calculated as 80 times mPAP divided by CO.

Supplemental Figure 1 – RV adaptation in pulmonary arterial hypertension, a schematic overview

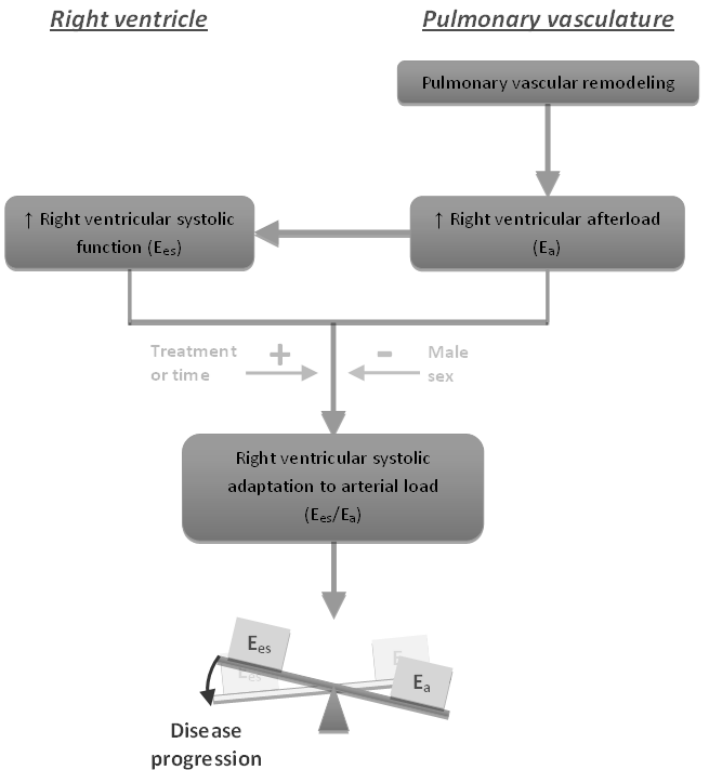

Data analysis

Ees, Ea and RV-arterial coupling

Part of the data analysis has been previously described.[1] The slope of the ESPVR (Ees) was calculated as follows: Ees = (Piso-mPAP)/SV. In this calculation mPAP is mean pulmonary artery pressure and taken as a surrogate of RV end-systolic pressure.[3-5] RV isovolumic pressure (Piso) per beat was determined according the single-beat method of Sunagawa.[6-8] With this method an inverted cosine wave was fitted over the RV pressure curve using the isovolumic contraction period (from end-diastole to the point of maximal rate of pressure rise (dP/dtmax)) and the isovolumic relaxation period (from minimal dP/dt to start diastole) by a semi-automatic Matlab R2008a program (The MathWorks, Natick, MA).

The point of end-diastole was identified using the R-wave of the ECG, and when needed manually shifted to the point before the upslope of the ascending limb. To compensate for beat-to-beat variations, the so calculated RV isovolumic pressures were averaged over at least five heartbeats. Stroke volume was calculated by dividing CO by heart rate. Diastolic elastance was assessed by a non-linear single-beat diastolic PV relation using the following formula: $P=\alpha (eV\beta -1)$ where P: pressure; α: curve-fitting constant; β: diastolic stiffness constant; V: volume.

The exponential term β was further used to quantify RV diastolic stiffness. The three pressure points used to construct the PV relation were recorded at:

1) the minimal pressure decrease of the beginning of the filling phase: begin diastolic pressure (BDP)
2) the maximal pressure rise of the filling phase: end diastolic pressure (EDP)
3) the 0pressure, point

The three volume points used were as follows:
1) end systolic volume (ESV) was calculated by: EDV-SV, where SV was determined from CO divided by HR
2) end diastolic volume (EDV) was set at an arbitrary value of 260 ml as described previously
3) the 0volume point

The exponential pressure-volume relation was constructed using:
1) BDP-ESV point
2) EDP-EDV point
3) 0pressure-0volume point.[2]

Arterial elastance (Ea) was calculated by dividing mPAP by SV. RV-arterial coupling was then calculated as the ratio between Ees and Ea.

Statistical analysis

Part I & II - Baseline and treatment analysis

An independent T-test or Mann-Whitney test was used to compare controls with I/HPAH-patients at baseline, to compare I/HPAH age groups (division based on median age), and to compare the follow-up I/HPAH population with the total baseline population. A chi-squared test was used to compare categorical variables. Linear regression analysis was used to assess differences between sexes with correction for age as confounding factor. A paired T-test or Wilcoxon signed rank test was used to compare baseline and follow-up measurements.

Part III - Survival analysis

Follow-up was until 31 October 2013 and survival was calculated from time of diagnosis with all-cause mortality or lung transplantation as end point. Optimal cut-off values were determined by ROC analysis. A Kaplan-Meier analysis was subsequently performed for dichotomized Ees, Ea, and Ees/Ea-values and compared by the log-rank test. The association between these parameters and survival was further explored by Cox-regression analysis with correction for age differences.

Stable vs. progressive I/HPAH

One-way ANOVA or Kruskal-Wallis test with post-hoc Bonferroni analysis was used to compare continuous variables of controls and I/HPAH patient groups. A chi-squared test was used to compare categorical variables. Differences between stable and progressive I/HPAH were further tested with linear regression analysis with correction for the difference in sex distribution. ROC analysis was additionally used to determine the discriminative value of Ees/Ea in stable and progressive I/HPAH.

REFERENCES

1. Trip P et al. Accurate assessment of load-independent right ventricular systolic function in patients with pulmonary hypertension. J Heart Lung Transplant. 2013; 32:50-5.
2. Rain S et al. Right Ventricular Diastolic Impairment in Patients with Pulmonary Arterial Hypertension. Circulation.2013; 128:2016-25.
3. Chemla D et al. Matching dicrotic notch and mean pulmonary artery pressures: implications for effective arterial elastance. Am JPhysiol. 1996; 271:H1287-95.
4. Curtiss EI et al. Alterations of right ventricular systolic time intervals by chronic pressure and volume overloading. Circulation. 1976; 53:997-1003.
5. Dell'Italia LJ et al. Can indices of left ventricular function be applied to the right ventricle? Prog Cardiovasc Dis. 1998; 40:309-24.
6. Brimioulle S et al. Singlebeat estimation of right ventricular end-systolic pressure-volume relationship. Am J Physiol Heart Circ Physiol. 2003; 284:H1625-30.
7. Sunagawa K et al. Estimation of the hydromotive source pressure from ejecting beats of the left ventricle. IEEE Trans Biomed Eng. 1980; 27:299-305.
8. Takeuchi M et al. Single-beat estimation of the slope of the end-systolic pressure-volume relation in the human left ventricle. Circulation. 1991; 83:202-12.

Chapter 7

Clinical relevance of right ventricular diastolic stiffness in pulmonary hypertension

Trip P, Rain S, Handoko ML, Bogaard HJ, Marcus JT, Boonstra A, Westerhof N, Vonk-Noordegraaf A, de Man FS

European Respiratory Journal 2015
doi: **10.1183/09031936.00156714**

ABSTRACT

Background – Right ventricular (RV) diastolic-stiffness is increased in pulmonary arterial hypertension (PAH) patients. We investigated whether RV diastolic-stiffness is associated with clinical progression and assessed the contribution of RV wall-thickness to RV systolic and diastolic-stiffness.

Methods and Results – Using single-beat pressure-volume-analyses, we determined RV end-systolic-elastance (E_{es}), arterial-elastance (E_a), RV-arterial-coupling (E_{es}/E_a), and RV end-diastolic-elastance (stiffness, E_{ed}) in controls (n=15), baseline PAH (n=63) and treated PAH-patients (survival>5 years, n=22, and survival<5 years, n=23). We observed an association between E_{ed} and clinical progression, with baseline E_{ed}>0.53 mmHg/ml associated with worse prognosis (age-corrected hazard-ratio 0.27, p=0.02). In treated patients, E_{ed} was higher in patients with survival<5 years (0.91±0.50 vs. 0.53±0.33 mmHg/ml in patients with survival>5 years, p<0.01). Wall-thickness-corrected E_{ed}-values in PAH-patients with survival>5 years were not different from control values (0.76±0.47 vs. controls 0.60±0.41 mmHg/ml, ns), whereas in patients with survival<5 years, values were significantly higher (1.52±0.91 mmHg/ml, p<0.05 vs. controls).

Conclusions – RV diastolic-stiffness is related to clinical progression in both baseline and treated PAH-patients. RV diastolic-stiffness is explained by the increased wall-thickness in patients with >5years survival, but not in <5years survival patients. This suggests that intrinsic myocardial changes play a distinctive role in explaining RV diastolic-stiffness in different PAH stages.

INTRODUCTION

In pulmonary arterial hypertension (PAH) pulmonary vascular remodeling leads to a typical fourfold increase in pulmonary artery pressure. The right ventricle (RV) copes with this increased pressure by converting from a low- to high-pressure pump. As long as this adaptation process is successful, cardiac output and oxygen supply to all organs are assured. Important mechanisms to adapt to an increase in pressure include increased muscle mass and enhanced intrinsic myocyte contractility. Both adaptations have been described in PAH-patients and explain the observed increase in RV systolic elastance (E_{es}, a measure of ventricular contractile function) in PAH-patients.[1,4-6]
However, potential consequences of RV systolic adaptation are increased myocardial stiffness and impaired relaxation. Indeed, we recently showed impaired RV diastolic function in PAH-patients.[1] Hypertrophy, fibrosis and stiffening of the RV cardiomyocytes all appeared to contribute to the observed RV diastolic stiffness.[1] However, this analysis was performed in end-stage PAH-patients. Therefore, it remains unclear whether RV diastolic impairment already plays a role at earlier stages of the disease, and whether it is associated with clinical progression. Because RV hypertrophy is already present at early stages of the disease, it could be hypothesized that the initial increase in RV diastolic stiffness is explained by the increase in wall thickness. This in contrast with end-stage PAH, in which further increases in diastolic stiffness may relate to intrinsic sarcomere stiffening.
Therefore, the aim of this study is twofold:
1. To investigate whether increased RV diastolic stiffness is associated with clinical progression in baseline and treated PAH-patients
2. To assess the contribution of RV wall thickness to RV diastolic stiffness in different disease stages.

METHODS

Subjects: control, baseline and treated cases

All patients diagnosed with idiopathic and heritable PAH at the VU University Medical Center from August 10 1989 until 25 February 2014 (n=267) were evaluated for inclusion in the current study.[7] Part of the patient selection procedure has been described before.[6]

Baseline patients

For the assessment of the relation between diastolic stiffness and clinical progression and RV systolic adaptation, baseline treatment-naïve patients with digitally stored good quality RV pressure recordings and a cardiac MRI performed within four weeks from right heart catheterization were included (figure 1, n=63). Reasons for excluding patients were: no stored RV pressure curves at the time of diagnosis (n=48) and RV pressure curves that were of poor quality (n=15).

Treated patients

The association between a high diastolic stiffness and clinical progression was further assessed in treated patients. In addition, these patients were used to determine a) the relation between RV diastolic stiffness and RV systolic adaptation and b) the

interaction between RV wall thickness and RV systolic and diastolic function (Fig. 1). We retrospectively determined the availability of good quality RV pressure curves recorded during follow-up and within four weeks from a cardiac MRI in all idiopathic and heritable PAH patients seen in our hospital. We included patients with these measurements based on their survival time after their follow-up measurement. Patients who were alive and who had a follow-up time <5 years after the measurement were not included. The remaining patients either survived >5 years or died or underwent lung transplantation. These patients were divided into two groups, i.e. survival <5 and >5 years after the follow-up measurements ($PAH_{survival<5yrs}$ and $PAH_{survival>5yrs}$). Of the latter group, only 2 out of 22 included patients had an event during follow-up.

Controls

Subjects referred to the VU University Medical Center between 1 January 2003 and 1 January 2014 for the evaluation of pulmonary hypertension, but who had normal pulmonary artery pressures (mean pulmonary artery pressure (mPAP) <20 mmHg) were included as controls if RV pressure recordings with a concomitant cardiac MRI were available (n=15). Due to the retrospective character of this study using data obtained for clinical purposes, the Medical Ethics Review Committee of the VU University Medical Center did not consider this study to fall within the scope of the Medical Research Involving Human Subjects Act. Therefore, no additional approval was acquired.

Figure 1 - Schematic overview of study populations and study aims

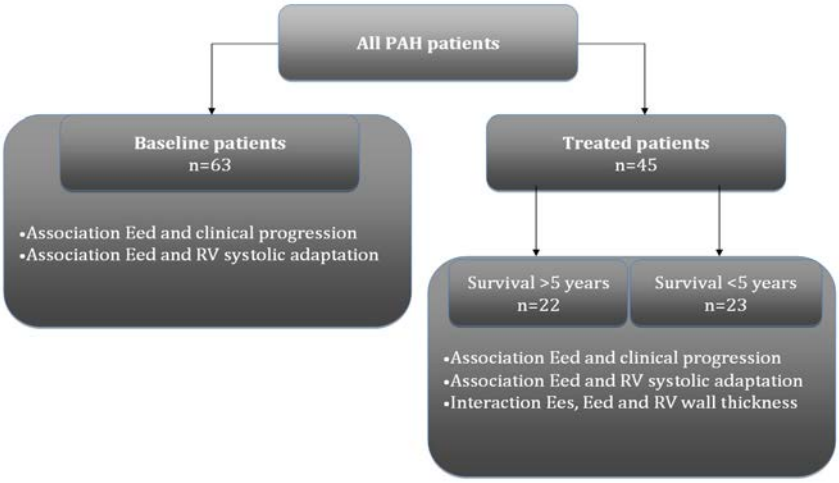

PAH: idiopathic and heritable pulmonary arterial hypertension patients; E_{ed}: end-diastolic elastance; E_{es}: end-systolic elastance.

Right heart catheterization

Right heart catheterization was performed as previously described.[6] A detailed description can be found in the online data supplement. Mean PAP was averaged over at least two respiratory cycles. Cardiac output (CO) was measured by either the direct Fick method or thermodilution. Stroke volume (SV) was calculated as CO divided by

heart rate. CO and SV were indexed for body surface area (BSA). Total pulmonary vascular resistance (TPVR) was calculated as mPAP and divided by CO (Woods units, mmHg/min/L).

Cardiac magnetic resonance imaging

All MR images were acquired with a 1.5 Tesla Avanto or Sonata MRI system equipped with a 6-element phased array coil (Siemens Medical Solutions, Erlangen, Germany) as previously described.[6] A stack of short-axis images was taken at breath-hold per slice, with a slice thickness and interslice gap of 5mm. RV volumes and mass were determined by manually drawing endocardial and epicardial borders at end-diastole and end-systole using Mass Analysis software (MEDIS Medical Imaging Systems, Leiden, The Netherlands). End-diastole was defined as the onset of the R-wave of the ECG. End-systole was determined visually as the smallest volume during the cardiac cycle. Relative wall thickness was calculated by dividing RV mass by RV end-diastolic volume. RV ejection fraction (RVEF) = (RVEDV-RVESV)/RVEDV*100%, where RVEDV is RV end-diastolic volume and RVESV is RV end-systolic volume.

Data analysis

Part of the data analysis has been previously described.[1,6] A detailed description of the data analysis can be found in the online data supplement. The slope of the end-systolic pressure-volume relation (E_{es}, a measure of RV systolic function) was calculated as follows: E_{es} = (P_{iso}-mPAP)/(EDV-ESV). RV isovolumic pressure (P_{iso}) per beat was determined according to the single-beat method of Sunagawa.[8,9] Arterial elastance (E_a, a measure of afterload) was calculated by dividing mPAP by SV. RV-arterial coupling (RV systolic adaptation to arterial load) was then calculated as the ratio between E_{es} and E_a. Diastolic stiffness was assessed by end-diastolic elastance (E_{ed}).

Statistical analysis

The data are presented as means ± SEM unless stated otherwise. A p-value < 0.05 was considered significant. Survival was calculated from the time of diagnosis to death (all-cause mortality) or lung transplantation. Follow-up was till March 1 2014. A Kaplan-Meier analysis was performed for dichotomized E_{ed} based on the median and ROC derived cut-off values (supplement). The association between these parameters and survival was further explored by Cox-regression analysis with correction for age differences. Patient characteristics of baseline patients divided in high and low E_{ed} were tested using an independent T-test or Mann-Whitney test, depending on normal distribution. A chi-squared test was used to compare categorical variables. A one-way analysis of variance with Bonferroni's multiple comparison test or a Kruskal-Wallis test with Dunn's multiple comparison was performed, depending on normal distribution, to compare controls and treated PAH patient groups.

Table 1 - General characteristics and hemodynamics of the total cohort of baseline PAH-patients divided as low and high RV diastolic stiffness

	Baseline	**PAH - Low E_{ed}**	**PAH - High E_{ed}**
Patient number	n=63	N=32	n=31
Age (years)	56 (35-71)	58 (40-73)	49 (30-67)
Gender (n, %)	41 (65%)	21 (66%)	20 (65%)
BSA (m^2)	1.9 (1.7-2.1)	1.9 (1.7-2.1)	1.9 (1.7-2.1)
Follow-up time (y)	2.7 (1.4-4.7)	2.7 (1.2-8.5)	2.4 (1.5-3.9)
Events (n, %)	16 (25%)	5 (16%)	11 (36%)
Hemodynamics			
mPAP (mmHg)	53 (46-59)	50 (45-54)	56 (47-67)*
CI ($L/min/m^2$)	2.3 (2.0-2.7)	2.5 (2.1-2.9)	2.2 (2.0-2.7)
HR (bpm)	80 (71-91)	78 (68-87)	80 (74-97)
TPVR (mmHg/min/L)	12.3 (8.3-15.2)	11.0 (7.6-12.9)	14.5 (9.5-19.5)*
mRAP (mmHg)	6 (4-11)	5 (4-9)	8 (5-11)*
SvO_2 (%)	63 (56-68)	67 (58-70)	61 (55-65)
Cardiac MRI			
RVEDV (ml)	142 (122-175)	149 (134-166)	140 (117-191)
RVESV (ml)	93 (70-128)	91 (73-112)	99 (66-145)
RVEF (%)	36 (23-45)	39 (35-47)	27 (18-38)*
RV mass (g)	98 (78-118)	90 (77-113)	112 (81-132)*
WT(g/ml)	0.65 (0.55-0.82)	0.59 (0.51-0.70)	0.76 (0.57-0.84)*
Pressure-volume analysis			
E_{es} (mmHg/ml)	1.35 (0.99-1.94)	1.12 (0.87-1.49)	1.64 (1.18-2.59)*
E_a (mmHg/ml)	1.14 (0.78-1.44)	0.86 (0.64-1.20)	1.38 (1.05-2.09)*
E_{ed} (mmHg/ml)	0.52 (0.37-0.86)	0.37 (0.27-0.45)	0.86 (0.62-1.22)*
E_{es}/E_a	1.29 (0.99-1.57)	1.32 (1.00-1.66)	1.25 (0.90-1.56)

Data are presented as median (25-75%) or n (%). *p<0.05 vs. PAH - Low E_{ed}. PAH: idiopathic and heritable pulmonary arterial hypertension patients; E_{ed}: end-diastolic elastance; BSA: body surface area; mPAP: mean pulmonary artery pressure; CI: cardiac index; HR: heart rate; WT: wall thickness; TPVR: total pulmonary vascular resistance; mRAP: mean right atrial pressure; SvO_2: mixed venous oxygen saturation; RVEDV: right ventricular end-diastolic volume; RVESV: right ventricular end-systolic volume; RVEF: right ventricular ejection fraction; P_{iso}: right ventricular isovolumic pressure; Ees: end-systolic elastance; E_a: arterial elastance. E_{ed} was calculated as the slope of the diastolic pressure-volume relation at end-diastole, see online data supplement. The diastolic pressure-volume relation was determined as described previously.[1]

Table 2 - Clinical characteristics and right ventricular MRI parameters of controls and the cohort of treated PAH patients divided based on survival (<5 or >5 years)

	Controls	**$PAH_{survival>5yrs}$**	**$PAH_{survival<5yrs}$**
Patient number	n=15	n=22	n=23
General characteristics			
Age (years)	49 (34-59)	37 (31-51)	43 (36-54)
Gender (n, %)	13 (87%)	18 (82%)	18 (78%)
BSA (m^2)	1.91 (1.70-2.04)	1.82 (1.68-2.04)	1.75 (1.62-1.92)
Hemodynamics			
mPAP (mmHg)	14 (12-16)	50 (40-61)*	50 (43-60)*
CI ($L/min/m^2$)	3.6 (3.1-5.1)	3.1 (2.3-3.4)*	2.8 (2.2-3.5)*
HR (bpm)	79 (72-87)	78 (68-90)	89 (77-100)
TPVR (mmHg/min/L)	2.1 (1.5-2.5)	9.1 (6.6-13.8)*	10.2 (7.9-14.7)*
mRAP (mmHg)	4 (3-5)	5 (2-8)	9 (4-13)*
SvO_2 (%)	75 (71-80)	67 (63-72)*	63 (56-69)*
Cardiac MRI			
RVEDV (ml)	120 (94-135)	138 (118-159)	200 (136-269)*†
RVESV (ml)	44 (37-50)	75 (66-114)*	143 (92-227)*
RVEF (%)	63 (54-68)	42 (33-47)*	22 (14-33)*†
RV mass (g)	37 (31-48)	96 (81-116)*	125 (86-149)*
WT (g/ml)	0.33 (0.27-0.39)	0.70 (0.64-0.80)*	0.61 (0.47-0.80)*

Data are presented as median (25-75%) or n (%). *p<0.05 vs. controls, †p<0.05 vs. $PAH_{survival>5yrs}$. PAH: idiopathic and heritable pulmonary arterial hypertension patients; BSA: body surface area; WT: wall thickness; mPAP: mean pulmonary artery pressure; CI: cardiac index; HR: heart rate; TPVR: total pulmonary vascular resistance; mRAP: mean right atrial pressure; SvO_2: mixed venous oxygen saturation.

RESULTS

Relation between RV diastolic stiffness and clinical progression

To investigate whether RV diastolic stiffness is related to clinical progression, we first compared clinical characteristics of baseline patients with a low and high RV diastolic stiffness (median-based cut-off value 0.53 mmHg/ml). Table 1 shows that patients with a high diastolic stiffness had a higher mPAP, TPVR and mean right atrial pressure (mRAP) when compared to patients with a low diastolic stiffness. RV volumes were similar in the two groups, while patients with a high diastolic stiffness exhibited a lower RV ejection fraction and a higher RV mass and relative wall thickness. Interestingly, pressure-volume analysis revealed that despite of the higher afterload seen in patients with a higher diastolic stiffness, RV-arterial coupling was similar. A

survival analysis based on baseline values of RV diastolic stiffness showed that age-corrected survival was worse for patients with a high diastolic stiffness (Fig. 2).

Figure 2 - Survival of baseline patients according to low or high

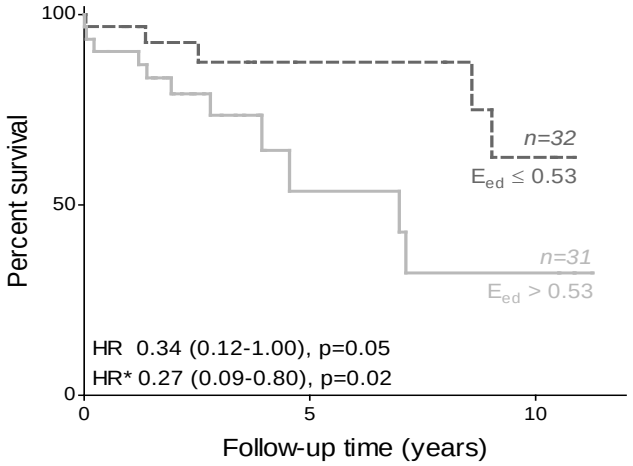

E_{ed}. *age-corrected

Similar findings were observed when using an ROC analysis-based optimal E_{ed} cut-off value as presented in the online supplement (supplemental figure 2).
To further investigate the association between RV diastolic stiffness and clinical progression in PAH-patients, we divided treated patients into two groups
1) survival >5 years after a follow-up right heart catheterization ($PAH_{survival>5yrs}$)
2) death occurring within 5 years of a follow-up right heart catheterization ($PAH_{survival<5yrs}$).
Table 2 shows general characteristics, hemodynamics and cardiac MRI measurements of $PAH_{survival>5yrs}$ and $PAH_{survival<5yrs}$, as well as control subjects. As expected, $PAH_{survival<5yrs}$ had a higher RV end-diastolic volume and a lower RV ejection fraction in comparison to $PAH_{survival>5yrs}$. No difference was observed between E_{es} en E_a in $PAH_{survival>5yrs}$ and $PAH_{survival<5yrs}$, albeit that E_{es}, E_a and E_{ed} were all increased in comparison to controls (Fig. 3). However, in $PAH_{survival<5yrs}$ but not in $PAH_{survival>5yrs}$, the reduced RV-arterial coupling coincided with increased RV diastolic stiffness. Together, these data together suggest that RV diastolic stiffening is closely associated with clinical progression in both baseline as well as treated PAH-patients.

Relative wall thickness and diastolic stiffness in different disease stages

To investigate whether the increased E_{es} and E_{ed} in $PAH_{survival>5yrs}$ and $PAH_{survival<5yrs}$ are a sole consequence of increased RV wall thickness, we subsequently calculated wall thickness corrected E_{es} and E_{ed} values. As can be observed in Figure 4, E_{es} values remained increased after correction for RV wall thickness. In contrast, wall thickness-corrected E_{ed} values were normal in $PAH_{survival>5yrs}$, whereas in $PAH_{survival<5yrs}$ wall thickness-corrected E_{ed} values was significantly increased. These data suggest that diastolic stiffness in stable patients may be largely explained by hypertrophy, while in progressive patients additional intrinsic factors may play a role in increasing diastolic stiffness.

Relation between RV diastolic stiffness and systolic adaptation

To assess whether diastolic stiffness is associated with impaired RV systolic adaptation, we investigated the relation between E_{ed} and E_{es}/E_a in baseline and treated patients. In baseline patients, E_{ed} showed no correlation with E_{es}/E_a (r^2=0.01, p=0.53). In treated patients, only a weak correlation between E_{ed} and E_{es}/E_a was observed (r^2=0.17, p=0.005), suggesting that RV diastolic stiffening and systolic adaptation are largely independent processes.

Figure 3 - Pressure-volume analysis

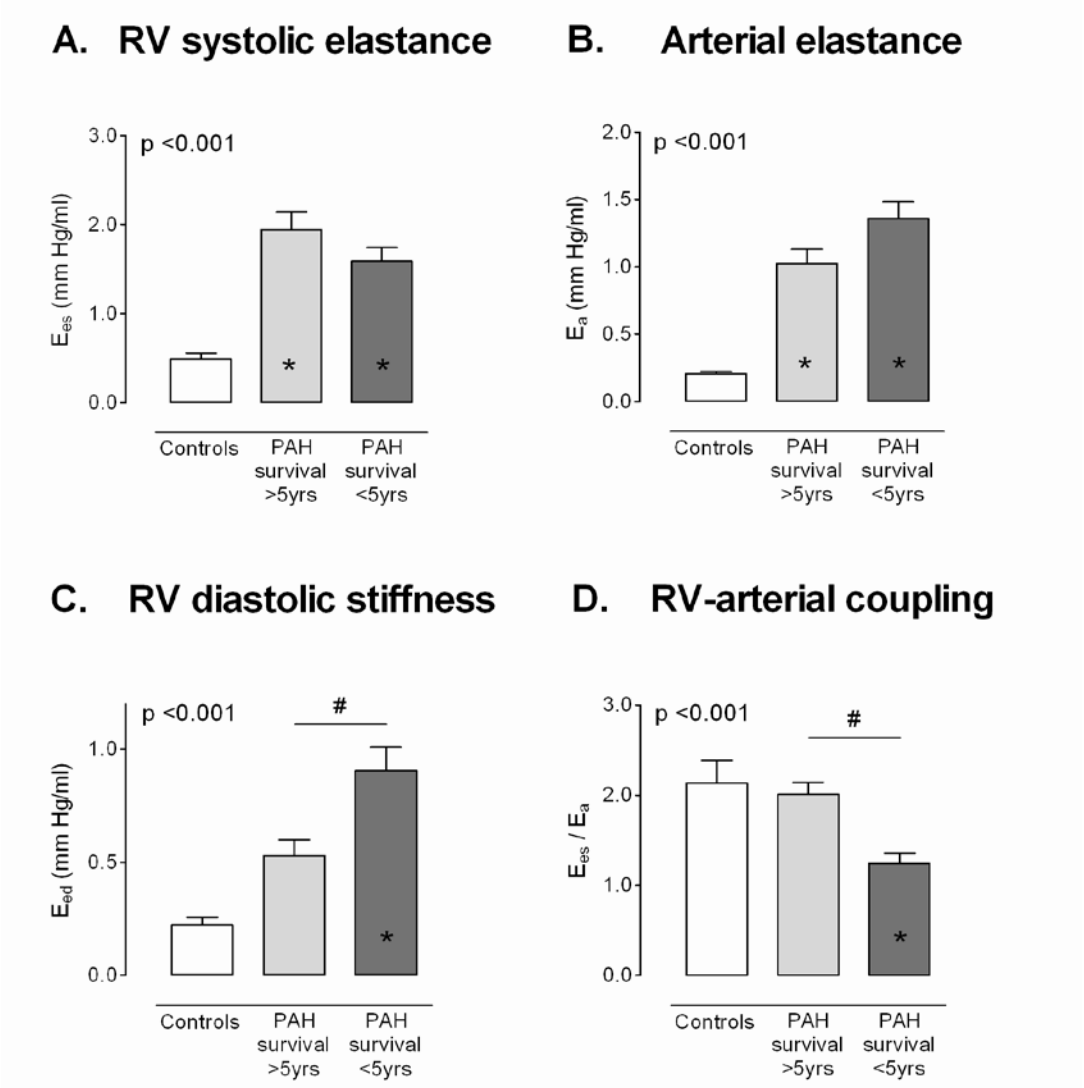

Ees, Ea, Eed and Ees/Ea were performed in controls (n=15), treated $PAH_{survival>5yrs}$ (n=22) and $PAH_{survival<5yrs}$ (n=23). *p<0.05 vs. controls. #p<0.05 vs. $PAH_{survival>5yrs}$.

Figure 4 - Right ventricular function corrected for wall-thickness

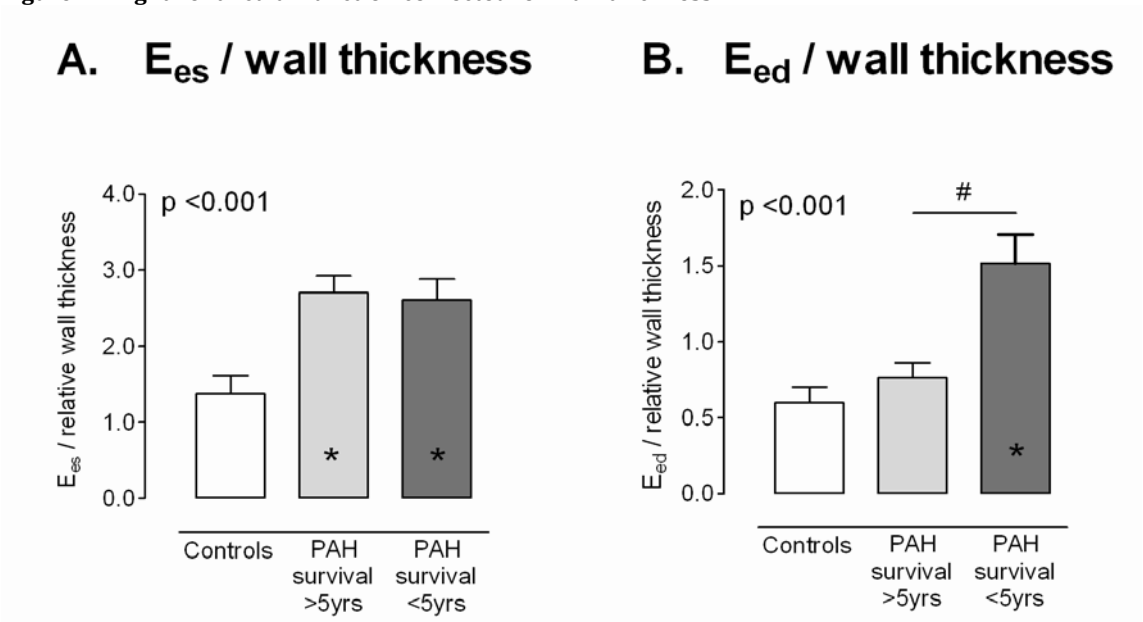

Ees and Eed were corrected for RV wall thickness in controls, and treated PAH-patients: $PAH_{survival>5yrs}$ and $PAH_{survival<5yrs}$.

DISCUSSION

In the present study we assessed RV diastolic stiffness in a large cohort of baseline and treated PAH-patients and demonstrated that:
1) diastolic stiffening is closely associated with clinical progression in both baseline as well as treated PAH-patients
2) diastolic stiffness in treated PAH-patients with a survival >5 years is largely explained by increased RV wall thickness, whereas in PAH-patients RV with a survival <5 years diastolic stiffness remains increased after correction for RV wall thickness
3) RV diastolic stiffness is only weakly associated with impaired RV systolic adaptation in treated PAH-patients, while no relation exists in baseline PAH-patients.

The clinical importance of RV diastolic stiffness

Previous large PAH-patient cohort studies have demonstrated the clinical importance of load-dependent measures of RV diastolic stiffening such as RA pressure, increased atrium-dependent RV filling, and prolonged RV isovolumic relaxation.[10-14] Especially RA pressure is one of the parameters that is frequently identified as predictor of survival in multivariate survival analyses.[10] We have recently introduced a novel method to assess RV diastolic stiffness in a load-independent fashion using a single-beat, diastolic pressure-volume analysis.[1] Load-independent assessment of RV diastolic stiffness is scientifically important, as it provides insight in the intrinsic alterations of the RV myocardium independently from the degree of pressure overload. However, what remained unanswered is whether load-independent RV diastolic stiffness is related to clinical progression and development of right heart failure. Therefore, we investigated

the association between clinical progression and RV diastolic stiffness and observed a close association in both treated as well as baseline PAH-patients.
Subsequently, we were interested in the relation between RV diastolic stiffness and RV systolic adaptation. Both systolic and diastolic function are closely modulated on a cellular level by calcium flux and sarcomeric function, and on ventricular level by wall mass.[12,15] Recently, we identified in tissue samples from end-stage PAH-patients, changes in protein expression of important calcium handling proteins indicating prolonged diastolic calcium clearance.[16] Furthermore, increased calcium sensitivity of the sarcomeric proteins may add to RV systolic adaptation as less calcium would be needed to obtain a similar force development.[1,16] However, at the same time increased calcium sensitivity will affect relaxation of the RV cardiomyocytes, thereby inducing diastolic stiffening of the RV. Therefore, we recently proposed that in early stages of PAH, RV diastolic stiffness may result from the adaptation mechanisms that are induced to preserve RV systolic adaptation as long as possible, such as ventricular wall mass and increased calcium sensitivity.[17] In later stages, RV diastolic stiffness will become more prevalent due to stiffening of the RV cardiomyocytes itself, which will eventually hamper RV systolic adaptation in end-stage PAH.[14,17,18] In this study, support for this hypothesis was provided by finding increased RV diastolic stiffness in baseline PAH-patients in whom RV systolic adaptation was relatively preserved. Moreover, only in treated PAH-patients, RV diastolic stiffness coincided with impaired RV systolic adaptation.

Possible mechanisms of RV diastolic stiffness in PAH

To obtain more insight into the mechanism of RV diastolic stiffness and systolic function in different stages of PAH, we calculated systolic elastance corrected for wall thickness. After correction for wall thickness, RV systolic function was increased in all PAH-patients in comparison to controls. This indicates that in addition to the increased RV wall mass, intrinsic alterations in the cardiac muscle are important in determining increased systolic function of the RV in PAH. RV diastolic stiffness corrected for wall-thickness was not different from control subjects in PAH-patients with a survival >5 years. This may indicate that RV diastolic stiffness in early or stable PAH is a mere consequence of RV systolic adaptation. In PAH-patients with a survival <5 years, RV diastolic stiffness is increased out of proportion to the increase in wall thickness, which indicates that intrinsic cardiac muscle alterations play an additional role in determining diastolic stiffness in more advanced PAH. One such intrinsic alteration could be RV cardiomyocyte stiffening due to hypo-phosphorylation of the giant sarcomeric protein titin, which we recently showed in RV samples of end-stage PAH-patients.[16] Another possible mechanism of RV diastolic stiffness may be increased collagen deposition, although until now only modest increases in RV fibrosis have been reported in clinical PAH.[1]

Clinical implications

With the present study we show that in a large baseline and treated PAH patient cohort RV diastolic stiffness is associated with clinical progression. A high diastolic stiffness has little relationship to a reduced RV systolic adaptation, indicating that the relation between diastolic stiffness and clinical progression in PAH is not mediated through influences on RV systolic function. This finding further marks the importance of RV

diastolic function in PAH and underscores the need to further explore the additive value of the determination of diastolic stiffness in predicting patient outcome. Moreover, future studies are needed to provide tools to noninvasively assess RV diastolic function. Currently, the available noninvasive techniques have significant drawbacks which limits the clinical applicability of noninvasive RV diastolic evaluation.[19-21] However, studies on the assessment of diastolic wall strain in patients with left ventricular diastolic dysfunction have shown promising results, making diastolic wall strain a possible future evaluation tool for RV diastolic dysfunction in PAH.[2, 22-24]

CONCLUSIONS

With the present study we demonstrate that RV diastolic stiffening is closely associated to clinical progression in both baseline as well as treated PAH-patients. We additionally show that RV diastolic stiffness in treated PAH-patients with a survival >5 years is largely explained by increased RV wall thickness, whereas in PAH-patients with a survival <5 years the further increase in RV diastolic stiffness is most likely related to additional intrinsic alterations of the myocardium. Furthermore, RV diastolic stiffness is only weakly associated with impaired RV systolic adaptation in treated PAH-patients, while no relation exists in baseline PAH-patients.

REFERENCES

1. Rain S *et al.* Right Ventricular Diastolic Impairment in Patients with Pulmonary Arterial Hypertension. *Circulation.* 2013; 128:2016-2025
2. de Man FS *et al.* Bisoprolol delays progression towards right heart failure in experimental pulmonary hypertension. *Circ Heart Fail.* 2012; 5:97–105.
3. de Man FS *et al.* Dysregulated renin-angiotensin-aldosterone system contributes to pulmonary arterial hypertension. *Am J Respir Crit Care Med.* 2012; 186:780–789.
4. Kuehne T *et al.* Magnetic resonance imaging analysis of right ventricular pressure-volume loops: in vivo validation and clinical application in patients with pulmonary hypertension. *Circulation.* 2004; 110:2010–2016.
5. Tedford RJ *et al.* Right Ventricular Dysfunction in Systemic Sclerosis Associated Pulmonary Arterial Hypertension. *Circ Heart Fail.* 2013; 6:953-63
6. Trip P *et al.* Accurate assessment of load-independent right ventricular systolic function in patients with pulmonary hypertension. *J Heart Lung Transplant Off Publ Int Soc Heart Transplant.* 2013; 32:50–55.
7. Galiè N *et al.* Guidelines for the diagnosis and treatment of pulmonary hypertension: the Task Force for the Diagnosis and Treatment of Pulmonary Hypertension of the European Society of Cardiology (ESC) and the European Respiratory Society (ERS), endorsed by the International Society of Heart and Lung Transplantation (ISHLT). *Eur Heart J.* 2009; 30:2493–2537.
8. Brimioulle S *et al.* Single-beat estimation of right ventricular end-systolic pressure-volume relationship. *Am J Physiol Heart Circ Physiol.* 2003; 284:H1625–1630.
9. Sunagawa K *et al.* Estimation of the hydromotive source pressure from ejecting beats of the left ventricle. *IEEE Trans Biomed Eng.* 1980; 27:299–305.
10. Benza RL *et al.* The REVEAL Registry risk score calculator in patients newly diagnosed with pulmonary arterial hypertension. *Chest.* 2012; 141:354–362.
11. D'Alonzo GE *et al.* Survival in patients with primary pulmonary hypertension. Results from a national prospective registry. *Ann Intern Med.* 1991; 115:343–349.
12. Gan CT *et al.* Right ventricular diastolic dysfunction and the acute effects of sildenafil in pulmonary hypertension patients. *Chest.* 2007; 132:11–17.
13. Vonk Noordegraaf A *et al.* The role of the right ventricle in pulmonary arterial hypertension. *Eur Respir Rev Off J Eur Respir Soc.* 2011; 20:243–253.
14. Vonk-Noordegraaf A *et al.* Right heart adaptation to pulmonary arterial hypertension: physiology and pathobiology. *J Am Coll Cardiol.* 2013; 62:D22–33.
15. Eichhorn EJ *et al.* Are contraction and relaxation coupled in patients with and without congestive heart failure? *Circulation.* 1992; 85:2132–2139.
16. Rain S *et al.* Protein changes contributing to right ventricular cardiomyocyte diastolic dysfunction in pulmonary arterial hypertension. J Am Heart Assoc 2014; 3:e000716.
17. Rain S *et al.* Pressure overload-induced right heart failure. *Pflügers Arch Eur J Physiol.* 2014; 466:1055–1063.
18. Voelkel NF *et al.* Right Ventricular Function and Failure Report of a National Heart, Lung, and Blood Institute Working Group on Cellular and Molecular Mechanisms of Right Heart Failure. *Circulation.* 2006; 114:1883–1891.
19. Leong DP *et al.* Heart failure with normal ejection fraction: the complementary roles of echocardiography and CMR imaging. *JACC Cardiovasc Imaging.* 2010; 3:409–420.
20. Maurer MS *et al.* Diastolic dysfunction: can it be diagnosed by Doppler echocardiography? *J Am Coll Cardiol.* 2004; 44:1543–1549.
21. Paulus WJ *et al.* How to diagnose diastolic heart failure: a consensus statement on the diagnosis of heart failure with normal left ventricular ejection fraction by the Heart Failure and Echocardiography Associations of the European Society of Cardiology. *Eur Heart J*. 2007; 28:2539–2550.
22. Ohtani T *et al.* Diastolic stiffness as assessed by diastolic wall strain is associated with adverse remodelling and poor outcomes in heart failure with preserved ejection fraction. *Eur Heart J*. 2012; 33:1742–1749.
23. Takeda Y *et al.* Noninvasive assessment of wall distensibility with the evaluation of diastolic epicardial movement. *J Card Fail.* 2009; 15:68–77.
24. Bogaard HJ *et al.* Adrenergic receptor blockade reverses right heart remodeling and dysfunction in pulmonary hypertensive rats. *Am J Respir Crit Care Med.* 2010; 182:652–660.

SUPPLEMENTAL METHODS

Right heart catheterization and cardiac MRI

Right heart catheterization was performed as previously described.[1,2] Under local anesthesia and constant ECG monitoring, a balloon-tipped Swan-Ganz catheter (Edwards Lifesciences, LLC, Irvine, CA) was inserted via the jugular vein and pulmonary artery, right ventricular and right atrial pressures were measured. A Powerlab data acquisition system (AD Instruments, Sydney, Australia) was used to register pressure curves alongside the standard pressure recordings. To obtain high quality pressure curves without artifacts we used shielded pressure transducers with a resistance serially connected to increase damping and flushed the catheter repeatedly with heparin to avoid potential underdamping due to blood clots. Mean PAP was averaged over at least two respiratory cycles. Cardiac output (CO) was measured by either the direct Fick method or thermodilution. Stroke volume (SV) was calculated as CO divided by heart rate. Cardiac output and SV were indexed for body surface area (BSA). Total pulmonary vascular resistance was calculated as mPAP divided by CO (Woods units, mmHg/min/L).

Supplemental Figure 1 – Two methods to calculate diastolic stiffness

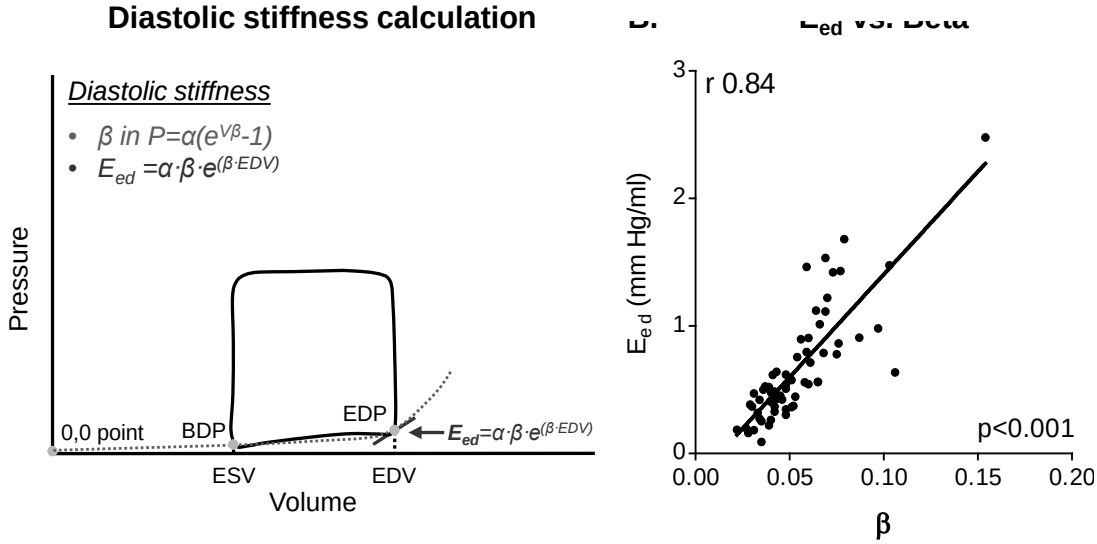

A. β (dotted line) has been used in previous studies and describes only part of the end-diastolic pressure-volume relation. E_{ed} (end-diastolic elastance) is used in the present study and describes the slope of the end-diastolic pressure-volume relation at end-diastole (continuous line).[2] B. Correlation between the previously used measure of diastolic stiffness β and E_{ed} in baseline PAH-patients.

Data analysis

E_{es}, E_a and RV-arterial coupling

Part of the data analysis has been previously described [1]. The slope of the ESPVR (E_{es}) was calculated as follows: E_{es} = (P_{iso}-mPAP)/(EDV-ESV). In this calculation mPAP

is mean pulmonary artery pressure and taken as a surrogate of RV end-systolic pressure.[3-5]

Supplemental Figure 2 – Baseline survival

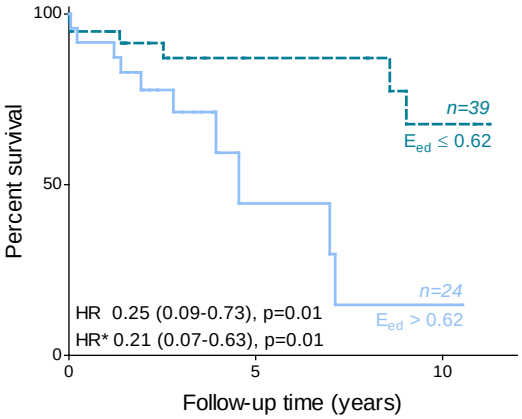

Survival of baseline patients according to low or high E_{ed} based on an E_{ed} cut-off value determined with ROC analysis. *age-corrected.

RV isovolumic pressure (P_{iso}) per beat was determined according the single-beat method of Sunagawa.[6-8] With this method an inverted cosine wave was fitted over the RV pressure curve using the isovolumic contraction period (from end-diastole to the point of maximal rate of pressure rise (dP/dt_{max})) and the isovolumic relaxation period (from minimal dP/dt to start diastole) by a semi-automatic Matlab R2008a program (The MathWorks, Natick, MA). The point of end-diastole was identified using the R-wave of the ECG, and when needed manually shifted to the point before the upslope of the ascending limb. To compensate for beat-to-beat variations, the so calculated RV isovolumic pressures were averaged over at least five heartbeats. End-diastolic volume (EDV) and end-systolic volume (ESV) were determined with cardiac MRI. Arterial elastance (E_a) was calculated by dividing mPAP by EDV-ESV. RV-arterial coupling was then calculated as the ratio between E_{es} and E_a. A non-linear single-beat diastolic pressure-volume relation was determined using the following formula: $P=\alpha\ (e^{V\beta} -1)$ where P: pressure; α: curve-fitting constant; β: diastolic stiffness constant; V: volume. The three pressure points used to construct the PV relation were recorded at: 1) the minimal pressure decrease of the beginning of the filling phase: begin diastolic pressure (BDP) 2) the maximal pressure rise of the filling phase: end diastolic pressure (EDP) 3) the $0_{pressure}$, point

To avoid measurement errors caused by the positioning of the catheter, BDP was normalized at 1 mm Hg, whereas the EDP was calculated with the following formula: $EDP_{normalized}=1+EDP_{initial}-BDP_{initial}$.[2] The three volume points used were as follows:

1) end systolic volume (ESV)

2) end diastolic volume (EDV)

3) the 0_{volume} point .

The exponential pressure-volume relation was constructed using:

1) $BDP_{normalized}$-ESV point

2) $EDP_{normalized}$-EDV point

3) $0_{pressure}$-0_{volume} point.[2]

Subsequently, end-diastolic elastance (E_{ed}) was determined at end-diastolic volume using α and β in the following formula: $\alpha \cdot \beta \cdot e^{(\beta \cdot EDV)}$.

REFERENCES

1. Trip P *et al.* Accurate assessment of load-independent right ventricular systolic function in patients with pulmonary hypertension. *J Heart Lung Transplant.* 2013; 32:50-5.
2. Rain S *et al.* Right Ventricular Diastolic Impairment in Patients with Pulmonary Arterial Hypertension. *Circulation.* 2013; 128:2016-25.
3. Chemla D *et al.* Matching dicrotic notch and mean pulmonary artery pressures: implications for effective arterial elastance. *Am J Physiol.* 1996; 271:H1287-95.
4. Curtiss EI *et al.* Alterations of right ventricular systolic time intervals by chronic pressure and volume overloading. *Circulation.* 1976; 53:997-1003.
5. Dell'Italia LJ *et al.* Can indices of left ventricular function be applied to the right ventricle? *Prog Cardiovasc Dis.* 1998; 40:309-24.
6. Brimioulle S *et al.* Single-beat estimation of right ventricular end-systolic pressure-volume relationship. *Am J Physiol Heart Circ Physiol*. 2003; 284:H1625-30.
7. Sunagawa K *et al.* Estimation of the hydromotive source pressure from ejecting beats of the left ventricle. *IEEE Trans Biomed Eng*. 1980; 27:299-305.
8. Takeuchi M *et al.* Single-beat estimation of the slope of the end-systolic pressure-volume relation in the human left ventricle. *Circulation*. 1991; 83:202-12

Chapter 8

Conclusions and future perspectives

CONCLUSIONS

Part 1 – Molecular pathways associated with RV diastolic impairment

In figure 1 the most important molecular mechanisms underlying RV diastolic dysfunction in PAH are summarized. Based on the findings in this thesis we propose that altered neurohormonal signaling is at the origin of diastolic dysfunction in PAH patients. An overactive noradrenergic (NA) system is known to induce a protective downregulation of cardiomyocyte membrane-bound β-adrenergic receptors (β-AR), with a net downstream effect of reduced protein kinase A (PKA)-mediated phosphorylation of target proteins.

Figure 1 – Molecular mechanisms of RV diastolic dysfunction.

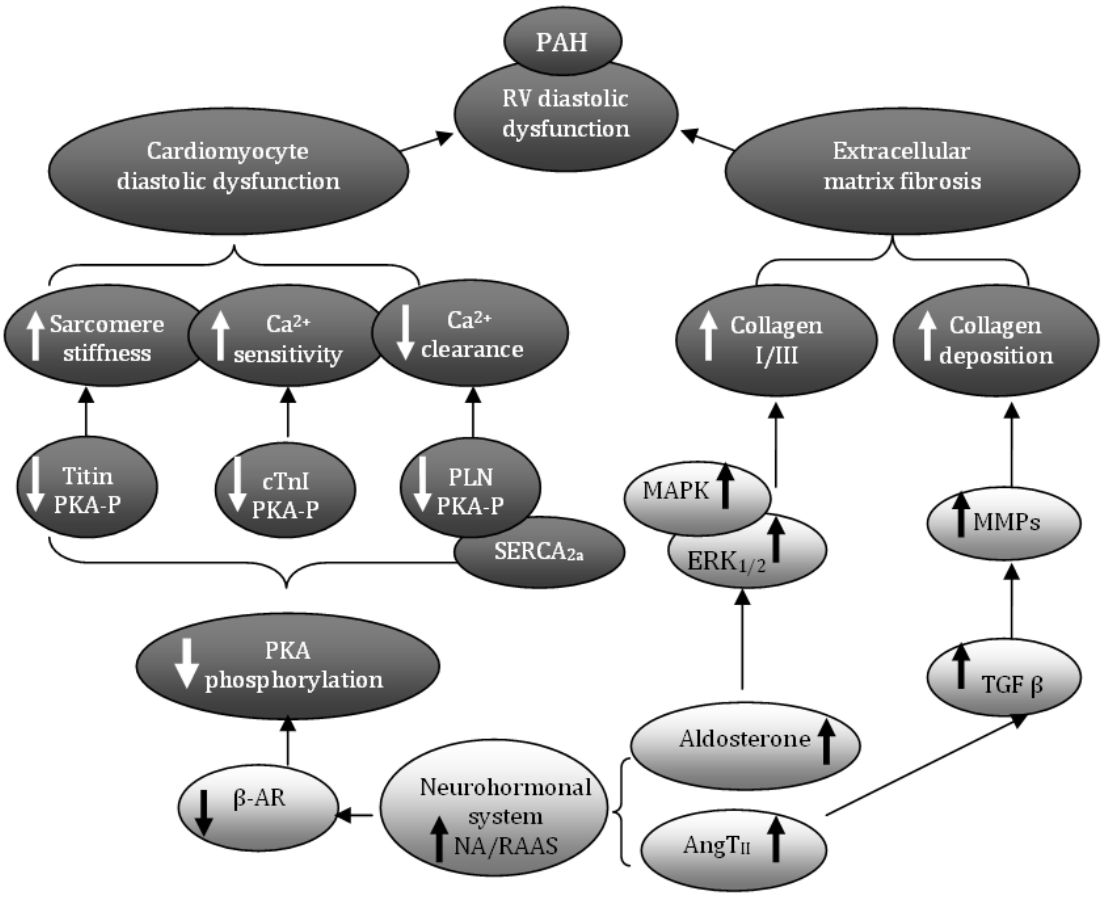

PAH: pulmonary arterial hypertension; PKA-P: protein kinase A phosphorylation; cTnI: cardiac troponin I; PLN: phospholamban; $SERCA_{2a}$: sarcoplastmic reticulum calcium ATPase 2a (cardiac isoform); β-AR: β-adrenergic receptors; NA: noradrenalin; RAAS: renin-angiotensin-aldosterone system; $AngT_{II}$: angiotensin II; TGF-β: transforming growth factor; MMPs: matrix metalloproteinases; $ERK_{1/2}$: extracellular signal-regulated kinases; MAPKs: mitogen-activated protein kinases

In our studies we show that a series of key-proteins regulating cardiomyocyte relaxation are insufficiently phosphorylated by PKA and contribute to increased cardiomyocyte stiffness in the failing RV of PAH patients.

In addition to the NA system, the exacerbated renin-angiotensin-aldosterone (RAAS) system may also play an important part in altering the diastolic function of the right ventricle by increasing extracellular fibrosis. Increased levels of angiotensin II could lead to the activation of TGF-β in the RV fibroblasts, which would 1) increase collagen fiber secretion, 2) decrease MMPs and increase TIMPS, with a net effect of enhancing collagen production and deposition. Furthermore, via the aldosterone signaling pathways the activation of mitogen-activated protein kinases (MAPKs) and extracellular signal-regulated kinases (ERK1/2) could lead to an increase in the mRNA levels of type I collagen, which is the stiff collagen isoform.

Part 2 – Clinical relevance of RV diastolic impairment

In figure 2 we give an overview of the clinical relevance of RV diastolic dysfunction in patients with PAH. The presence of RV diastolic dysfunction in treated PAH patients was associated with worse clinical and hemodynamic parameters and shorter survival. At baseline diastolic dysfunction is an independent predictor of survival. Therefore we believe that in PAH patients an altered diastolic function contributes to the severity of disease and is not solely a benign phenomenon which accompanies the systolic impairment.

Figure 2 – Clinical relevance of RV diastolic dysfunction.

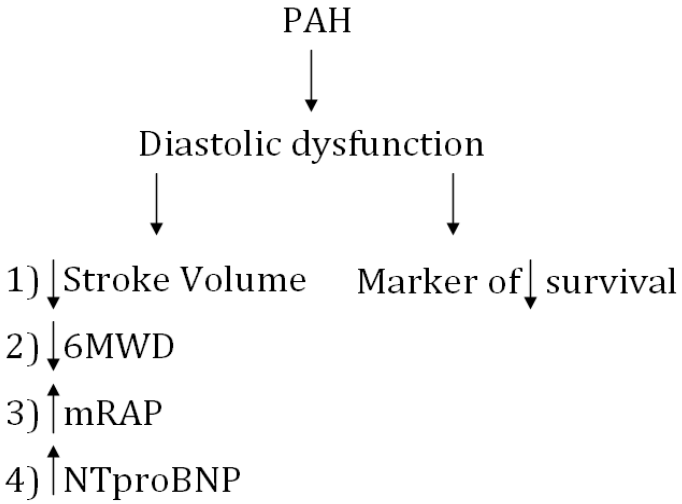

PAH: pulmonary arterial hypertension; 6MWD: 6 minutes walk distance test; mRAP: mean right atrial pressure; NTproBNP: N-terminal prohormone of brain natriuretic peptide

FUTURE PERSPECTIVES

Titin and RV hypertrophy

Background

The survival in PAH patients is related to the capacity of the RV to preserve its function. Regardless of pulmonary arterial pressure, patients who present with a relatively hypertrophied RV tend to preserve the pump function and cope better with the high afterload. Nevertheless, in most patients this initial hypertrophic step is quickly followed by extensive RV dilation and failure.

Figure 3 – Titin and the transition from a stable RV function to RV failure

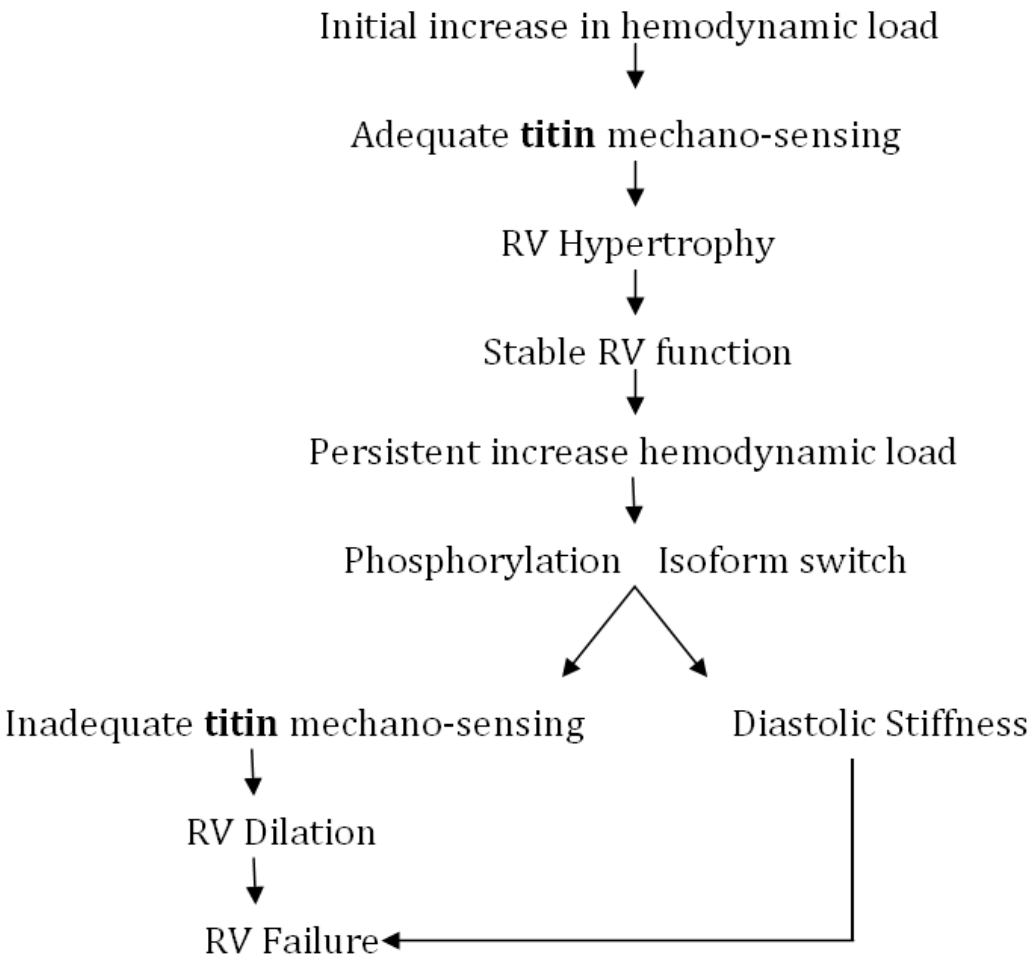

The transition from an adaptive RV hypertrophic response to the inability of the RV to maintain hypertrophy is crucial for the progression of cardiac disease. However, the molecular mechanisms which govern this process are not understood, despite their prognostic importance. A clear understanding of the molecular steps involved in the

remodeling of the RV could further lead to appropriate medical treatment to preserve RV hypertrophy and stop the progression towards failure.
Titin plays a major role in determining the diastolic stiffness of RV cardiomyocytes. However titin also plays a central function in cellular-extracellular mechano-sensing.[1-4] The relation between cardiac cells and the surrounding extracellular matrix involves not only the close contact between the two, but also a continuous bidirectional communication which is dependent on adequate sensing and responding to the local mechanical stimuli.

Hypothesis

We believe that as the afterload increases, titin function is altered with two important functional consequences 1) increased diastolic stiffness and 2) altered mechano-sensing. The incapacity of titin to correctly sense the extracellular strain may underlie cessation of the transmission of hypertrophic stimuli to the nucleus. Eventually, myocardial hypertrophy stops and the progression to RV dilation and failure occurs. (Figure 3)

Figure 4 – Titin and mechano-sensing associated proteins

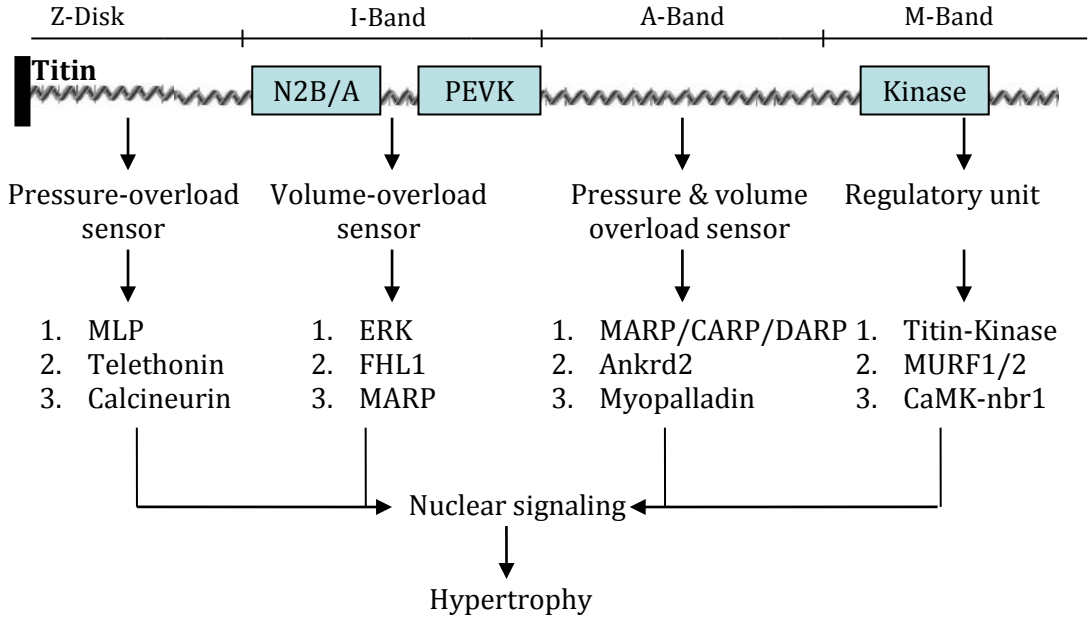

The mechanisms by which titin may incorrectly sense the myocardial mechanical stretch could be diverse. In figure 4 we describe what is currently known about titin and its sarcomeric protein partners involved in the mechano-sensory process.[5-8] Furthermore the newly discovered titin-kinase was shown to be activated by increased myocardial strain and upon ATP binding and autophosphorylation to induce hypertrophic signaling helping cardiomyocytes to adapt to the loading conditions.[9-11]

Methods

The progress from hypertrophic remodeling to RV dilation and failure is difficult to study in human material, since RV tissue samples are usually gathered after cardiac explanation and therefore are in the end-stage failing stage. Nevertheless, careful RV biopsy at different RV remodeling time-points may provide sufficient tissue to perform important molecular studies and determine the mechanisms involved in the transition to heart failure.

Furthermore, PAH animal models of different severity stage are very useful on this perspective. The induction of PAH by pulmonary arterial banding (PAB) is suitable for the following reasons. Firstly, by PAB one can study exclusively the RV response to the afterload, without the pulmonary vascular remodeling as confounding factor. Secondly, by performing a PAB of variable diameter, the severity of the disease can be modulated and distinct RV remodeling (hypertrophic, dilative) can be induced. Third, therapeutic options can be implemented and their effect solely attributed to the right ventricle.

Future Aims

We would like to determine whether the changes in titin and its mechano-sensory partner proteins are altered in PAH. If indeed the case, it is further important to understand 1) the initial molecular pathways which induce adaptive RV hypertrophy; 2) the alterations in signaling pathways which eventually lead to the cessation of the hypertrophic response and 3) which therapy options could be applied to target these pathways.

REFERENCES

1. Arimura T *et al.* Structural analysis of four and half LIM protein-2 in dilated cardiomyopathy. *Biochem Biophys Res Commun*. 2007;357:162–167.
2. Bos JM *et al.* Genotype-phenotype relationships involving hypertrophic cardiomyopathy-associated mutations in titin, muscle LIM protein, and telethonin. *Mol Genet Metab*. 2006;88:78–85.
3. Brancaccio M *et al.* Melusin, a muscle-specific integrin beta1-interacting protein, is required to prevent cardiac failure in response to chronic pressure overload. *Nat Med*. 2003;9:68–75.
4. Fink MA *et al.* AKAP-mediated targeting of protein kinase a regulates contractility in cardiac myocytes. *Circ Res*. 2001;88:291–297.
5. Gautel M *et al.* Cytoskeletal protein kinases: titin and its relations in mechanosensing. *Pflugers Arch*. 2011;462:119–134.
6. Hayashi T *et al.* Tcap gene mutations in hypertrophic cardiomyopathy and dilated cardiomyopathy. *J Am Coll Cardiol*. 2004;44:2192–2201.
7. Knöll R *et al.* The cardiac mechanical stretch sensor machinery involves a Z disc complex that is defective in a subset of human dilated cardiomyopathy. *Cell*. 2002;111:943–955.
8. Linke WA *et al.*. The giant protein titin as an integrator of myocyte signaling pathways. *Physiology (Bethesda)*. 2010;25:186–198.
9. Linke WA *et al.* Sense and stretchability: the role of titin and titin-associated proteins in myocardial stress-sensing and mechanical dysfunction. *Cardiovasc Res*. 2008;77:637–648.
10. Pare GC *et al.* The mAKAP complex participates in the induction of cardiac myocyte hypertrophy by adrenergic receptor signaling. *J Cell Sci*. 2005;118:5637–5646.
11. Sheikh F *et al.* An FHL1-containing complex within the cardiomyocyte sarcomere mediates hypertrophic biomechanical stress responses in mice. *J Clin Invest*. 2008;118:3870–3880.

Summary

This thesis describes the diastolic function of the right ventricle in pulmonary arterial hypertension.

Chapter 2: Right ventricular diastolic impairment in patients with pulmonary arterial hypertension

We developed a load-independent method which estimates RV diastolic stiffness and is suitable for clinical practice. This is based on a modified end-diastolic elastance (Eed) estimation of the diastolic stiffness of the right ventricle. The classical Eed is only applicable for animal models since it requires preload reduction maneuvers. These can not be performed in PAH patients since they carry out risks associated with the hemodynamic instability of the patients. Nevertheless, the advantage of Eed over other estimates of RV diastolic function (right atrial pressure (RAP), E/A, E'/E, tau) is related to its load-independence and reflection of intrinsic RV properties. Therefore we developed a single-beat Ed method which circumvents the preload reduction maneuvers and measures load-independent intrinsic RV diastolic function in PAH patients. Furthermore, we observed that RV diastolic stiffness significantly associates with parameters of clinical worsening, such as RAP, stroke volume (SV), 6-minutes-walk-distance (6MWD) and NT-proBNP levels.
To understand the molecular mechanisms involved in the diastolic impairment of the right ventricle we assessed the passive properties of RV cardiomyocyte and the amount of myocardial fibrosis. RV cardiomyocytes were hypertrophied in PAH patients compared with controls and showed an increased sarcomeric stiffness and myofilament Ca^{2+}-sensitivity. We indicated that the giant protein titin may be responsible for the increase in sarcomeric stiffness in PAH cardiomyocytes. Furthermore, we found a significant but small increase in the fibrotic content of the RV, which could also contribute to myocardial stiffness.

Chapter 3: Protein changes contributing to right ventricular cardiomyocyte diastolic dysfunction

Important proteins regulating RV cellular diastolic function were found to contribute to the increased cardiomyocyte stiffness. A decreased Protein Kinase A (PKA) -dependent phosphorylation was observed in: 1) titin N2B domain leading to an increase in sarcomere stiffness, 2) troponin I leading to increased myofilament Ca^{2+}-sensitivity and 3) phospholamban (PLN), which via SERCA2a inhibition alters diastolic Ca^{2+}-clearance. We speculate that an abnormal adrenergic neurohormonal system is at the origin of the diastolic dysfunction of RV cardiomyocytes. The excessive neurohormonal activation present in heart failure ultimately leads to beta1-adrenergic receptor (β1-AR) downregulation on the RV cardiomyocyte membrane as a protective mechanism

against its apoptotic side-effects. However, reduced β1-AR signaling may also lead to a decrease in the adenylate-cyclase – PKA signaling pathway and an abnormal function of proteins modulated by PKA phosphorylation.

Chapter 4: Fibrosis- and cardiomyocyte-mediated stiffness in pulmonary arterial hypertension

Both the increase in cardiomyocyte diastolic stiffness and extracellular fibrosis contribute to the RV diastolic stiffness. However their relative contribution may be different in relation to the stage of the disease. Therefore we used two groups of rats with different PAH severity (mild RV dysfunction and severe RV dysfunction) to distinguish between the two components for diastolic stiffness. We found that RV myocardial stiffness is increased in rats with mild and severe RV dysfunction. In mild RV dysfunction, stiffness is mainly determined by increased cardiomyocyte stiffness. In severe RV dysfunction, both cardiomyocyte and fibrosis-mediated stiffness contribute to increased RV myocardial stiffness.

Chapter 5: Pressure-overload-induced right heart failure

In this review we discuss the integrative role of RV diastolic function in the progression of PAH to heart failure and give an overview of the mechanisms and molecular pathways incriminated in this process.

Chapter 6: Right ventricular-arterial coupling in patients with pulmonary arterial hypertension

A more pronounced diastolic impairment is associated with worse hemodynamic parameters and functional markers of disease severity (mean RAP, stroke volume, NT-proBNP levels and 6MWD). In this chapter we investigated whether RV diastolic dysfunction contributes to worsening of the disease or is merely an epiphenomenon of disease progression. We found that diastolic stiffness is compromised from an early disease stage and further increases as disease progresses. Unlike diastolic stiffness, systolic parameters are impaired only in a late disease stage. RV diastolic stiffness can be significantly decreased by current PAH treatment, an effect which is most likely due to a reduction of RV afterload.

Chapter 7: Clinical relevance of right ventricular diastolic stiffness in pulmonary hypertension

We further investigated whether diastolic stiffness in idiopathic PAH (iPAH) patients was associated with disease progression and survival. Treatment naïve patients had a better survival if they presented with lower RV diastolic stiffness, while in treated patients, those who maintained a high diastolic stiffness had a significantly lower survival. Interestingly, RV hypertrophy was not responsible for the high diastolic stiffness in the low-survival iPAH group. Rather than the hypertrophic response of the right ventricle, intrinsic molecular wall changes may influence RV diastolic properties.

Acknowledgements

For the first time I set foot in a lab I knew I wanted to do basic research. I knew I would love to do a PhD. Looking back it was a great adventure, diving deep in the world of molecules and cells, understanding how every protein is an "important member" of the cellular "society", how ATP is the currency of all transactions, how titin the "the big guy", how everybody gets a little "tense" when he stretches his muscles, how the kinases are the "bankers" of the cells deciding who gets poor and who gets rich on ATP, how mitochondria are the biggest power plants where specialised engineer-molecules turn glucose into energy and how beyond the protective cellular walls lies a "dark forest" of dense collagen "trees", with branches interconnecting and regulating who can pass through. This fascinating microscopic world is what makes us who we are and its complexity will never cease to amaze me.

Four years went on so fast and looking back I realize how lucky I was to be surrounded by so many great people from whom I learnt immensely. To them I will always be thankful. Without them these amazing four years would not have been possible.

First of all I would like to thank my PhD team: Anton and Jolanda, my promoters and Frances, my co-promoter.
Dear Jolanda, you are a true leader. I admire so much how you can manage the group with your optimism, kind encouragements and clear advices. You stimulate people to be creative, enjoy science but also to look critically at the data and make the best out of it. I always left our meetings with a very clear idea of how to interpret my results and what needed to be done further.
Dear Anton, you were always there for me when I needed advice for the clinical part of my study. During the PH meetings you encourage the young researchers to ask questions to take their projects one step further. Your first concern is helping the PH patients. You understand the physiology of the disease is indeed the first step in finding new ways to treat these patients. Furthermore, you are very interested in basic research. Although sometimes what we do in the lab may not be immediately applicable for the patients, you understand the importance of every cell and molecule can be in the disease progression.
Dear Frances, it is amazing to see a young researcher who recently finished her PhD become a great scientist, respected in the international group for her work, always looking for new ideas to develop and keeping a sharp eye on the ongoing projects. It was a pleasure working with you. You are demanding but also very friendly, you are ambitious but also relaxed, you stimulated me to work hard but also to love research.

I would also like to thank the reading committee. Prof.dr. Robert Naeije, Prof.dr. Yigal Pinto, Dr. Paul Knaapen, Prof.dr. Dirkje S. Postma, thank you all for accepting to review

my PhD thesis. Looking forward to our discussion. Dear Dr. Naeije, thank you for inviting me to present my research in Brussels and for all the interesting discussions during the ATS and ERS congresses.

A special thanks to our collaborators Prof. Humbert, Dr. Guignabert and Dr. Dorfmuller in Paris and and Prof. Dos Remedios in Sydney. Thank you for kindly providing us with human right ventricular tissue. Without this the experiments presented in this book would not have been possible.
Prof. Granzier in Tucson, thank you for having me in Arizona and teaching me to perform titin experiments. The research you are leading is impressive and I am very proud to have been part of our group, even for a short while.

The pulmonology group, dear Nico, Harm Jan and Louis, thank you so much for all the stimulating discussions and advice. Nico, I really admire you passion for research and devotion to the PhD students. Even after so long you still find great joy in doing science. Dear Harm Jan and Louis, you are both very busy doctors but make time for research as well. I hope in my future career as a doctor to be like you: spending my free time reading a scientific paper and contributing to research.

To the physiology group, dear Ger, Coen, Walter and Ed, thank you for your critical questions during the meetings and the precious advice regarding my experiments. I learnt so much from all of you. I hope in the future to see many more great papers from your groups.

Dear PhD-colleagues, dear roommates Barbara, Emmy, Michiel, Rosalie and for a short while Josien and Wies, we had rough times and we had great times. We respected each other's space and quiet moments, but we also laughed together, worried together and gave each other advice. We decorated the room for our birthdays and made our room a cosy one. We also suffered together in the heat of the summer, never actually fixed the broken fridge and had to deal with a dead mouse once. Looking back those were the funny times! I wish you all the best in your future careers, I hope you find the jobs that you love. I know I did!
Dear Vasco and Robert, we started the adventure together, been so close these years and now we sadly have to go separate ways. I will never forget you. You are my closest friends in Amsterdam.
Dear Joana, Diederik, Nina, Rick, Rob W, Rob J, Melissa, Paul, Chris, Aref, Denielli, Ali, Elsa, Dimitar, Ilse, Vaishali, Pleuni, Josine, Erik and Max, we had a huge lunch group. It was always fun to be around you and share ideas with you. We still get together every now and then for a BBQ or dinner and it's always great. Best of luck with your projects and hope to see you at the party after the defence.
Dear pulmonology colleagues, dear Pia, Cathelijne, Onno, Paul, Marielle, Gerrina and Bart, it was great to have you around during all those congresses. Good luck with you PhDs and residencies. Wish you all the best.

The technician group, Ingrid, Sylvia, Ruud, Jan, Michiel, Max, Wies, Kim and Sanne, thank you for teaching me so many practical things. You were always there when I

needed you, always helpful and great to work with. The lab was very cheerful with you around.

Many thanks to Aimée, Ella and Anny who always helped me with the administrative problems, which can be overwhelming for a foreigner who doesn't speak Dutch. You made it very easy for me.

Special thanks to my paranymphs Nina and Barbara. I will have a great time together. Thank you for accepting to be there for me in such a nerve wracking moment.

Of course none of this would have been possible without the invaluable support of my family. Dear mom, you are my hero, my inspiration and my best friend. You taught me the most important lessons in life, you taught me to be down to earth, work and be realistic, but also encouraged me to dream and fly away in search of my passions. Dear Sebi, my little brother grew up into a fine young man. I am so proud of you. Good luck following your dreams.

I saved the last thank you for the most special person in my life. Dear Sebas, you have been next to me all this time, you cheered me when I was down, we laughed together when everything went well. Simply thank you for being awesome!

List of publications

Right ventricular diastolic impairment in patients with pulmonary arterial hypertension. Rain S, Handoko ML, Trip P, Gan CT, Westerhof N, Stienen GJ, Paulus WJ, Ottenheijm CA, Marcus JT, Dorfmüller P, Guignabert C, Humbert M, Macdonald P, Dos Remedios C, Postmus PE, Saripalli C, Hidalgo CG, Granzier HL, Vonk-Noordegraaf A, van der Velden J, de Man FS. Circulation. 2013;128(18):2016-25, 1-10.

Pressure-overload-induced right heart failure. Rain S, Handoko ML, Vonk Noordegraaf A, Bogaard HJ, van der Velden J, de Man FS. Pflugers Arch. 2014 ;466:1055-63.

Protein changes contributing to right ventricular cardiomyocyte diastolic dysfunction in pulmonary arterial hypertension. Rain S, Bos Dda S, Handoko ML, Westerhof N, Stienen G, Ottenheijm C, Goebel M, Dorfmüller P, Guignabert C, Humbert M, Bogaard HJ, Remedios CD, Saripalli C, Hidalgo CG, Granzier HL, Vonk-Noordegraaf A, van der Velden J, de Man FS. J Am Heart Assoc. 2014;3:e000716.

Clinical relevance of right ventricular diastolic stiffness in pulmonary hypertension. Trip P, Rain S, Handoko ML, van der Bruggen C, Bogaard HJ, Marcus JT, Boonstra A, Westerhof N, Vonk-Noordegraaf A, de Man FS. Eur Respir J. 2015; 45:1603-12.

The striated muscles in pulmonary arterial hypertension: adaptations beyond the right ventricle. Manders E, Rain S, Bogaard HJ, Handoko ML, Stienen GJ, Vonk-Noordegraaf A, Ottenheijm CA, de Man FS. Eur Respir J. 2015. pii: ERJ-02052-2014.

Dysregulated renin-angiotensin-aldosterone system contributes to pulmonary arterial hypertension. de Man FS, Tu L, Handoko ML, Rain S, Ruiter G, François C, Schalij I, Dorfmüller P, Simonneau G, Fadel E, Perros F, Boonstra A, Postmus PE, van der Velden J, Vonk-Noordegraaf A, Humbert M, Eddahibi S, Guignabert C. Am J Respir Crit Care Med. 2012; 186:780-9.

A full range of mouse sinoatrial node AP firing rates requires protein kinase A-dependent calcium signaling. Liu J, Sirenko S, Juhaszova M, Ziman B, Shetty V, Rain S, Shukla S, Spurgeon HA, Vinogradova TM, Maltsev VA, Lakatta EG. J Mol Cell Cardiol. 2011; 51(5):730-9.

Right Ventricular Myocardial Stiffness in Experimental Pulmonary Arterial Hypertension: Relative Contribution of Fibrosis and Cardiomyocyte Stiffness. Rain S, Andersen S, Schultz JG, da Silva Gonçalves Bos D, Handoko ML, Westerhof N,

Bogaard HJ, Vonk-Noordegraaf A, Andersen A, van der Velden J, Ottenheijm CA, de Man FS. Circ. Heart Fail. 2015. In revision.

Back to basic – The striated muscles in pulmonary arterial hypertension; adaptations beyond the right ventricle. Manders E, Rain S, Vonk-Noordegraaf A, Ottenheijm CA, de Man FS. Eur Respir J 2015. In press.

Curriculum Vitae

Silvia Rain was born on April 1st 1985 in Ploiesti, Romania. After finishing her secondary education from the "Mihai Viteazul" National College Ploiesti in 2004 she decided to further study medicine in "Carol Davila" Medical University Bucharest.

During her study she took a particular interest in cellular biology and basic research. The first contact with the fascinating cardiovascular research world was in 2008 during the "Heart failure –from bench to bedside" summer school at the Academic Medical Centre – Amsterdam, coordinated by Prof. Dr. J.H. Ravesloot. The research adventure continued the next summer at the National Institute of Health in Baltimore where Silvia studied the sinoatrial node function under the supervision of Dr. J. Liu and Prof. Dr.E. Lakatta.

After receiving her medical doctor degree in 2010 Silvia started her PhD at the department of Pulmonology and Physiology at the VU Medical Centre, Amsterdam, under the supervision of Prof. Dr. A. Vonk-Noordegraaf, Prof. Dr. J. van der Velden and Dr. F.S. de Man. The research focuses on the diastolic function of the right ventricle in pulmonary hypertension.

After finishing her PhD, Silvia embarked on a new adventure, this time focused on the human brain. Currently she is working as a medical doctor at the Neurology department at the WestfriesGasthuis in Hoorn.